Modeling of Hydraulic Systems

Tutorial for the Hydraulics Library®

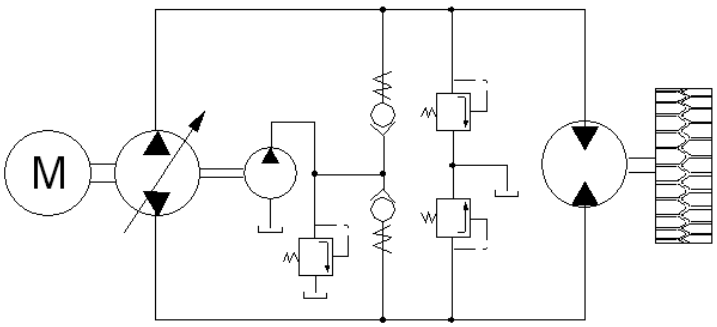

Modelon

Hydraulics Library Tutorial

The software described in this document is furnished only under license, and may be used or copied only in accordance with the terms of such license. Nothing contained in this document should be construed to imply the granting of a license to make, use, or sell any of the software described herein. The information in this document is subject to change without notice, and should not be construed to imply any representation or commitment by the author.

This document may not be reproduced in whole or in part without the prior written consent of the author.
MapleSim, Maple, and Maplesoft are trademarks of Waterloo Maple Inc.
Modelica® is a registered trademark of the Modelica Association.
PneuLib, HyLib, Pneumatics Library and Hydraulics Library are registered trademarks of Modelon AB.
Other product or brand names are trademarks or registered trademarks of their respective holders.

Hydraulics Library Manual and Tutorial
2013-09-04
© 1997 – 2013 Modelon AB. All rights reserved.

Modelon AB
IDEON Science Park
SE-223 70 LUND
Sweden

E-mail: support@modelon.com
URL: http://www.modelon.com/

Phone: +46 46 286 2200
Fax: +46 46 286 2201

Maplesoft
615 Kumpf Drive
Waterloo, ON, N2V 1K8
Canada

E-mail: support@maplesoft.com
URL: http://www.maplesoft.com/

Phone: +1-519-747-2373
Fax: +1-519-747-5284

“Everything should be made as simple as possible,
but not simpler.”

Albert Einstein

Preface

Modeling the static and dynamic response of hydraulic drives has been a research topic for a number a decades. In the fifties a number of models for analog computers have been developed and published. The restrictions of the analog computers limited the size of the models. Often they were linearized about an operating point and could therefore not predict the response of the system for large deviations from that operating point.

In the seventies digital computers became available and were used to model and simulate hydraulic systems. In the beginning only small models with few states were used because no simulation software was available. For each modeling task a new program had to be written in a programming language, e. g. ALGOL or FORTRAN. Later the first simulation languages, e. g. CSMP, were used. Because of the lack of reusable models these studies were very time consuming.

During that time a lot of research was done to develop mathematical models, i. e. to find mathematical equations that describe the response of a hydraulic component. This work, today's powerful digital computers and high level simulation languages enable us to quickly model and simulate even complex hydraulic circuits and study them before any hardware has been build.

This tutorial gives an overview about both modeling complex hydraulic systems and modeling typical components. For a number of components it lists several mathematical models and compares them. But it is not a standard text book on hydraulics because it doesn't explain the operation of these components.

This tutorial gives general remarks and examples of modeling hydraulic systems in chapter 2. In chapter 3 a number of component models is given. The reference section gives the details of the model implementation in the Hydraulics Library (formerly HyLib) in the Modelica language version 3.1.

TABLE OF CONTENTS

Hydraulics Library Tutorial 2

PREFACE 4

1 BASIC PRINCIPLES 0

2 SYSTEM MODELS 2

2.1 Hydraulic Drive 9

2.2 Hydrostatic Transmission (Closed Circuit) 10

2.3 Hydrostatic Transmission (Open Circuit) 11

2.4 Hydrostatic Transmission (Secondary Control) 12

2.5 Including mechanical parts 13

2.6 Semi-empirical models 14

2.7 Using Modelica's advanced features 15

3 COMPONENT MODELS 17

3.1 Hydraulic fluids 17
3.1.1 Compressibility 17
3.1.2 Viscosity 22
3.1.3 Inductance 25

3.2 Pumps 27
3.2.1 Theoretical Displacement, Power Flow of an Ideal Pump 27
3.2.2 Efficiency 27
3.2.3 Modeling the Losses 28
3.2.4 Physically Motivated Models 29
3.2.5 Abstract Mathematical Models 31
3.2.6 Models for Time Domain Simulation 33
3.2.7 Effects of Reduced Intake Pressure 35

3.3 Motors 38

3.4 Cylinders 40
3.4.1 Seal friction 40
3.4.2 Leakage 44
3.4.3 Fluid Compressibility and Housing Compliance 44
3.4.4 What happens if there is no flow but the rod is pulled out? 44

3.5 Restrictions **46**
3.5.1 Calculating Laminar Flow 47
3.5.2 Calculating Discharge Coefficient C_d For Turbulent Flow Through Orifices 50
3.5.3 Calculating Loss Coefficients or K-Factors 53
3.5.4 Cavitation 57
3.5.5 Metering Edges of Valves 58
3.5.6 Library Models for Orifices 58
3.5.7 Library Models for Metering Orifices of Valves 65

3.6 Spool Valves **66**
3.6.1 Servo and Proportional Valves 66
3.6.2 Directional Control Valves 69

3.7 Flow and Pressure Control Valves **71**

3.8 Long Lines **75**
3.8.1 Steady State Pressure Loss in Lines 75
3.8.2 Modeling the Dynamics of Long Lines 77
3.8.3 Examples using Model LongLine and LongLine_u_air 80

3.9 Accumulators **85**

3.10 Filters and Coolers **85**

REFERENCES **86**

INDEX **94**

1 Basic Principles

There are several ways to model a hydraulic system. Which is appropriate depends on the purpose of the simulation study. A model can be very small and linear to gain insight in the typical response of a system, e. g. stability or sensitivity to parameter changes. Or it can be very elaborate and consist of a lot of nonlinearities to predict the response of a particular machine and a particular load cycle.

Modeling a dynamic system is an engineering task and that means there are some guidelines but no fixed rules that will guarantee success, if followed, or lead to failure, if ignored. The main point is that a good model helps to get the work done, to answer the questions that were the reason it was made. Unfortunately it is not possible to say in advance which the answers to the questions are.

One reasonable approach is to start modeling "the heart of the system" assuming ideal boundary conditions. In case of a hydraulic control system this may be the inner loop consisting of a servovalve and a cylinder. Pressure supply, auxiliary valves and instrumentation can be modelled as ideal. The first simulation runs will show the influence of the valve characteristics, the internal leakage of the cylinder or the response of the external load. At this point more detailed information is usually needed about the key components which leads to questions to the manufacturer or own measurements. If the response of this small system is fully understood, more detailed models can be used for the auxiliary components. For instance the ideal pressure supply can be replaced by a model of a pump driven by an electric motor and a pressure valve. The model of the pump can include the torque and volumetric losses and the valve model can include leakage and saturation.

If stability problems occur it is always useful to look at the linearized system. While building the model one should therefore try to find out which component influences which eigenvalues, e. g. associate the very lightly damped mode with a pressure valve or the large time constant with the volume at the main pump.

The model should be as simple as possible but not simpler. It should describe the physical phenomena even if the used parameters are always somewhat wrong. This means that it always makes sense to model leakage even if it is small because it adds almost always damping to the system. And real systems are very often better damped than their models. It depends on the system and the experience of the analyst whether it is better to use "global" models of the components or "local" when modeling a system. For example a global model of a pump includes the reduction of output flow if the input pressure is too low while the smaller local model doesn't describe this effect. If the system works properly the pump's inlet pressure is always high enough and the global model is not necessary. If on the other hand the inlet pressure is too low the local model is not a valid representation of the system and leads to wrong results.

The algorithms should also be numerically sound. If the flow rate through an orifice is modelled by

$$Q = A \cdot C_D \cdot \sqrt{\frac{2}{\rho}} \cdot \sqrt{|\Delta P|} \cdot \text{sign}(\Delta P) \tag{1.1}$$

the physical effects of fluid flowing through a small hole are not always described adequately because (1.1) is only valid at high Reynolds numbers. At low Reynolds numbers there is a linear relationship between pressure drop and flow rate. And if (1.1) is used for $\Delta P \rightarrow 0$ the step size of an integration algorithm with variable step size becomes very small and the sign of Q may even change. The reason is that the gain of this model, $dQ/d(\Delta P)$, goes to infinity as ΔP goes to zero. This leads to numerical and stability problems. A better way is a model that switches between the describing equations, one for low and one for high Reynolds numbers, or a model that is valid for all Reynolds numbers

2 System Models

The conceptive easiest way to model a hydraulic system is to identify all important components, e. g. pump, valves, orifices, cylinders, motors, etc. connect their models according to the circuit diagram and place a lumped volume at each node, the connection of two or more components. This leads to a set of differential equations where the through variable, flow rate, can be easily calculated from the known state variables, i. e. the across variables, which are the pressures in the volumes (nodal analysis).

The laminar resistance is a typical example. The flow rate Q through that component is calculated by:

$$Q = G \cdot (P_A - P_B) \tag{2.1}$$

where G is the conductance, P_A is the pressure at port A and P_B is the pressure at port B. The flow rate is positive, $Q > 0$, if $P_A > P_B$. The through variable of this model is the mass flow rate $m_flow = Q \cdot \rho$ which is identical for the input and the output port. The across variables are the pressures P_A and P_B, which are usually different.

The library icons show the symbol of the component, the abbreviation and names the ports if necessary, the object diagram includes the across and through variables and the positive flow direction.

Figure 2.1 Diagram of laminar resistance.

In a lumped volume the flow rate is integrated with respect to time to calculate the pressure. The describing differential equation is:

$$\frac{dP}{dt} = \frac{\beta}{V} Q(t) \tag{2.2}$$

with the bulk modulus β, the volume V and the flow rate Q(t). Both β and V can be constants or depend on other system variables. The across variable is again the pressure P, the through variable the flow rate m_flow. In the library oil filled components are symbolized by the red background of the drawing, e. g. the model *OilVolume* or *ChamberA*.

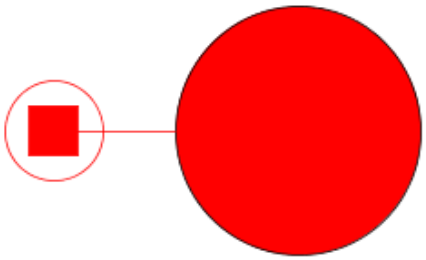

Figure 2.2 Icon of lumped volume, library model OilVolume

The *direct* connection of two lumped volumes leads usually to problems. If you look at the resulting system from a modeling point it is a poor model because there is always a resistance between two real energy storage devices (and this is not included in the model). In the electrical world this could be the resistance of the wire between two capacitors, in the hydraulic world the resistance of the connecting hose. System theory says that such a system is not completely controllable and observable, i. e. not a minimal realisation. Mathematicians say that the resulting differential equations form a higher index system that cannot be solved by the usual integration algorithms. However, when looking at such a system an engineer would simply eliminate one state (differential equation of a lumped volume) and add the amount of oil of that state to the other state. This can be done automatically by an appropriate algorithm that is implemented in MapleSim. It is then possible to connect lumped volumes directly to one another and this feature is used in the Hydraulics library.

For the proposed modeling approach the system in Figure 2.3 gives an example. It has a pump as flow source with a relief valve, a 4 port control valve, a hydraulic motor and a tank.

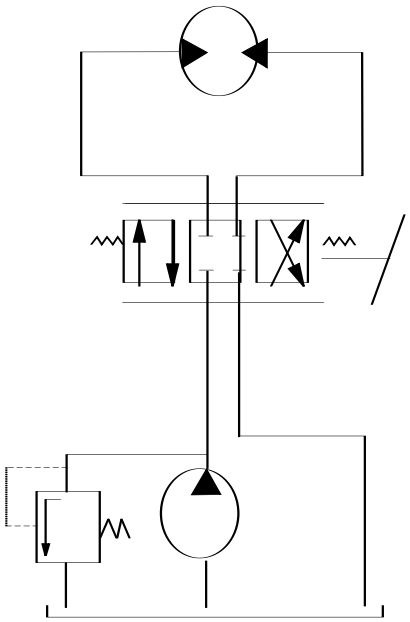

Figure 2.3 Example system

In most cases it is best to model a pump as a flow source because almost all pumps used for oil hydraulics displace the fluid with pistons, gears or vanes. This means they produce a flow rate while the pressure builds up according to the resistances the oil has to pass on its way to the tank. In this example the flow rate of the pump is constant, i. e. $Q_{pump} = 10^{-3}$ m^3/s. In the library SI units are used. This has the advantage that no conversions are needed during calculations. On the other hand the approach can lead to numerical problems because some of the numbers of the resulting set of equations are very big (e. g. pressure: 10^7 Pa) while others are very small (e. g. conductance: 10^{-12} $m^3/(s\ Pa)$).

In the model the tank has always a constant pressure regardless of the amount of oil coming in. In this example the preload pressure is 0 Pa (against the atmosphere).

The pressure relief valve can be described by a (static) relationship of the pressure differential between the inlet port and the outlet port and the resulting flow through the valve. In most cases this simple model is sufficient because the speed of response of a relief valve is usually many times faster than that of the driven load. A more detailed model can be derived from measurements of the input-output response (Viersma 1980) or by modeling all parts of the valve, like spool, springs, orifices (Merritt 1967). Unfortunately the necessary parameters for these dynamic models are not easily available.

A simple model of the control valve uses orifices to describe the resistances the oil has to pass depending on the position of the lever. A simple model of the hydraulic motor describes the torque τ at the shaft as a function of the pressure at the two ports and the motor displacement, D_{Motor}.

$$\tau(t) = D_{Motor} \cdot \frac{P_A(t) - P_B(t)}{2\pi} \tag{2.3}$$

This torque τ accelerates a rotating mass that has an angular velocity ω and an angle φ.

To model the complete system lumped volumes are added at the nodes. The pressures in these volumes are the state variables of the system and the across variables. No volume is needed at the tank because this component has always a fixed value for the pressure. Using the *basic component models*[1] of the library the following model can be build.

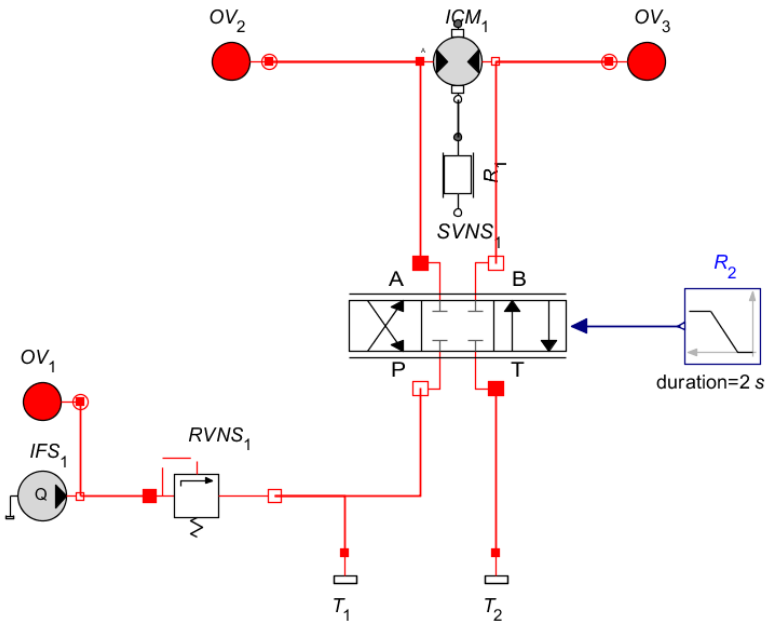

Figure 2.4 Simulation model of example system, using *basic component models*

Three volumes were used. As the state variables, pump flow rate and tank pressure are known all other flow rates can be calculated. The change of the pressure is given for each lumped volume by first order differential equations:

$$\frac{dP_i}{dt} = \frac{\beta}{V_i} \sum Q_j \tag{2.4}$$

The torque τ can be calculated from the known pressures P_A and P_B. The states ω and φ are calculated by integration of the torque and the angular velocity, respectively. For the mechanical part this procedure leads to:

$$\tau = \frac{(P_B - P_A) \cdot D_{Motor}}{2\pi} \tag{2.5}$$

and for the state variables (across variables):

$$\frac{d\omega}{dt} = \frac{\tau}{J} \tag{2.6}$$

[1] The basic components are printed in *blue* in the electronic form of the document.

$$\frac{d\varphi}{dt} = \omega \tag{2.7}$$

The placement of volumes at the nodes can be justified by the fact that there is very often a considerable amount of oil in the fittings and hoses between the components. The compliance of this oil and the housings can lead to lightly damped oscillations.

But while this *manual* placement of lumped volumes makes sense from a modeling point of view there are at least two drawbacks. In a typical hydraulic circuit diagram these volumes don't appear and therefore a number of engineers don't like them to be in the object diagram of the simulation model. Some component models already have a lumped volume included, e. g. the cylinder models. And if the placement of lumped volumes can be done automatically by the simulation program the modeller shouldn't be required to do so. In the *main windows* of the Hydraulics library almost all component models have therefore already added these volumes at the hydraulic ports. And if applicable the inertia of the moving parts is also included. Figure 2.5 shows the object diagram of the main motor model. It is composed of the ideal motor, laminar resistances to model the leakage and the rotor to describe the inertia of the motor shaft and the coupled load.

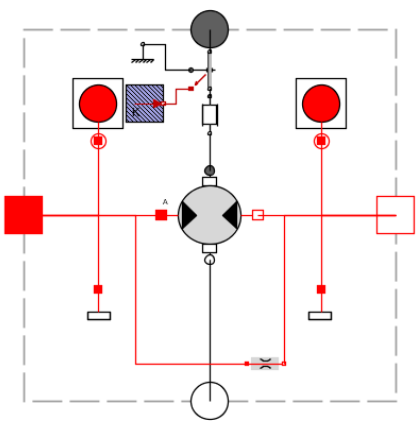

Figure 2.5 Object diagram of main motor model ConMot

Using the *main models* the object diagram looks very similar to a hydraulic circuit diagram; the user doesn't have to place lumped volumes at the nodes.

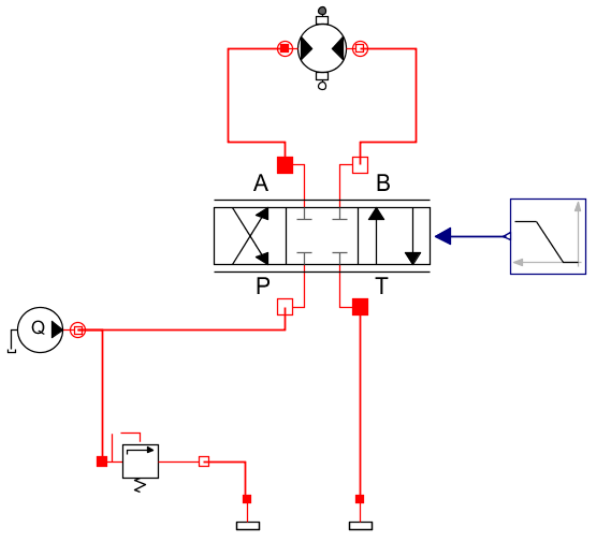

Figure 2.6 Simulation model of example system using *main models*

The amount of oil at a port becomes a parameter in the parameter window of the model.

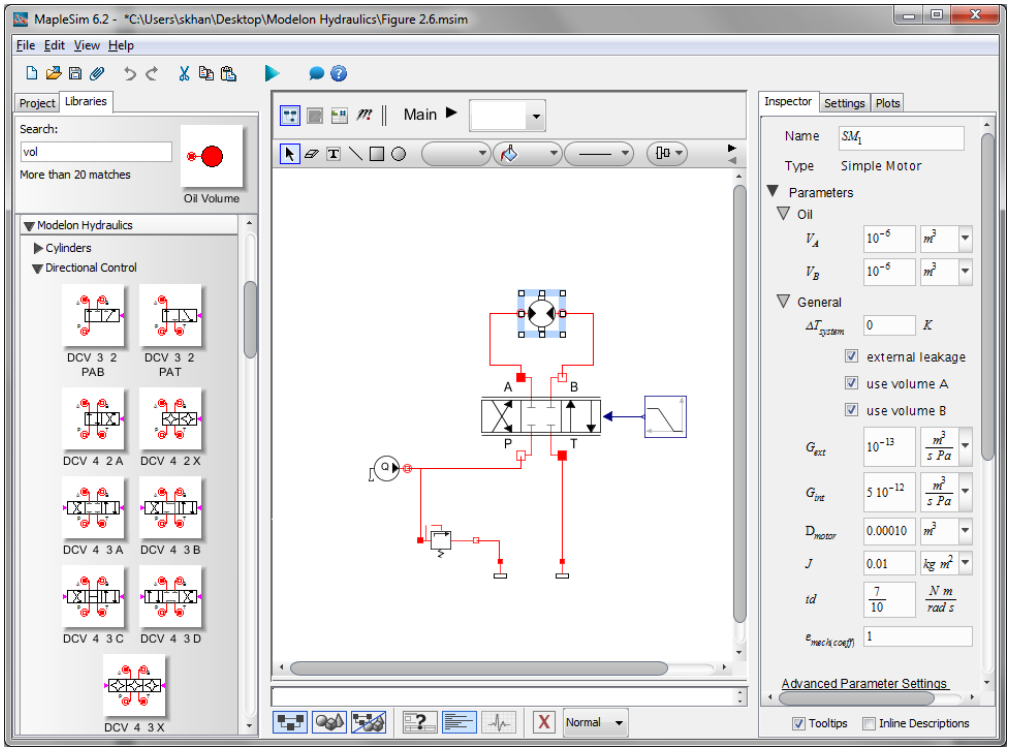

Figure 2.7 Parameter window of ConMot, model of a constant displacement motor

Sometimes however these volumes become very small and their time constants are negligible compared with the rest of the system dynamics. In this case the basic models can be used without the volumes and a numerical solution of the resulting equations can be used.

Besides the lumped volume there is a second energy storage element in hydrostatic systems: The inductance of an oil column. This storage element is equivalent to the inertia of a mass in translational mechanics. Usually it is not necessary to include this effect in a system model. However if there are high frequency excitations or long lines the effect of the inductance of the oil column cannot always be neglected.

Hydraulic systems are usually build to drive mechanical loads, e. g. propel a vehicle or move a mass. When modeling a system it is necessary to model these mechanical parts too. And detailed models of hydraulic components often require the modeling of the inertia of moving parts, e. g. spools or pistons. Simple mechanical models with one degree of freedom are therefore needed.

The easiest way to model a translational mechanical system with one degree of freedom is to identify all components that have a mass, regard them as rigid and connect them with compliant components, e. g. springs or dampers. This leads to a set of differential equations where the through variable, force F, can be easily calculated from the known state variables, i. e. the across variables, which can be the positions s and velocities, $v = d\,s/d\,t$, of the masses. It is important to use the same coordinate system throughout the model! The icons of the mechanical models show therefore a small arrow: All arrows must point to the same direction!

As with lumped volumes the direct connection of two masses leads to a singular problem. It is necessary to have one compliant component in between, e. g. a spring. However the mechanical libraries in the Modelica standard library and MapleSim are set up such that a rigid connection between two masses can be dealt with.

2.1 Hydraulic Drive

Figure 2.8 show the simulation diagram of a linear drive. It is built in a similar way as the previous example but with a linear actuator, a cylinder, instead of a rotational actuator, a hydraulic motor. The load, SlidingMass1, is coupled via Spring1 to the cylinder. The left position of the cylinder is defined by Fixed1.

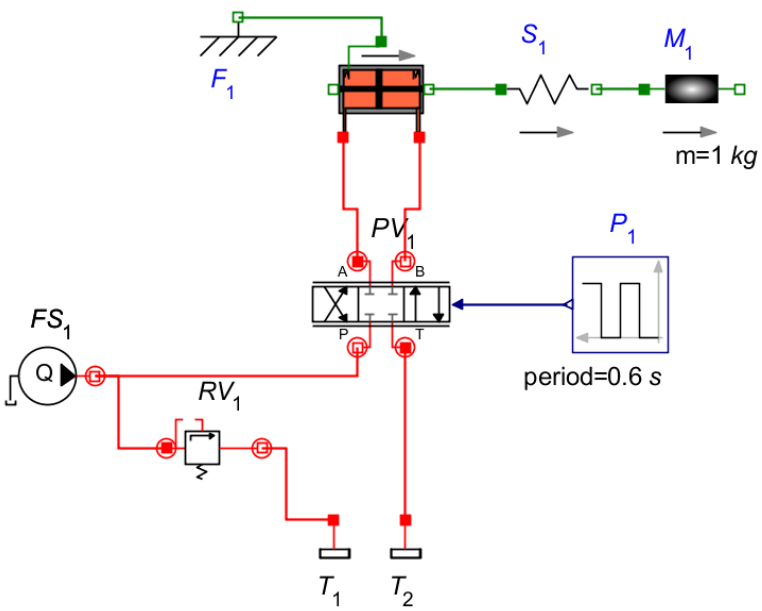

Figure 2.8 Simulation diagram of a hydraulic drive

2.2 Hydrostatic Transmission (Closed Circuit)

Figure 2.9 show the simulation model of a hydrostatic transmission. This kind of drive is used for small wheel loaders or fork lift trucks. There are many studies on the dynamic response of these drives (e. g. Knight et al. 1972, Hahmann 1973, Svoboda 1979, Wochnik and Frank 1993, Lennevi 1995, Sannelius 1999).

The necessary power is delivered by a diesel engine, symbolized by the rectangle. This engine drives the main pump and a charge pump. The main pump is a variable displacement pump that can produce an oil flow in both directions, depending on the command signal. The main pump is connected to the wheel motor which has a constant displacement. This kind of circuit is called “closed circuit” because the pump output flow is sent directly to the hydraulic motor and then returned in a continuous motion back to the pump. The charge pump is needed to maintain a minimum pressure in the return line from the motor to the pump, i. e. replenish the oil that has left the circuit as leakage. The pressure in the return line is limited by the relief valve. There are two more relief valves to limit the pressure in the high pressure line.

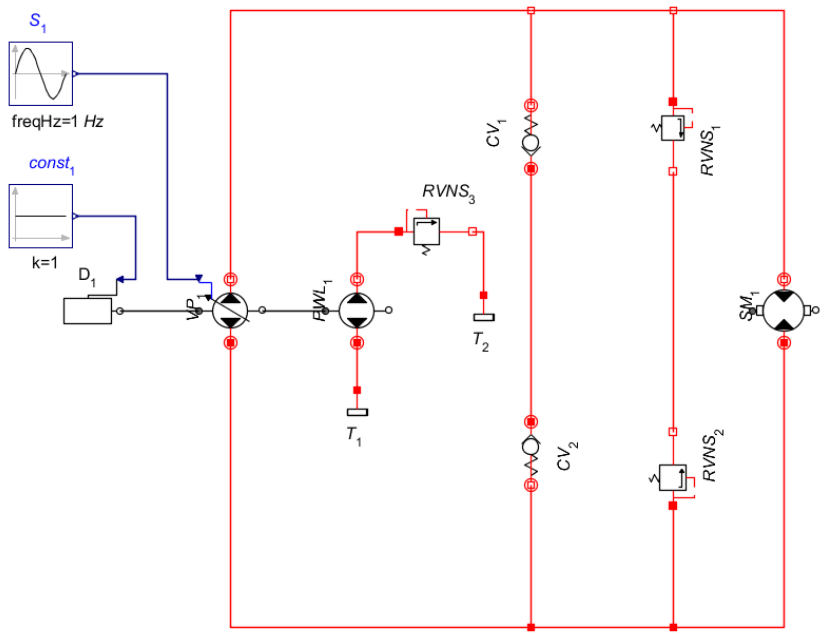

Figure 2.9 Object diagram of a closed circuit hydrostatic transmission

This system shows the importance of “global” component models. If for example the diameter of the check valves is too small or the charge pressure is too low the pressure in the return line will drop below atmospheric pressure at high speed. If the reduction of output flow and the limit of the pressure to the vapour pressure were not modelled the simulation would show negative pressure values in the return line.

To use this hydrostatic transmission a controller is necessary to give input signals to the Diesel engine and the main pump. In the past different concepts have been used. The simplest way was to give the operator

two levers to change both signal manually. Another machine used an open loop strategy to command the swash angle of the main pump and the engine speed as a function of commanded speed. An important feature of the controller was overload detection and deswashing of the pump to prevent the Diesel engine from stalling if the required torque was too high. Newer concepts use nonlinear decoupling controllers that are realized electronically (Wochnik and Frank 1993, Lennevi 1995).

2.3 Hydrostatic Transmission (Open Circuit)

The hydrostatic transmission in Sect. 2.1 is a closed circuit system. The drive in Figure 2.10 is an *open circuit system* because the oil flows from the motor into the tank and not to the pump. This kind of circuit is used if the pump delivers oil to several actuators including double-acting cylinders with differential area because then the return flow differs from the pump flow. This is a common situation for excavators which have cylinders with differential area for the boom, arm and bucket and motors for the swing and propel.

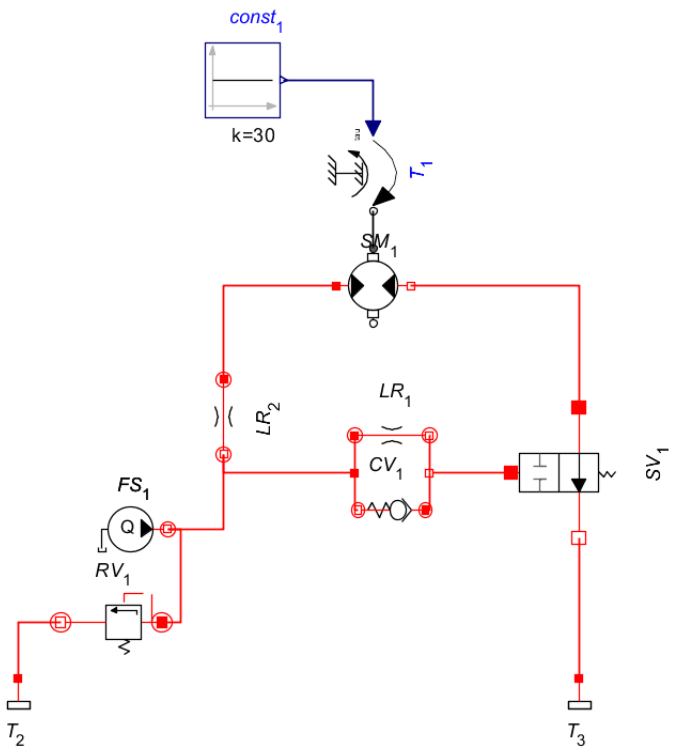

Figure 2.10 Simulation diagram for hydraulic drive with counterbalance valve

When using a motor in an open circuit a counterbalance valve is needed to decelerate the load. Figure 2.10 show the circuit. If the pump pressure is high enough the counterbalance valve is wide open and the oil flows from the pump to the motor, through the counterbalance valve to the tank. If the pump pressure is about the atmospheric pressure the spring in the counterbalance valve moves the spool to the left and

the valve is closed. If the motor is rotating there will be a pressure build up at motor port B which leads to a torque that decelerates the motor. The vehicle stops.

These systems tend to be oscillatory when decelerating the motor. In that operating condition the needed pump power is small (the pressure is low) and it is therefore not necessary to model the Diesel engine and the pump in detail. A constant flow source is used instead. The check valve is used to provide more damping of the system. The intention is to close the valve fast, and open it slowly.

The external torque to the motor can be used to analyse different operating conditions, e. g. model an uphill or downhill slope. The model is very well suited to look at the sensitivity to parameter changes, e. g. the effect of a reduction of the internal or external leakage of the motor or a change of the amount of oil in the lumped volumes. A detailed study of this kind of drive system was done by Kraft (1996).

2.4 Hydrostatic Transmission (Secondary Control)

Open circuit systems tend to have a good dynamic response but poor efficiency. To avoid the throttle losses in valves without impairing the dynamics *secondary control of hydrostatic transmissions* was designed. The key element is a constant pressure system that can store energy in a hydraulic accumulator. All motors have a variable displacement volume and are usually operated with closed loop velocity control. This circuit has considerable advantages if there are number of motors with alternating load cycles. In that case some of the motors will take hydraulic energy out of the circuit, while others act as generators and put hydraulic energy into the circuit.

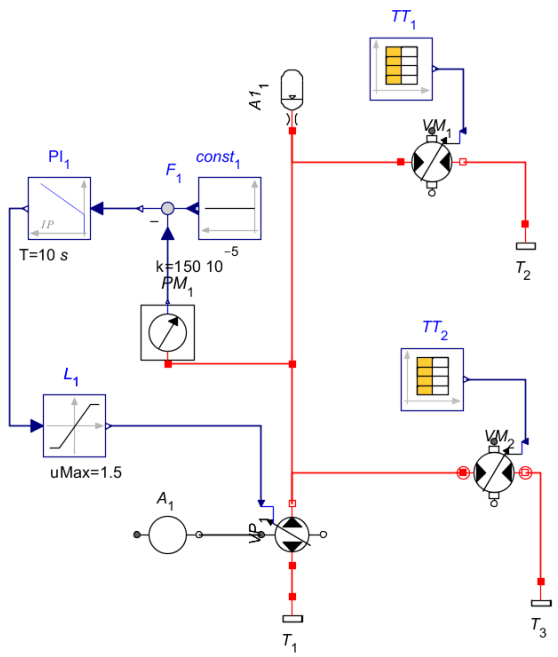

Figure 2.11 Object diagram for hydraulic drive with secondary control

2.5 Including mechanical parts

The model of the double acting cylinder is a good example of a model that consists both of hydraulic and mechanical parts. The inertia and the friction of the piston, rods and the stops at both ends of the housing can't usually be neglected. Figure 2.12 show the used coordinate system and the variable names. Figure 2.13 show the used submodels and their connections. At connector flange_aref the left end of the cylinder housing is defined. The spring-damper combination models the hydraulic cushion if the piston is near the left end of the housing. A rod models the housing length and another spring-damper the cushion at the right end. To model the piston dynamics the submodel *Mass* is used. The inertia of the piston and the rods and if appropriate the driven load is lumped into one mass. The rods at the left and right end of the piston transmit the forces to the piston. The hydraulic part is modelled by two chambers where the pressures build up according to the flow rates and the piston movements. The internal leakage is modelled by the laminar resistance. Note that the arrows of all mechanical submodels point to the same direction.

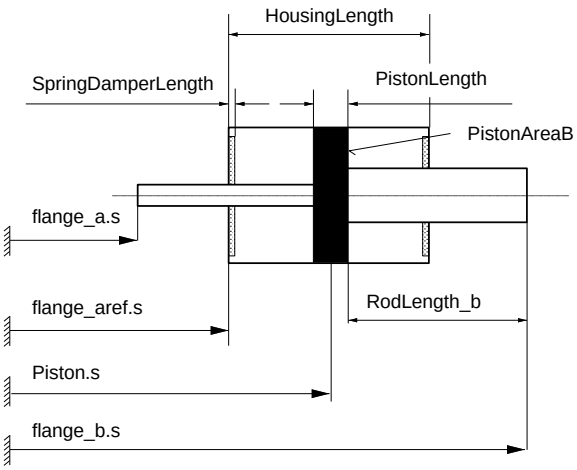

Figure 2.12 Coordinates and variable names of the cylinder model

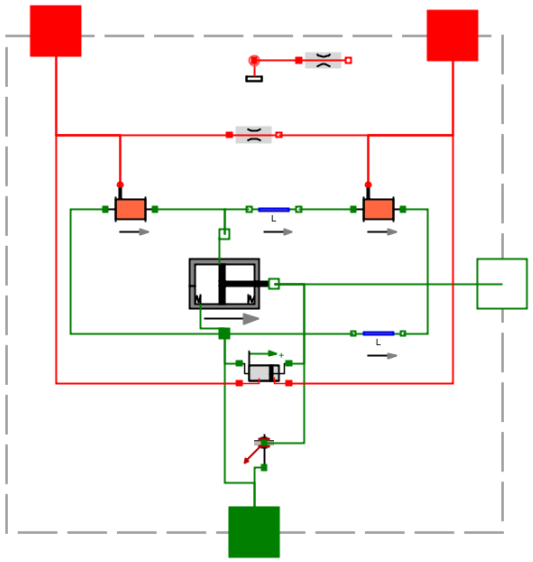

Figure 2.13 Diagram of cylinder model composed of submodels

2.6 Semi-empirical models

"An analytical model for a fluid power component has a large number of parameters that has to be identified. This means, in practice, that the component has to be dismantled in order to measure the dimensions of internal elements, spring constants etc. When using the model for designing a component its form is the most appropriate but using it as a part of a circuit model has its drawbacks" (Handroos 1996).

In this case semi-empirical models can be suited better. Starting from the analytical equations, the model is simplified and the resulting small number of parameters estimated. This requires of course a working component and some signal processing. Therefore none of the models given by Handroos is included in the library, but the approach can be the best compromise between a too simple and an overly complex model.

2.7 Using Modelica's advanced features

The library is set up in such a way that for typical hydraulic systems Modelica's advanced features are best used. Sometimes however the modeller may wish to override these default settings.

State selection is automatically done by MapleSim and is usually not a critical point for hydraulic systems. The lumped volumes in the Hydraulics library have therefore the default setting *stateSelect=StateSelect.default* with the exception of the models from the package Volumes that are deliberately chosen by the user (OilVolume, OilVolume2, VolumeConst, VolumeTemp). They have the next higher priority (stateSelect=StateSelect.prefer). This ensures that the index reduction algorithm selects these volumes as states and thus keeps their attributes, like initial conditions. The default setting for all volumes can be overridden by the modifier stateSelect=StateSelect.xxx where xxx is one of (never, avoid, default, prefer, always).

Selecting *initial conditions* is easy for most hydraulic systems because typically it is best to start with a system at rest, i.e. all pressures are equal to zero. Then appropriate control signals drive the system to the operating point of interest. Another way is to set some initial conditions to the desired values and have MapleSim calculate all other required variables, e. g. Chamber(port_A(p(start=1e5, fixed=true))).

Modelica uses SI units for all models. That has the advantage that the user doesn't have to convert units when writing models, e. g. l/min to m^3/s or bar to Pa. The numerical range of variables becomes very big however. Pressures can reach up to 10^8 Pa while conductance may be in the range of 10^{-12} $m^3/(s*Pa)$. To ease the burden on the numerical integrator the attribute *nominal* has been introduced in the Modelica language. It enables automatic scaling of variables. In the Hydraulics library a value of p_nominal=1e6 is used in the definition of the oil pressure p(nominal=p_nominal). This constant is defined under package Hydraulics.

For additional information about state selection, initialisation and scaling see the MapleSim manual and on-line help and the Modelica manuals.

3 Component Models

This chapter gives mathematical models of the most important components of hydraulic systems, e. g. pumps, motors, valves etc. For a number of components there is more than one model and a discussion which model is appropriate.

3.1 Hydraulic fluids

In a hydraulic system the fluid is needed to transport energy. As a string can only transmit a tensile force a technical fluid can only transmit positive pressure. In the library this effect is described in the component models, e. g. the pump stops delivering fluid if the intake pressure is too low. All components based on TwoPortComp limit the internally used pressure at a port to the vapour pressure. Only very pure fluids can transmit negative pressure. Experimental results show values of 25 MPa for water (Briggs 1950).

3.1.1 Compressibility

There are several properties of a fluid that may need modeling. Most important for hydraulic control systems is the spring effect of a liquid leading, together with the mass of mechanical parts, to a resonance that very often is the chief limitation to dynamic performance. The stiffness of the fluid spring is characterized by the *bulk modulus* β. Hayward (1970) gives several definitions of the bulk modulus and some simple formulas for the bulk modulus of water, mercury and mineral oil that is *free from entrained* air.

Effect of Wall Thickness

The *effective bulk modulus* depends on the fluid bulk modulus β and the bulk modulus of the container due to mechanical compliance. Equation 3.1 shows the effect of the wall thickness (Theissen 1983).

$$\beta_e = \beta \frac{1}{1 + \frac{\beta}{E_{St}} W} \tag{3.1}$$

with: β_e effective bulk modulus,
β fluid bulk modulus,
E_{St} Young's modulus of elasticity for metal.

W is given for thick walled steel tubes by:

$$W = \frac{2\left(\frac{D_o}{D_i}\right)^2 (1+\nu)+3(1-2\upsilon)}{\left(\frac{D_o}{D_i}\right)^2 - 1} \tag{3.2}$$

with: D_o outside diameter,
D_i inside diameter,
ν Poisson's ratio, 0.3 for steel.

For thin walled tubes with a wall thickness S and $S/D_o < 0.1$ this equation can be simplified to:

$$W = \frac{D_i}{S} \tag{3.3}$$

with: D_i inside diameter,
S wall thickness.

For rubber hoses Martin (1981) gives an empirical formula that works well up to $P = 0.5\ P_{max}$:

$$\beta(P) = (614D - 2.18)(P_{max})^{1.5}\left(1.11 - e^{\frac{-2P}{Pmax}}\right) \tag{3.4}$$

with: D internal diameter in m,
P_{max} maximum allowable working pressure in MPa.

Effect of Entrained Air

There is always a certain amount of air in a hydraulic fluid. While the *dissolved* air has almost no effect on the bulk modulus (Stern 1997), the *entrained* air in the form of bubbles reduces the effective bulk modulus especially if the pressure is below 10 MPa. Equation 3.5 models this effect assuming that the change of state is isentropic and that no air will be dissolved by the oil (Backé and Murrenhoff 1994):

$$\beta_{Isen} = \beta \frac{1 + \frac{V_{L0}}{V_{Oil0}}}{1 + \left(\frac{P_0}{P}\right)^{1/\kappa} \frac{V_{L0}}{V_{Öl0}} \frac{\beta}{\kappa P}} \tag{3.5}$$

with: β_{Isen} bulk modulus by isentropic change of state,
β_{bulk} modulus of air free oil,
V_{L0} Volume of undissolved air at atmospheric pressure,
V_{Oil0} Volume of oil at atmospheric pressure,
P_0 atmospheric pressure,
P oil pressure,
κ polytropic expansion index.

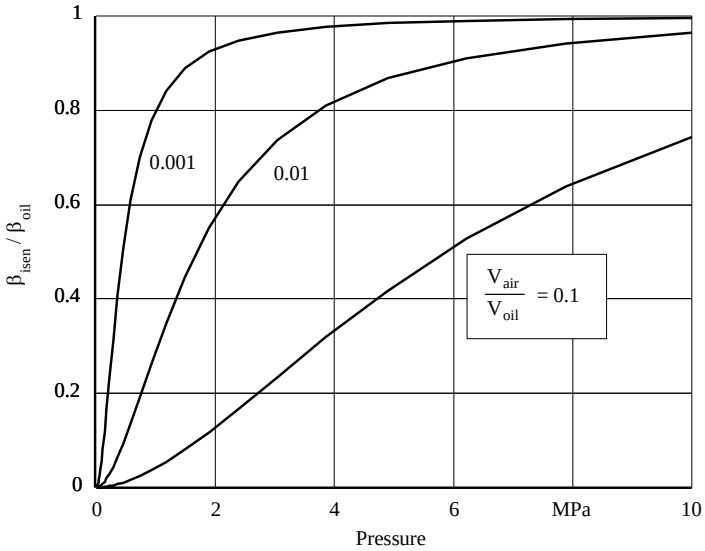

Figure 3.1 Bulk modulus as a function of entrained air

Bowns et al. (1973) showed that when a greater amount of dissolved air is in the hydraulic fluid at start up of a system this air will be completely released quite rapidly. They measured a time of two hours or less for all test cases. There are however no models that describe the rate of solution of air bubbles under (varying) pressure (Hayward 1962).

Effective Bulk Modulus

The value of the bulk modulus depends on the fluid, the pressure, the entrained air, the container and the temperature. The low values of the bulk modulus at low pressure lead to low corner frequencies of hydraulic motors and may cause stability problems. It is therefore important to model this effect if the working pressure is below 10 MPa. As the housings of hydraulic components aren‘t infinitely stiff their compliance has to be included in the calculations. To simplify modeling an *effective bulk modulus* has been defined as (Backé and Murrenhoff 1994, Martin 1995):

$$\beta_e = \frac{V \cdot \Delta P}{\Delta V}. \tag{3.6}$$

It can be measured by setting the component under pressure and recording the pressure drop ΔP while letting a small amount of oil, ΔV, out of the component. Figure 3.2 shows the measured bulk modulus of oil at 20 and 50 °C and the effective bulk modulus of oil in a high pressure hose, a tube or a housing (Zimmermann 1985).

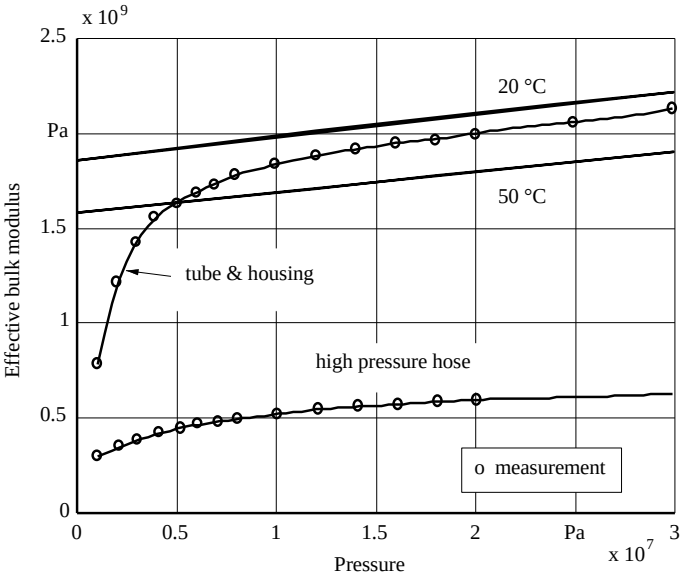

Figure 3.2 Effective bulk modulus as a function of pressure

As the effective bulk modulus depends on a number of parameters it should be measured with the actual component. Kürten (1993) and Manring (1997) describe suitable procedures. If this is not possible numbers from literature can be used. Four different models are shown in Figure 3.3. The biggest difference between the models is the behaviour at low pressure. Those of Eggerth and Boes have a bulk modulus of almost zero while Lee‘s has a value that is approximately 19 % and Hoffmann‘s 33 % of the maximal value. Eggerth‘s model also includes the effect of the oil temperature.

Boes's Model

$$\beta_e(P) = 0.5 \cdot \beta \cdot \log\left(99\frac{P}{P_{ref}} + 1\right) \tag{3.7}$$

with: $\beta = 1.2 \cdot 10^9$ Pa,
$P_{ref} = 10^7$ Pa.

Hoffmann's Model

$$\boldsymbol{\beta_e(P) = \beta_{P_{max}}[1 - exp(-0.4 - 2 \cdot 10^{-7} P)]} \tag{3.8}$$

with: P in Pa,
$\beta_{Pmax} = 1.8 \cdot 10^9$ Pa,

Jinghong's Model

$$\beta_e(P) = \frac{\beta(1+10^{-5}P)^{\left(1+\frac{1}{\gamma}\right)}}{(1+10^{-5}P)^{\left(1+\frac{1}{\gamma}\right)} + 10^{-5}R(1-c_1P)\left(\frac{\beta}{\gamma} - 10^5 - P\right)} \tag{3.9}$$

with: $\beta = 1.701 \cdot 10^9$ Pa,
$\gamma = 1.4$,
$c_1 = -9.307 \cdot 10^{-6}$,
$R = 4 \cdot 10^{-5}$.

Lee's Model

$$\beta_e(P) = 0.5 \cdot \beta \cdot \log\left[100 \cdot \left(0.9\frac{P}{P_{max}} + 0.03\right)\right] \tag{3.10}$$

with: $\beta = 1.8 \cdot 10^9$ Pa,
$P_{max} = 2.8 \cdot 10^7$ Pa,
P in Pa.

Eggerth's Model

Compressibility value c:

$$c = \frac{1}{\beta_e} \tag{3.11}$$

For oil HLP 36 Table 3.1 gives the parameters for a model according to equation 3.12

$$c = C_1 + C_2\left(\frac{P}{P_0}\right)^{\lambda} \tag{3.12}$$

with: $P_0 = 10^6$ Pa and pressure P between $0 < P < 5$ MPa.

Table 3.1 Temperature dependent parameters of Eggerth's compressibility model

Temperature	C_1	C_2	λ
20 °C	$4.943 \cdot 10^{-10}$ m²/N	$1.9540 \cdot 10^{-10}$ m²/N	-1.480
50 °C	$5.469 \cdot 10^{-10}$ m²/N	$3.2785 \cdot 10^{-10}$ m²/N	-1.258
90 °C	$5.762 \cdot 10^{-10}$ m²/N	$4.7750 \cdot 10^{-10}$ m²/N	-1.100

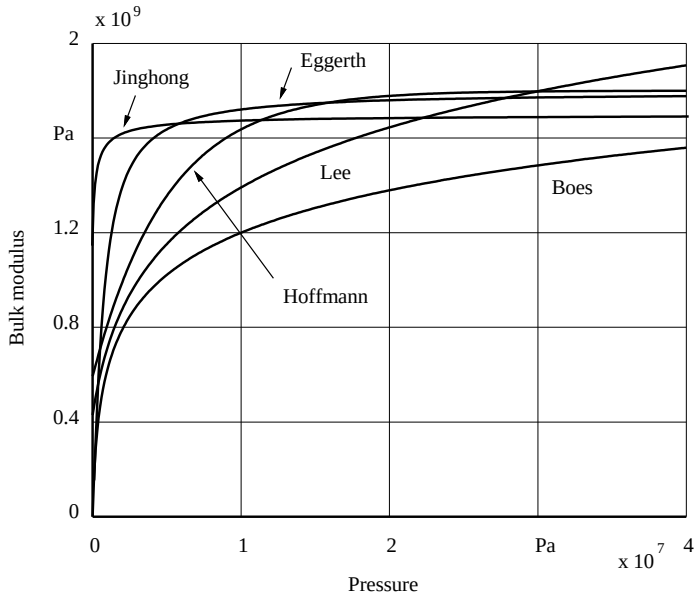

Figure 3.3 Comparison of models of effective bulk modulus

There is one side effect of the compressibility that is not included in the library models: the volume that leaves the high pressure port of a pump is smaller than the volume entering at the low pressure suction port. If the pressure differential is $4 \cdot 10^7$ Pa this volume difference is about 2 %.

3.1.2 Viscosity

The *absolute* or *dynamic viscosity* μ (mu) is a measure of the shearing stress τ between a stationary plate and a parallel moving plate, see Figure 3.4. Assuming a Newtonian fluid, the viscosity is independent of shear rate. Many calculations require the ratio of the absolute viscosity μ to the oil mass density ρ. This ratio is called *kinematic viscosity* ν (nu).

$$\tau = \frac{F}{L \cdot B} = \mu \frac{dw}{dy} = \nu\rho \frac{dw}{dy} \tag{3.13}$$

with: τ shearing stress,
F pulling force,
L length of plate,
B width of plate,
μ dynamic viscosity,
ν kinematic viscosity,
ρ oil mass density, mass per unit volume,
w flow velocity,
y distance to the stationary plate.

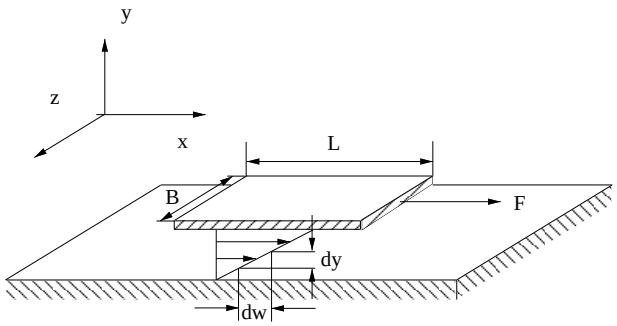

Figure 3.4 Velocity gradient in fluid between a stationary plate and a parallel moving plate

The SI-Unit for dynamic viscosity μ is Pa · s and m²/s for kinematic viscosity ν. Table 3.2 gives conversion factors to older units and typical values of oil HLP 68 that is used for mobile applications.

Table 3.2 Units and values of the viscosity of HLP 68

	Unit	Value for HLP 68 at 60 °C
dynamic viscosity μ	1 cP = 1 mPa · s = 10^{-3} Pa · s	0.025 Pa · s
kinematic viscosity ν	1 cSt = 1 mm^2 / s = 10^{-6} m^2 / s	$27 \cdot 10^{-6}$ m^2/s

The oil temperature has a great influence on the viscosity. At 20 °C the viscosity changes 7 % with 1 °C, at 100 °C still 2 % per 1 °C. Figure 3.5 show the kinematic viscosity as a function of temperature.

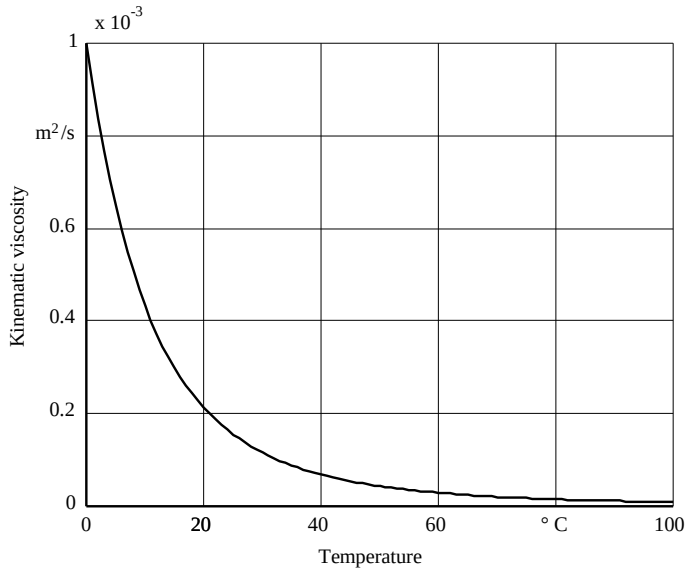

Figure 3.5 Kinematic viscosity as a function of temperature, oil HLP 68

If the kinematic viscosity is plotted as a function of temperature, with the absolute temperature in K on the x-axis in a logarithmic scale, and the term ln(ln(ν+0.8)) on the y-axis, straight lines result (see e.g. DIN 51 563). The slope of the straight lines is given by:

$$m = \frac{W_1 - W_2}{\ln(T_2) - \ln(T_1)} \tag{3.14}$$

with: $W_i = \ln(\ln(\nu_i + 0.8))$,
ν_i Value of kinematic viscosity in mm²/s at temperature T_i,
T_i temperature in K.

The kinematic viscosity at an arbitrary temperature T_x can be calculated by:

$$W_X = m\,(ln(T_1) + \ln(T_X)) + W_1 \tag{3.15}$$

At very low temperatures the viscosity changes drastically and equation 3.15 is no longer valid. Another important parameter is the pressure. The viscosity increases with increasing pressure. This is very important for hydrostatic bearings because the load capacity goes up when the load increases. This effect can be described by:

$$\mu(P) = \mu_0 e^{\alpha P} \tag{3.16}$$

with: μ_0 viscosity at atmospheric pressure,
α viscosity-pressure-coefficient.

The coefficient α depends on the temperature. Table 3.3 give values for a mineral oil HLP 32 (Ivantysyn and Ivantysynova 1993). Johnson (2000) has a long list of the viscosity of serval brands of hydraulic oil.

Table 3.3 Viscosity-pressure-coefficient for oil HLP 32

Temperature in °C	0	10	20	30	40	50	60	70	80	90	100
α in 10^{-8} Pa^{-1}	3.268	2.900	2.595	2.339	2.121	1.933	1.770	1.626	1.499	1.385	1.283

The viscosity of oil leads to *viscous drag*. This can be used to model the force resisting the motion of a spool. Assuming an annular clearance between spool and bore the viscous drag can be described by:

$$F_{Drag} = \frac{v\mu\pi DL}{S} \tag{3.17}$$

with: F_{Drag} viscous friction force,
v spool velocity,
μ absolute viscosity,
D inner diameter of bore,
L spool length,
S clearance between spool and bore.

The model is valid, if:

$$Re = \frac{S|v|}{\nu} < 1000\,. \tag{3.18}$$

3.1.3 Inductance

Newton‘s second law gives the force F to accelerate a mass m:

$$F = m \cdot a = m\frac{dv}{dt}. \tag{3.19}$$

Equation 3.19 is analogous to the expression for voltage drop u across an inductance:

$$u = L\frac{di}{dt}. \tag{3.20}$$

By analogy the inductance L_{th} of a fluid is defined as:

$$L_{th} = \frac{\Delta P}{\frac{dQ}{dt}}. \tag{3.21}$$

Assuming a one-dimensional flow, where all fluid particles have identical velocities at any instance of time, and a tube length *l*, an interior area A and a fluid density ρ and combining equation 3.19 and 3.21 leads to the theoretical inductance L_{th}:

$$L_{th} = \frac{\Delta P}{\frac{dQ}{dt}} = \frac{\rho\, l}{A}\ . \tag{3.22}$$

The inductance plays an important role for high frequency changes, e. g. switching of *fast* valves. When modeling typical valves it is not necessary to include the inductance in the model (Ramdén 1999).

If oil has to pass through a small hole or slot into a larger container the measured inductance L_{re} is higher than calculated by equation 3.21. For sharp-edged holes with 0.5 mm < D < 1 mm, 1 < *l*/D < 20 Tsung (1991) found:

$$L_{re} = L_{th}\left(1.54 + 5\frac{l}{D}e^{\frac{-l}{D}}\right) \tag{3.23}$$

with: D inner diameter,
l length.

Lau et al. (1995) and Johnston (2002) give formulas to calculate the inductance of the oil column in orifices in the freuqency domain.

To derive the theoretical inductance a uniform velocity profile was assumed. But the velocity profile for stationary laminar flow is not uniform but parabolic (Doebelin 1972), given by:

$$w(r) = w_{max}\left(1 - \left(\frac{r}{R}\right)^2\right) \tag{3.24}$$

with: R inner radius.

The mean velocity w_{mean} for this velocity profile is given by:

$$w_{mean} = \frac{1}{2} w_{max} \cdot \tag{3.25}$$

The kinetic energy is:

$$E_{kin} = \frac{4}{3} \rho \pi R^2 w_{mean}^2 \cdot \tag{3.26}$$

The inductance therefore has an (upper) value of:

$$L_{max} = \frac{4}{3} \rho \frac{l}{A} . \tag{3.27}$$

If the flow is turbulent or laminar with a harmonic excitation, equation 3.24 is no longer valid. Figure 3.6 show the velocity profiles for turbulent flow or laminar flow with harmonic excitation (Ham 1982). As frequency increases or the flow becomes turbulent the velocity profile becomes more square and the correct mass approaches $\rho \cdot A \cdot l$. The flow mode dependent value L_{re} of the inductance is therefore bounded by:

$$\rho \frac{l}{A} \le L_{re} \le \frac{4}{3} \rho \frac{l}{A} \tag{3.28}$$

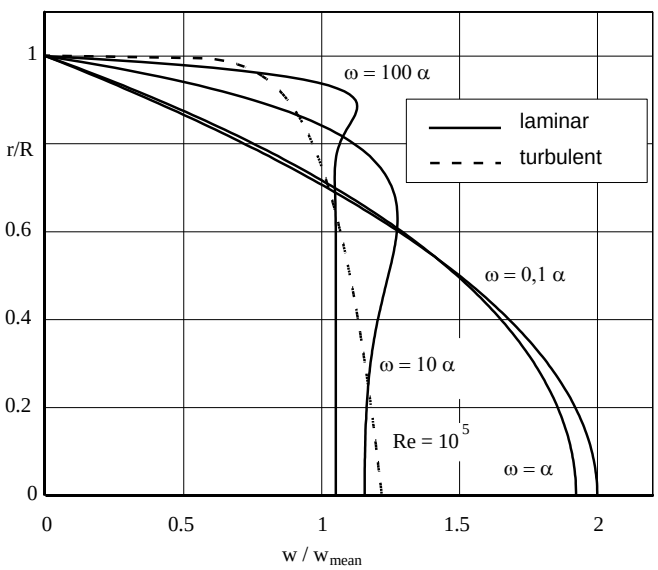

Figure 3.6 Velocity profile as a function of flow mode

The frequency in Figure 3.6 is normalized by:

$$\alpha = \frac{8\nu}{R^2} \tag{3.29}$$

with: ν kinematic viscosity,
R tube radius.

3.2 Pumps

Pumps are needed to convert mechanical energy into hydraulic energy and vice versa. There are two different types: Turbine pumps, impeller pumps and propeller pumps which are rarely found in hydraulic power systems. Most power systems require *positive displacement pumps*. At high pressures, piston pumps are often preferred to gear or vane pumps. These pumps should be modelled as flow sources because they displace the fluid with pistons, vanes or gears. This means they *produce a flow* while the pressure at the outlet port builds up according to the resistance the oil has to pass on its way to the tank.

3.2.1 Theoretical Displacement, Power Flow of an Ideal Pump

For an *ideal pump* there is only one equation to describe the input torque τ and the delivered flow rate Q, respectively:

$$\tau = \frac{D_{Pump} \cdot \Delta P}{2\pi} \tag{3.30}$$

with: τ required input torque,
D_{Pump} volumetric displacement,
ΔP pump differential pressure.

$$Q = D_{Pump} \cdot n \tag{3.31}$$

with: Q flow rate,
D_{Pump} volumetric displacement,
n shaft speed in rpm.

The theoretical displacement D_{Pump} of a gear or piston pump is given by its displacement volume *per revolution*. Sometimes the displacement is given in volume / rad. For mobile systems typical values vary from $12 \cdot 10^{-6}$ m^3 for small gear pumps up to $160 \cdot 10^{-6}$ m^3 for piston pumps.

3.2.2 Efficiency

In all real pumps there is a flow from the high pressure port to the low pressure port called *internal* or *cross-port* leakage. There is also an *external* leakage from each pump chamber past the pistons to the case drain. For swash plate-type axial piston pumps the external leakage is usually smaller than the internal leakage.

The internal and external leakage reduces the theoretical flow rate. This reduction is described by the *volumetric efficiency*, η_{vol}:

$$Q_{port} = \eta_{vol} \cdot Q_{theo} . \tag{3.32}$$

Due to friction there are mechanical losses in a pump. They result from bearings, seals and friction at rotating parts. Due to these losses the input torque must be higher than the theoretical values. The torque loss is described by the *torque efficiency*, η_{tor}:

$$\tau = \frac{D_{pump} \cdot \Delta P}{2\pi\eta_{tor}} . \tag{3.33}$$

The *over-all efficiency* η is defined as the ratio of actual hydraulic horsepower output to the mechanical horsepower supplied. The over-all efficiency is the product of volumetric and torque efficiencies:

$$\eta = \eta_{vol}\eta_{tor} \tag{3.34}$$

A comparison of the efficiencies of piston, gear and vanes pumps as a function of viscosity, pressure and speed is given by Yeaple (1990).

3.2.3 Modeling the Losses

Figure 3.7 shows the total efficiency of an axial piston pump with a displacement volume of 43 cm^3 as a function of speed and pressure. Figure 3.8 gives a contour plot of Figure 3.7. The figure gives also the necessary input torque and input horsepower.

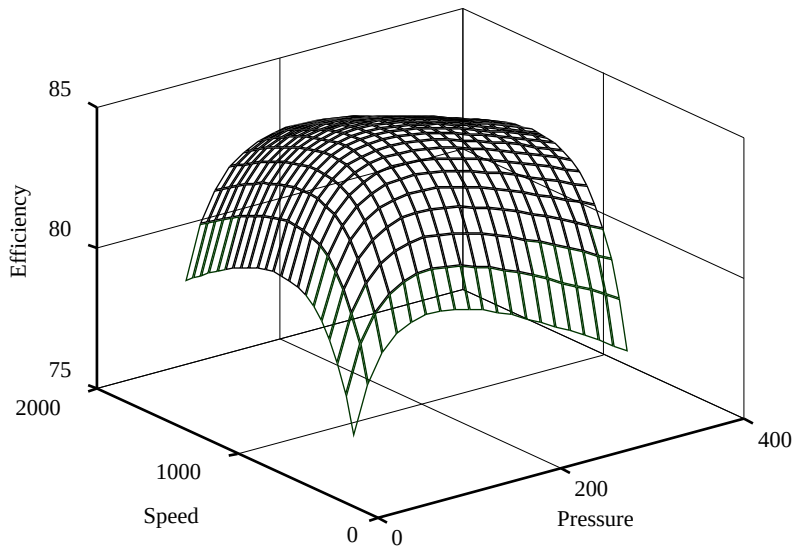

Figure 3.7 Total efficiency as a function of the speed and pressure of an axial piston pump, D = 43 cm^3

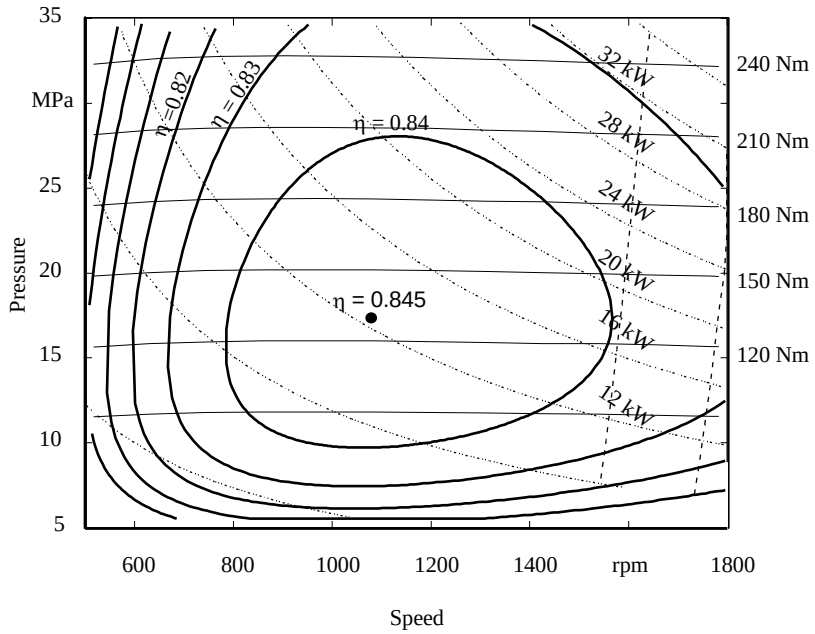

Figure 3.8 Contour plot of Figure 3.7.

The shape of Figure 3.7 cannot be easily described by geometric bodies or simple algebraic functions. A number of models has therefore been proposed to describe the volumetric and power losses of pumps. There are *abstract mathematical models* that fit algebraic equations to measured data. The parameters of these models have no physical meaning. On the other hand there are more or less elaborate models that try to describe the actual leakage flows and the friction losses in a pump. The losses depend also on the viscosity, i. e. the fluid type and the temperature. Most pump manufacturers give plots of the power losses or efficiencies but usually no mathematical models.

3.2.4 Physically Motivated Models

One of the well-known models was developed by Wilson (1948). This model assumes laminar leakage in the pump.

$$Q_{loss} = C_{SV} \frac{V\Delta P}{2\pi\mu} \tag{3.35}$$

Wilson assumed that there are three basic forms of friction responsible for torque losses in axial piston pumps. These are dry friction, viscous friction and constant friction. Equation 3.36 shows that the dry friction, coefficient C_f, is assumed to be proportional to the load pressure, but independent of the sliding velocity. The viscous friction with coefficient C_d is proportional to viscosity and speed but independent of the pump pressure. The constant term τ_c in Wilson‘s model represents for example seal friction.

$$\tau = \varepsilon \frac{D\Delta P}{2\pi} + C_f \frac{D\Delta P}{2\pi} + C_d \mu D n + \tau_c \tag{3.36}$$

For a gerotor motor with a displacement volume of D = 80.46 cm³ Conrad et al. (1993) give the following coefficients:

C_{sv} = 5.6148e-7
C_{pv} = 9.4792e-2
C_{vv} = 6.3688e2
M_c = 5.7898e0

Schlösser (1968) also used physical reasoning to model the losses in a pump:

$$Q_{loss} = A\Delta P + B\sqrt{\Delta P} = Q_{SV} + Q_{ST} \tag{3.37}$$

with: $Q_{SV} = C_{SV}\frac{\Delta P}{2\pi\eta}D_{th}$ and $Q_{ST} = C_{ST}\sqrt{\frac{2\Delta P}{\rho}}\sqrt[3]{\left[\frac{D_{th}}{2\pi}\right]^2}$.

The torque losses are given by:

$$\tau_{loss} = C\Delta P + D\omega + E\omega^2 + F = \tau_p + \tau_v + \tau_T + \tau_c . \tag{3.38}$$

with: $\tau_p = C_{PV}\frac{\Delta P D_{th}}{2\pi}$, $\tau_v = C_{VV}\frac{\eta\omega D_{th}}{2\pi}$, $\tau_T = C_{TV}\frac{\rho\omega^2}{2}\sqrt[3]{\left[\frac{D_{th}}{2\pi}\right]^5}$, $\tau_C = \text{const.} \approx 0$.

Schlösser (1968) gives minimum and maximum values for this model for pumps with a theoretical displacement D_{th} between 10 and 50 cm^3. The interesting point is that the values vary between the different pump types considerably. This shows that the characteristic behaviour of different pump types is different.

Table 3.4 Parameters for different pump types

	C_{SV}	C_{ST}	C_{PV}	C_{VV}	C_{TV}
Screw pumps	$45 \cdot 10^{-8}$	$38 \cdot 10^{-4}$	0.06	$0.4 \cdot 10^5$	1400
	$10 \cdot 10^{-8}$	$8 \cdot 10^{-4}$	0.03	$0.2 \cdot 10^5$	500
Gear pumps	$40 \cdot 10^{-8}$	$30 \cdot 10^{-4}$	0.06	$0.6 \cdot 10^5$	270
	$2 \cdot 10^{-8}$	$2 \cdot 10^{-4}$	0.03	$0.3 \cdot 10^5$	60
Vane pumps	$4.3 \cdot 10^{-8}$	$9.0 \cdot 10^{-4}$	0.30	$1.6 \cdot 10^5$	60
	$3.0 \cdot 10^{-8}$	$3.5 \cdot 10^{-4}$	0.02	$0.4 \cdot 10^5$	10
Axial piston pumps	$2.0 \cdot 10^{-8}$	$2.8 \cdot 10^{-4}$	0.10	$2.0 \cdot 10^5$	250
	$0.5 \cdot 10^{-8}$	$0.5 \cdot 10^{-4}$	0.01	$0.2 \cdot 10^5$	100
Radial piston pumps			0.08	$0.8 \cdot 10^5$	50
			0.01	$0.2 \cdot 10^5$	10

For pumps the overall efficiency is given by:

$$\eta = \frac{1 - \frac{C_{SV}}{\lambda} - \frac{C_{ST}}{\sigma}}{1 + C_{PV} + \lambda C_{VV} + \sigma^2 C_{TV}} \tag{3.39}$$

with the non dimensional numbers λ and σ:

$$\lambda = \frac{\omega \eta}{\Delta P} = \frac{\text{viscous forces}}{\text{hydrostatic forces}}, \tag{3.40}$$

$$\sigma = \omega \sqrt[3]{\frac{V_{th}}{2\pi}} \sqrt{\frac{\rho}{2\Delta P}} = \sqrt{\frac{\text{inertial forces}}{\text{hydrostatic forces}}}. \tag{3.41}$$

For motors the overall efficiency is given by:

$$\eta = \frac{1 - C_{PV} - \lambda C_{VV} - \sigma^2 C_{TV}}{1 + \frac{C_{SV}}{\lambda} + \frac{C_{ST}}{\sigma}}. \tag{3.42}$$

3.2.5 Abstract Mathematical Models

To describe the efficiency of a pump, *abstract mathematical models* can also be used. These models are not derived by describing the actual reasons of the losses, e. g. speed depending friction or pressure depending leakage, but by fitting the coefficients of a given equation to measured data. Often two equations are used. One to compute the mechanical power loss P_{Lmech} and the other for the volumetric power loss P_{Lvol}. The equation may look like this (Ivantysyn and Ivantysynova 1993)

$$\begin{aligned} P_{Lvol} = {} & A_1 + A_2 \cdot \alpha + A_3 \cdot \alpha^2 + (A_4 + A_5 \cdot \alpha + A_6 \cdot \alpha^2) \cdot n \\ & + (A_7 + A_8 \cdot \alpha + A_9 \cdot \alpha^2) \cdot n^2 + [A_{10} + A_{11} \cdot \alpha + A_{12} \cdot \alpha^2 \\ & + (A_{13} + A_{14} \cdot \alpha + A_{15} \cdot \alpha^2) \cdot n \\ & + (A_{16} + A_{17} \cdot \alpha + A_{18} \cdot \alpha^2) \cdot n^2] \cdot P \\ & + [A_{19} + A_{20} \cdot \alpha + A_{21} \cdot \alpha^2 + (A_{22} + A_{23} \cdot \alpha + A_{24} \cdot \alpha^2) \cdot n \\ & + (A_{25} + A_{26} \cdot \alpha + A_{27} \cdot \alpha^2) \cdot n^2] \cdot P^2 \end{aligned} \tag{3.43}$$

with: α angle of the swash plate,
n speed of rotation,
P pressure.

For axial piston pumps it often suffices to use only the linear dependency of the speed n and the angle α. To model the torque losses an equivalent polynomial is needed. Another type of equation is:

$$P_{Lmech}(P, n, \alpha) = \sum_{i=1}^{l} k_{i_1} \left[P^{k_{i_2}} + k_{i_3}\right]\left[n^{k_{i_4}} + k_{i_5}\right]\left[\alpha^{k_{i_6}} + k_{i_7}\right]. \tag{3.44}$$

The number of terms used is given by *l*. Suitable values range from 3 to 10 where higher values usually give better models. Heumann (1987) proposed the following model for variable displacement swash plate type pumps:

Delivered *flow rate Q in l/min*:

$$Q = c_{1q} \cdot n \cdot h + c_{2q} \cdot n \cdot \Delta P^2 \cdot h + c_{3q} \cdot n \cdot \Delta P + c_{4q} \cdot \Delta P \cdot h / n \,, \tag{3.45}$$

required input *horsepower P in kW:*

$$P = c_{1p} \cdot n \cdot h + c_{2p} \cdot n \cdot \Delta P \cdot h + c_{3p} \cdot n \cdot \Delta P \tag{3.46}$$

with: n in 1/min,
ΔP in MPa,
$h = D_{eff} / D_{max}$,
D_{eff} effective displacement volume of variable displacement pump,
D_{max} maximum displacement volume.

Parameters for variable displacement swash plate type pumps, equation 3.46, are given in Table 3.5.

Table 3.5 Parameters for Heumann's model for axial piston pumps

D [cm^3]	C_{1q}	C_{2q}	C_{3q}	C_{4q}	C_{1p}	C_{2p}	C_{3p}
2.0e+2	1.7538e-1	-9.35e-6	-1.898e-4	-1.13e+1	2.098e-3	2.91390e-3	6.240e-5
5.0e+2	4.2953e-1	-2.85e-5	-4.653e-4	-1.50e+1	3.752e-3	6.81720e-3	3.252e-4
8.0e+2	7.2818e-1	-3.75e-5	-7.853e-4	-1.92e+2	7.917e-3	1.12033e-2	6.715e-4
5.0e+1	4.8429e-2	-2.30e-8	-6.476e-5	-1.30e+1	1.880e-4	7.27800e-4	6.730e-5
1.0e+2	1.0044e-1	-1.80e-8	-2.140e-4	-1.30e+2	2.890e-4	1.48260e-3	1.291e-4
5.0e+1	4.8603e-2	-2.08e-7	-7.582e-5	-2.0000	9.030e-4	7.61700e-4	1.260e-5
6.3e+1	7.1395e-2	-6.65e-7	-9.490e-5	-2.47e+1	1.314e-3	1.17300e-3	3.540e-5
1.0e+2	1.0413e-1	-1.21e-7	-1.226e-4	-1.37e+1	2.757e-3	1.57730e-3	9.110e-5

The model for gear pumps is given by:

$$Q = c_{1q} \cdot n + c_{2q} \cdot n \cdot \Delta P + c_{3q} \cdot \Delta P + c_{4q} \cdot \Delta P / n \,, \tag{3.47}$$

$$P = c_{1p} \cdot n + c_{2p} \cdot n \cdot \Delta P \,. \tag{3.48}$$

Parameters for gear pumps, equations 3.47 and 3.48 , are given in Table 3.6.

Table 3.6 Parameters for Heumann's model for gear pumps

D [cm^3]	C_{1q}	C_{2q}	C_{3q}	C_{4q}	C_{1p}	C_{2p}
1.25	1.302e-3	-2.00e-7	-2.920e-2	-1.5000	5.80e-5	2.44e-5
2.00	1.981e-3	-5.70e-6	-1.200e-3	-7.56e+1	1.08e-4	3.54e-5
3.20	3.009e-3	-1.59e-5	-1.040e-2	-1.90e+1	9.80e-5	5.48e-5
5.00	4.745e-3	-1.17e-5	-4.310e-2	-1.26e+1	1.31e-4	8.33e-5
8.00	8.020e-3	-1.78e-5	-1.001e-1	-8.2000	2.79e-4	1.401e-4
1.25e+1	1.1826e-2	-1.20e-6	-1.090e-1	-1.570e+1	2.27e-4	2.307e-4
2.00e+1	1.8192e-2	-2.93e-5	-1.430e-1	-5.510e+1	3.80e-4	3.501e-4
3.20e+1	3.0196e-2	-5.45e-5	-2.272e-1	-1.231e+2	1.068e-3	5.296e-4
5.00e+1	4.5972e-2	-1.84e-4	-2.726e-1	-6.920e+1	7.540e-4	8.961e-4
8.00e+1	7.0201e-2	-1.50e-5	-8.500e-1	-6.000e+1	2.389e-3	1.266e-3

Conrad et al. (1993) give the following model for effective flow rate Q_E and the torque τ_E of gerotor type motors.

$$Q_E = A_{00} + A_{10}\Delta P + A_{01}n + A_{20}\Delta P^2 + A_{02}n^2 + A_{11}\Delta Pn \tag{3.3.49}$$

$$\tau_E = B_{00} + B_{10}\Delta P + B_{01}n + B_{20}\Delta P^2 + B_{02}n^2 + B_{11}\Delta Pn \tag{3.50}$$

They used two sets of measured data to determine two sets of coefficients by a least square approach, see Table 3.7 and Table 3.8. The motor was a D = 80.46 cm³ gerotor motor. The modeling error was much smaller than with Wilson‘s model. More models are given in (Huhtala and Vilenius 1997).

Table 3.7 Coefficients of flow models

Coefficient	Small data-set model	Large data-set model
A00	2.3568e-2	1.0482e-1
A10	-3.6810e-3	-3.1476e-3
A01	8.0040e-2	8.0232e-2
A20	2.110e-4	2.2340e-4
A02	7.9515e-7	2.7568e-7
A11	-9.9693e-7	2.0684e-6

Table 3.8 Coefficients of torque models

Coefficient	Small data-set model	Large data-set model
B00	2.9459e0	7.7526e-1
B10	1.1001e0	1.1611e0
B01	-4.7932e-3	-2.5872e-3
B20	1.6019e-4	-2.0801e-4
B02	-3.1621e-5	-3.31163e-5
B11	1.5056e-5	-2.0430e-6

3.2.6 Models for Time Domain Simulation

The models in Sects. 3.2.4 and 3.2.5 can describe the behaviour of pumps or motors very accurately. Unfortunately they require a number of parameters that are not readily available. They also need a considerable amount of computing time. For many simulation studies it is therefore better to use a simple, Wilson type model. The required parameters for this model have a physical meaning (e. g. internal or external conductance) and can be estimated from simple measurements or manufacturer data sheets. Usually the overall error of this approach won‘t be greater than the uncertainty of a number of parameters used in that simulation run.

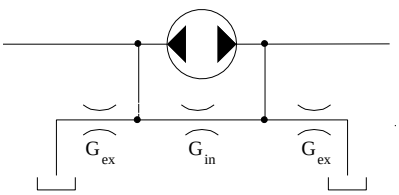

Figure 3.9 Simulation model

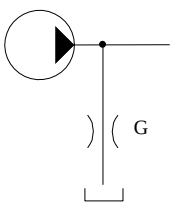

Figure 3.10 Simulation model

The internal conductance G_{in} is often much higher than the external conductance G_{ex} (G_{in} = 2 ... 6 G_{ex}). A rough estimate of the total conductance G is given by:

Axial piston pumps, $25 \cdot 10^{-6}\ m^3 < D_{Pump} < 200 \cdot 10^{-6}\ m^3$

$$G = 8 \cdot 10^{-8} \cdot D_{Pump} - 1.2 \cdot 10^{-12} \qquad (3.51)$$

with: G conductance in $m^3 / (s \cdot Pa)$,
D_{Pump} volumetric displacement in m^3.

Gear pumps with

22 cm^3: $G = 5 \cdot 10^{-13}\ m^3/(s \cdot Pa)$; 36 cm^3: $G = 6 \cdot 10^{-13}\ m^3/(s \cdot Pa)$ ... $2 \cdot 10^{-12}\ m^3/(s \cdot Pa)$.

An appropriate model for the overall torque losses is given by:

$$\tau_{loss} = c_c + c_p \cdot P + c_n \cdot n \ . \qquad (3.52)$$

Figure 3.11 shows the measured and modelled torque losses of a gear pump, Table 3.9 gives typical values for conductance and torque losses of axial piston pumps.

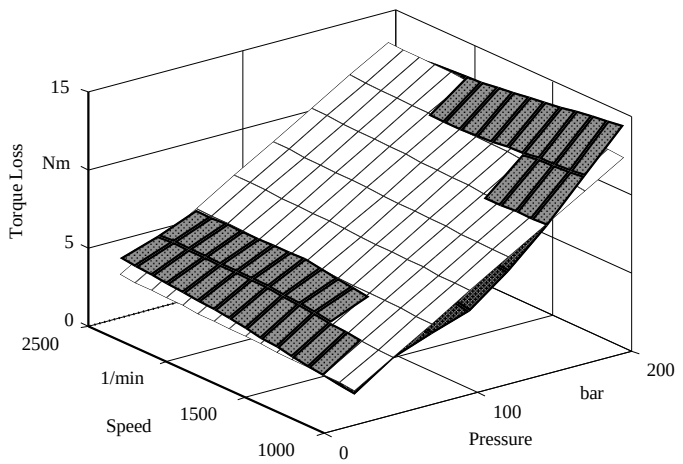

Figure 3.11 Torque loss of a gear pump, measurement (grey) and model (white)

Table 3.9 Volume and torque losses of axial piston pumps (c : pump for closed circuit hydrostatic transmission)

Volumetric displacement		Conductance	Constant Friction	Pressure dependent friction	Speed dependent friction
D in m^3		G [$m^3 / (s \cdot Pa)$]	c_c [Nm]	c_p [Nm / Pa]	c_n [Nm / (rad/s)]
$30 \cdot 10^{-6}$		1.492e-012	8.4088e+000	6.1968e-007	5.5188e-003
$43 \cdot 10^{-6}$		3.466e-012	4.7536e+000	5.5081e-007	4.5970e-003
$50 \cdot 10^{-6}$	c	2.833e-012	1.5121e+000	1.5611e-007	3.4818e-002
$75 \cdot 10^{-6}$		3.112e-012	5.4443e+000	1.4415e-007	3.3614e-002
$100 \cdot 10^{-6}$	c	5.201e-012	3.7904e+000	7.7440e-007	9.2407e-002
$100 \cdot 10^{-6}$		8.017e-012	5.0966e+000	5.4058e-007	-1.3992e-002
$105 \cdot 10^{-6}$	c	5.03e-012	5.1283e+000	3.6003e-007	7.2576e-002
$130 \cdot 10^{-6}$		7.786e-012	-2.5540e-001	1.5723e-007	8.9084e-002
$160 \cdot 10^{-6}$		1.426e-011	7.8071e+000	6.9808e-007	3.9299e-002

Table 3.10 Volume and torque losses of gear pumps

Volumetric displacement	Conductance	Constant friction	Pressure dependent friction	Speed dependent friction
D in m^3	G [m^3 / (s · Pa)]	c_c [Nm]	c_p [Nm / Pa]	c_n [Nm / (rad/s)]
$28 \cdot 10^{-6}$	5.069e-013	6.6740e-001	5.9123e-007	3.4449e-003

3.2.7 Effects of Reduced Intake Pressure

The input pressure of a pump can fall below atmospheric pressure because there are hydraulic losses, occurring in suction pipe, pipe bends and filter. This leads to a decrease of the output flow. Typical allowed values of the inlet pressure are between 15 and 50 kPa below atmospheric pressure. Too low values of the input pressure should be avoided because a decrease of input pressure reduces the mechanical efficiency of the pump. If the input pressure is too low, *cavitation* will occur which can destroy the pump. Cavitation can be heard (strong noise) and felt (vigorous pulsations).

Most manufacturers specify a minimum pressure at the inlet port but they don‘t usually provide curves of the relation between flow and inlet pressure. Some manufacturers specify a maximum pressure at the inlet port of the pump. If the pressure is higher than a specified value, which is usually the atmospheric pressure, the pump delivers a higher output flow. Maximum values of the input pressure are between 0.15 and 0.3 MPa.

For a model of a pump it is necessary to model the decrease of delivered flow when the input pressure decreases especially when the input pressure goes towards the vapour pressure of the fluid. Otherwise the model would output a flow while the input pressure, e. g. the pressure in a lumped volume, is at the vapour pressure and no fluid can flow into the pump. There are several references for the reduction of flow rate as a function of input pressure. Zalka and Látrányi (1971) give measurements for gear pumps, Hibi et al. (1977) for axial piston pumps, Schulz (1979) gives a formula for piston pumps and Yeaple (1990) shows calculations to predict cavitations.

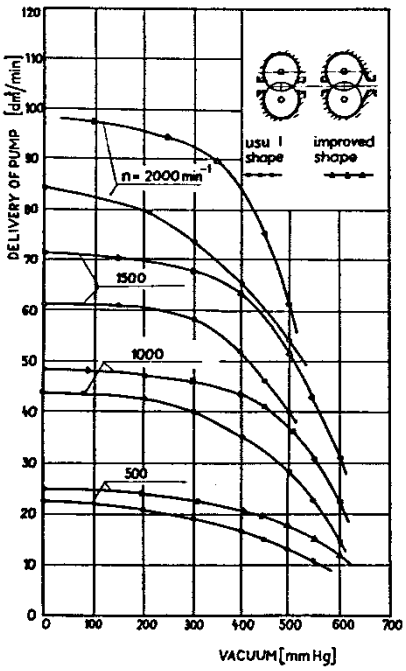

Figure 3.12 Influence of inlet pressure, given as vacuum in [mmHg], on delivered flow of a gear pump for two different shapes of the suction chamber (Zalka and Látrányi 1971)

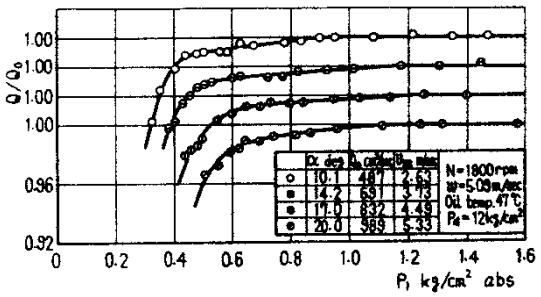

Figure 3.13 Influence of inlet pressure p1 and swash plate angle (of a axial piston pump on delivered flow, Hibi et al. 1977)

Schulz's model to calculate the flow rate reduction as a function of reduced inlet pressure is given by:

$$Q_{eff} = \begin{cases} Q_{nominal} & P_{input} \geq P_{atmosphere} \\ Q_{nominal}\left(1-\left(1-\frac{P_{input}}{P_{atmosphere}}\right)^2\right) & P_{input} < P_{atmosphere} \end{cases} \quad \text{if} \tag{3.53}$$

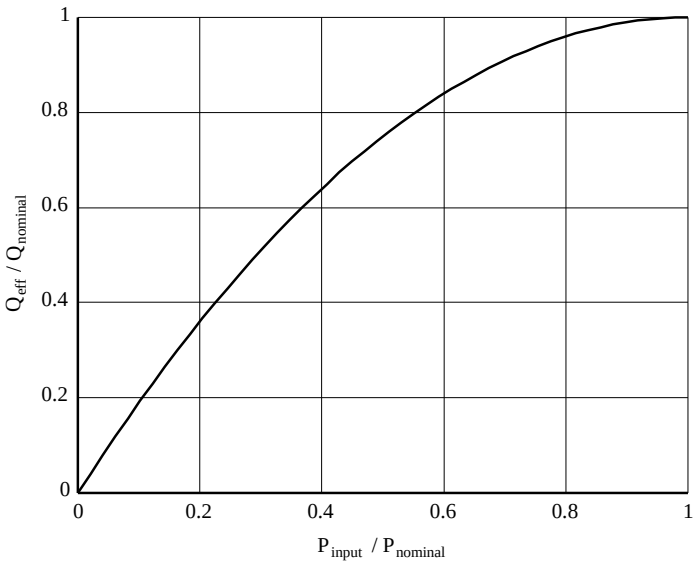

Figure 3.14 Delivered flow rate as a function of decreased input pressure using Schulz's model

Petterson et al. (1993) present results of modeling of cavitation and air release in a fluid power piston pump. Using a similar approach as in this text they state that a "simple model of cavitation only has proven unexpectedly accurate" when the effect on the pump delivery flow is of interest. However they caution that "to assume that this model is valid in another system with different range of dynamics would be hazardous".

3.3 Motors

From a modelling point of view there is no difference between an ideal pump and an ideal motor. Both are used to transform hydraulic energy to mechanical energy and some manufacturers even use the same parts, e. g. cylinder blocks or pistons. The equations of an ideal motor are therefore the same as for an ideal pump:

$$\tau = \frac{D_{Motor} \cdot \Delta P}{2\pi} \tag{3.54}$$

with: τ required input torque,
D_{Motor} volumetric displacement,
ΔP pump differential pressure,

$$Q = D_{Motor} \cdot n \tag{3.55}$$

with: Q flow rate,
D_{Motor} volumetric displacement,
n shaft speed.

The most important difference between a real pump and a real motor is that pumps are usually optimised for one direction of rotation and a certain speed range, e. g. 500 - 1800 revolutions per minute. Motors are used for both directions and all speeds between 0 and the maximum speed. Especially at low speeds the behaviour of a real motor may be different from the ideal model. Considerable pulsation of torque or speed may occur because of the low frequency change of pistons. And there may be a considerable increase in friction. In a closed circuit even the leakage may be important which varies with angular position during each revolution.

For torque loss of motors the same model can be used as for pumps:

$$\tau_{loss} = c_c + c_p \cdot P + c_n \cdot n \tag{3.56}$$

To model the speed dependency of the leakage a second term is added to the pump model:

$$Q_{loss} = G_p \cdot P + G_n \cdot n \tag{3.57}$$

Table 3.11 Volume and torque losses of axial piston motors

Volumetric displacement D [m^3]	Pressure-dependent conductance G_p [$m^3/(s \cdot Pa)$]	Speed dependent conductance G_n [m^3/ rad]	Constant friction c_c [Nm]	Pressure dependent friction c_p [Nm / Pa]	Speed dependent friction c_n [Nm / (rad/s)]
$35 \cdot 10^{-6}$	1.0565e-12	3.0393e-8	-2.8465e-1	3.7989e-7	2.1217e-2
$50 \cdot 10^{-6}$	1.2798e-12	5.9098e-8	4.0394	5.5825e-7	5.5243e-2
$75 \cdot 10^{-6}$	1.5489e-12	3.6158e-8	5.7974	4.7399e-7	4.1173e-2
$75 \cdot 10^{-6}$	1.8576e-12	5.1773e-8	3.4105	4.7974e-7	6.9763e-2

Table 3.12 Volume and torque losses of axial piston motors

Volumetric displacement D	Pressure-dependent conductance G_p	Speed and pressure dependent conductance
$[m^3]$	$[m^3/(s \cdot Pa)]$	$[m^3/(Pa \cdot rad)]$
$50.5 \cdot 10^{-6}$	3.6e-13	1.4e-14
$65.5 \cdot 10^{-6}$	1.2e-12	4.3e-14

3.4 Cylinders

The function of the cylinder in hydraulic systems is to convert the hydraulic energy supplied by the pump into useful work. The model of an ideal, mass less, single-acting, single ended cylinder is given by:

Balance of forces:

$$F = P \cdot A \tag{3.58}$$

with: F force,
P pressure in cylinder chamber,
A piston area.

Continuity:

$$Q = A \cdot \frac{dx}{dt} \tag{3.59}$$

with: Q flow rate,
x position,
dx / dt velocity.

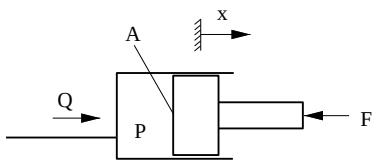

Figure 3.15 Ideal cylinder

However there are more effects that may need modeling:

- Seal friction
- Leakage
- Fluid compressibility and housing compliance
- Pulling rod force

3.4.1 Seal friction

There are many different designs of seals to get a good compromise between friction and leakage. Yeaple (1990) gives an example of a piston rod where the friction force could be reduced from 230 lb to 16 lb while the leakage increased from 0.4 g/1000 cycles to 11 g/1000 cycles. He also quotes a rule of thumb that “friction losses in hydraulic piston and rod seals represent an energy loss of less than 5 %” and shows that these 5 % sum up to 7 million barrels of fuel oil a year in the United States alone.

Armstrong-Hélouvry (1991) gives the following definitions:

Static Friction (Stiction)
The torque (force) necessary to initiate motion from rest. It is often greater than the kinetic friction.

Kinetic friction
(*Coulomb friction*, Dynamic friction)
A friction component that is independent of the magnitude of the velocity.

Viscous Friction
A friction component that is proportional to velocity and, in particular, goes to zero at zero velocity.

Break-Away
The transition from rest (static friction) to motion (kinetic friction).

Break-Away Force (Torque)
The amount of force (torque) required to overcome static friction.

Stribeck Friction or the Stribeck Effect
A friction phenomenon that arises from the use of fluid lubrication and gives rise to decreasing friction with increasing velocity at low velocity.

Negative Viscous Friction
Decreasing friction with increasing velocity. Stribeck friction is an example of negative viscous friction.

When modeling a cylinder the characteristic of the seal friction must be known. For control or servo systems it is important whether the static friction (stiction) is negligible and the speed dependent friction dominates, which means a linear relation between pressure and rod force, or if the high static seal friction gives rise to slip-stick effects at low speeds.

Friction as a function of speed can be modelled with the model *Stop* in the Modelica standard library, see Figure 3.16. This model uses the following equation (Tustin 1947):

$$F_{fric} = f_{prop} v + \left[F_{Coulomb} + F_{Stribeck} e^{-f_{exp}|v|}\right] sign(v) \tag{3.60}$$

with: F_{fric} total friction force,
f_{prop} coefficient of viscous, speed proportional friction,
v velocity,
$F_{Coulomb}$ speed independent, constant Coulomb friction force,
$F_{Stribeck}$ force modeling Stribeck effect,
f_{exp} coefficient of decay for Stribeck force.

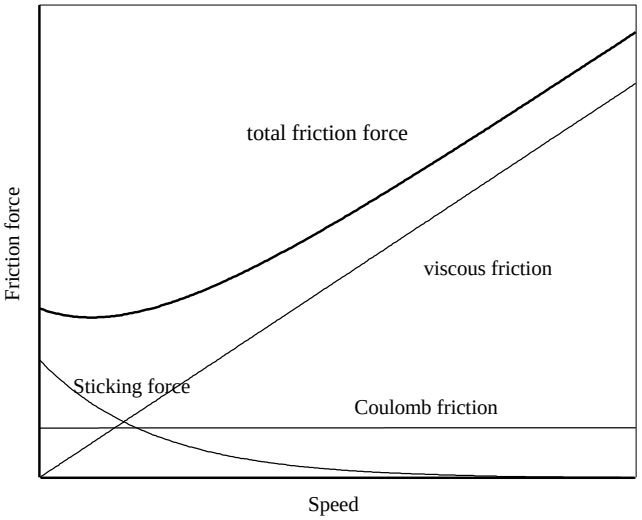

Figure 3.16 Friction model used in Modelica.Mechanics.Translational.Stop

This model is not valid for very small movements, several µm, when motion begins after a rest. It also doesn‘t include the time dependency of the static friction (it builds up after the motion stops) and the lag in friction force after a change in velocity. This time dependency has been observed both on (rubber) O-ring seals and on metal contacts, e. g. roller bearings. These points are significant for machines that have to operate at very low speed or make very small displacements, e. g. industrial robots.

To describe the friction both in single components or in complete drives the model, equation 3.60 has been found adequate. The library model can easily be changed to model different friction characteristics for positive and negative directions. A good introduction to more refined modeling of friction is given by Armstrong-Hélouvry (1991) and Armstrong and Canudas de Wit (1996). If the overall system is very sensitive to the friction (model) detailed measurements are necessary to determine the friction force as a function of speed, pressure, temperature and direction of stroke (extend or return). Figure 3.17 gives some results from Tao (1991). For low speeds there are slip-stick effects shown by upper and lower values of the friction force.

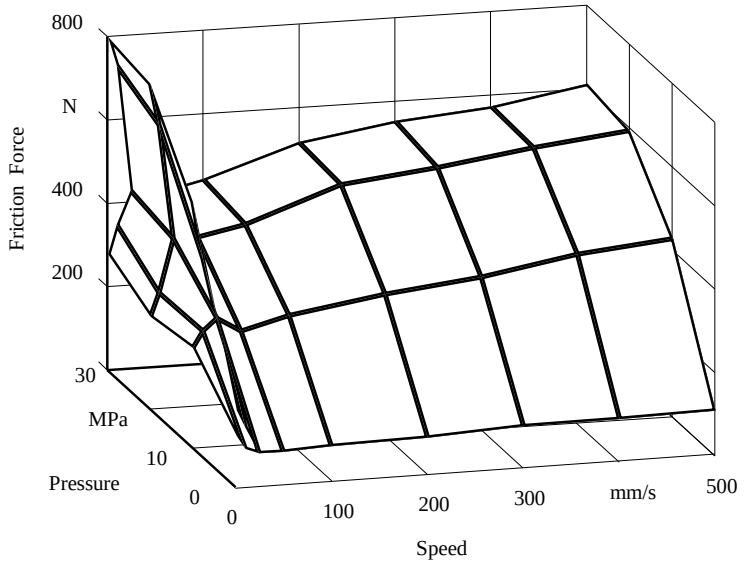

Figure 3.17 Friction force of piston seal as a function of speed and pressure

The 5 % rule of thumb mentioned above indicates that there may be a considerable power loss because of the seal friction. A mechanical efficiency of cylinders η_{mech} can be defined by:

$$\eta_{mech} = \frac{F}{P_1 A_1 - P_2 A_2} \tag{3.61}$$

with: F effective piston force,
P_i pressure in chamber i,
A_i piston area in chamber i.

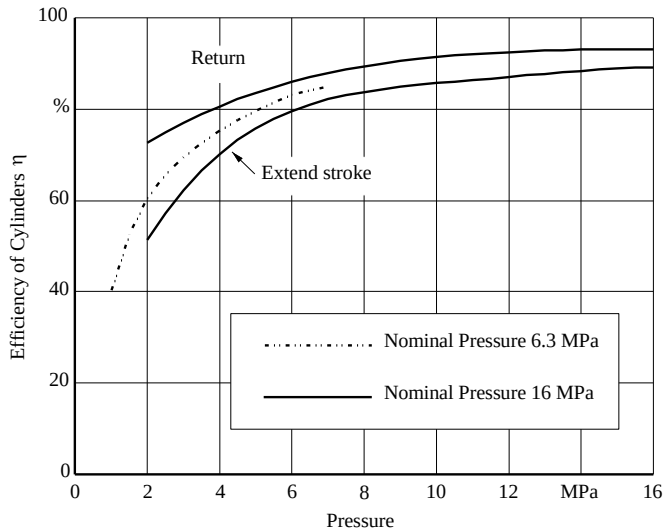

Figure 3.18 Efficiency of two different cylinders as a function of pressure (Will and Ströhl 1985)

3.4.2 Leakage

Some leakage is necessary to assure seal lubrication. In most cases the leakage doesn‘t affect the system behaviour considerably and there is no need to model it. As the leakage flow is always small it can be modelled as laminar flow described by a laminar resistance.

3.4.3 Fluid Compressibility and Housing Compliance

The oil in the cylinder chamber is compressible and the housing is not infinitely stiff. Both effects are modelled by the effective bulk modulus β_{eff}. In the cylinder chamber model Hoffmann‘s model is used.

3.4.4 What happens if there is no flow but the rod is pulled out?

To describe the pressure build up in one cylinder chamber the following differential equation is used:

$$\frac{dP}{dt} = \frac{\beta_{eff}(p)}{A \cdot x(t)} \left(Q(t) - A \frac{dx(t)}{dt} \right) \tag{3.62}$$

with: P pressure in cylinder chamber,
β_{eff} effective bulk modulus of oil, pressure dependent,
A piston area,
x position,
Q flow rate into chamber,
dx / dt velocity.

If there is no flow, Q(t) = 0, and an external force moves the piston in Figure 3.15 to the left, dx/dt becomes smaller than 0, and pressure builds up, dP/dt > 0. If the force moves the piston to the right, however, dx/dt becomes greater than 0 and pressure decreases. But as no negative pressure exists in technical fluids, equation 3.59 is then no longer valid. The pressure remains at a constant value that is given for pure fluids by the vapour pressure. For mineral oil Fassbender (1993) measured a minimum absolute pressure of 25 mbar while the vapour pressure is 0.03 mbar.

Figure 3.19 shows the measured pressure as a function of piston displacement when a rather compliant cylinder is used and the seal permits some air to enter the cylinder camber. The pressure falls from atmospheric pressure (0.1 MPa) to about 0.01 MPa. Figure 3.20 shows the pressure as a function of the relative increase in chamber volume. Even a modest increase in volume of 0.5 % is enough for the pressure to fall to the minimum value, this value doesn‘t change significantly if the volume is further expanded.

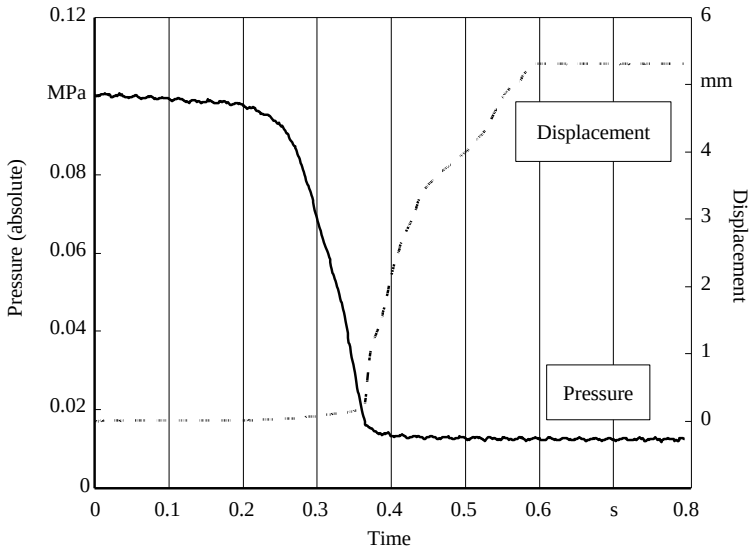

Figure 3.19 Measured pressure and piston displacement as function of time

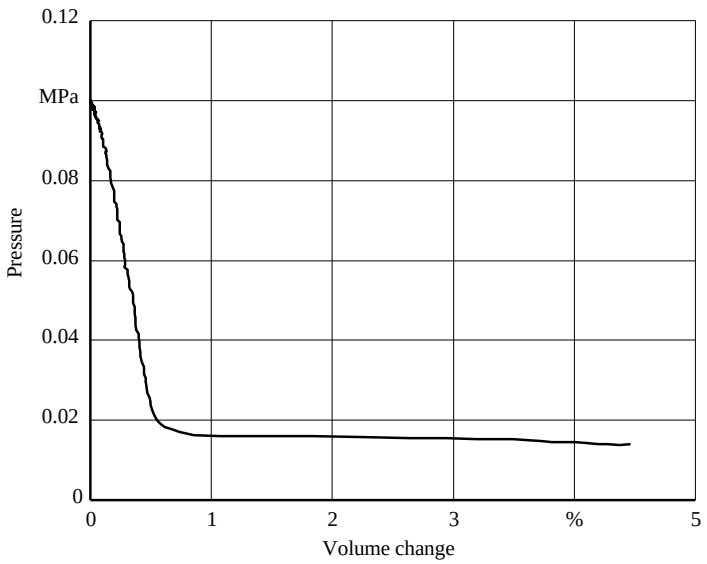

Figure 3.20 Pressure as a function of increased volume

To describe these effects there is a limiter in the library submodel *OilVolume*. It limits the value of the effective bulk modulus to β_{eff}(P=0 Pa).

3.5 Restrictions

While pumps, motors and cylinders are needed to transform mechanical energy to hydraulic energy and vice versa other components are needed to transport, filter and cool the oil or control the flow. When modeling the dynamic response of a system the resistance of these components has to be considered. The dc resistance R is the ratio of pressure drop ΔP, across variable, to volume flow rate Q, through variable:

$$R = \frac{\Delta P}{Q}\bigg|_{\substack{\Delta P=\text{const} \\ Q=\text{const}}} \tag{3.63}$$

The inverse of the resistance is the *conductance* G:

$$G = \frac{1}{R}. \tag{3.64}$$

When modeling flow in a hydraulic system there are two extreme cases:

1. $R = \text{const}$, (3.65)

   which leads to:

   $$Q = \frac{1}{R}\Delta P \sim \Delta P. \tag{3.66}$$

   The linearity between pressure drop and flow characterises *laminar flow*.

2. $R = R(\Delta P, Q)$, (3.67)

   which leads to:

   $$Q \sim \sqrt{\Delta P}. \tag{3.68}$$

   The "square root" dependency characterises *turbulent flow*.

A typical example of laminar flow is the leakage between the ports of a spool valve, an example of turbulent flow the flow through a sharp edged orifice. For a number of (technical) restrictions the flow is not exactly laminar or turbulent but best described by:

$$Q \sim \Delta P^n;\ 0.5 < n < 1. \tag{3.69}$$

The flow mode depends on the restriction, the flow velocity and the kinematic viscosity of the fluid and is characterized by the *Reynolds number* Re:

$$Re = \frac{u\ D}{\nu} \tag{3.70}$$

with: u flow velocity,
D diameter,
ν kinematic viscosity.

If the restriction has no circular cross section the diameter D can be approximated by the *hydraulic diameter*, D_h:

$$D_h = \frac{4A}{S} \tag{3.71}$$

with: D_h hydraulic diameter,
A flow section area,
S flow section perimeter.

If the Reynolds number is less than the critical value Re_{crit} the flow mode is laminar. If the Reynolds number is higher than the critical value Re_{crit}, the flow mode changes from laminar to turbulent. The transition length from laminar to turbulent takes only a length of 10 ... 20 D, while the transition from turbulent flow to laminar is about $0.03 \cdot D \cdot Re$.

Table 3.13 Critical Reynolds number (Ebertshäuser 1993, Findeisen and Findeisen 1994)

Component	Re_{crit}
smooth tube	2200 - 2320
concentric smooth clearance	1000 - 1200
eccentric smooth clearance	1000 - 1050
plug valve	550 - 750
passageway in valves	< 300
metering notch, slot	200 - 400
metering orifice in sliding spool valve	250 - 275
orifice	100 - 200
poppet valve	25 - 100

3.5.1 Calculating Laminar Flow

A typical example of laminar flow is the leakage between two cylinder chambers.

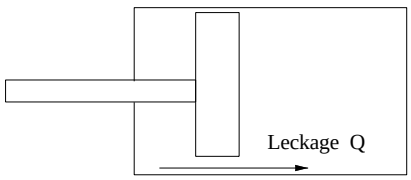

Figure 3.21 Leakage between two cylinder chambers

Table 3.14 Restrictions with laminar flow

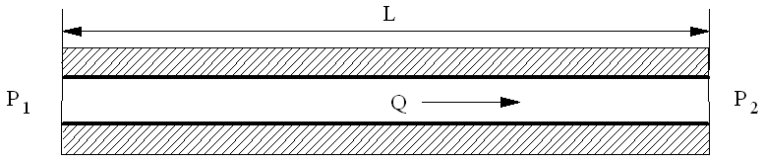

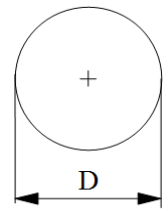 Circular tube.	$Q = \frac{\pi D^4}{128 \mu L}(P_1 - P_2)$ (Merritt 1967) velocity distribution: $u(r) = 2V_{ave}\left(1 - \frac{4r^2}{D^2}\right),\ U_{ave} = \frac{4Q}{\pi D^2}$
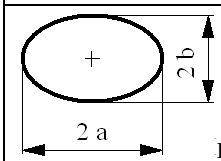 Elliptical tube.	$Q = \frac{\pi a^3 b^3}{4 \mu L (a^2 + b^2)}(P_1 - P_2)$ (Merritt 1967)
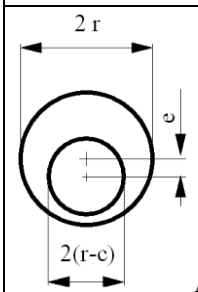 Annulus between cylinder and shaft.	$Q = \frac{\pi r c^3}{6 \mu L}\left[1 + \frac{3}{2}\left(\frac{e}{c}\right)^2\right](P_1 - P_2)$ $c \ll r$ (Merritt 1967) valid for Re < 1000 (see also Ellman et al. 1995) $Q = \pi(r^2 - (r-c)^2)\sqrt{\frac{2(P_1 - P_2)}{\rho}\left(\frac{2c}{\xi L} + \frac{1}{1.5^2}\right)}$ $\xi = \frac{0.316}{\mathrm{Re}^{0.21}} \frac{1}{1 + 0.2\left(\frac{e}{c}\right)}$ *turbulent flow* across annulus (Ellman et al. 1995) see also Bell and Bergelin (1957)
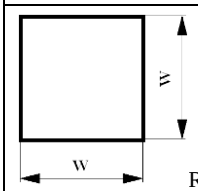 Rectangular passage, square cross section.	$Q = \frac{w^4}{28.4 \mu L}(P_1 - P_2)$ (Merritt 1967)
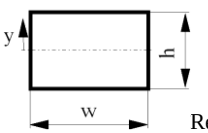 Rectangular passage, rectangular cross section.	$Q = \frac{w h^3}{12 \mu L}\left[1 - \frac{192h}{\pi^5 w}\tanh\frac{\pi w}{2h}\right](P_1 - P_2)$ (Merritt 1967) $u(y) = \frac{3}{2}V_{ave}\left(1 - \left(\frac{2y}{h}\right)^2\right),\ V_{ave} = \frac{Q}{hw}$

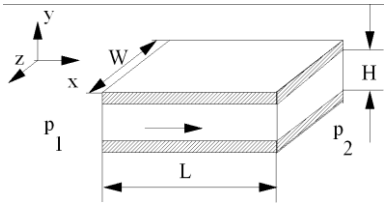	$Q = \frac{wh^3}{12\mu L}(P_1 - P_2)$ (Merritt 1967) Rectangular passage, two parallel plates,rectangular cross section with w >> h
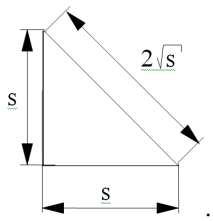	$Q = \frac{s^4}{155.5\mu L}(P_1 - P_2)$ (Merritt 1967) Triangular passage, right angle triangle cross section
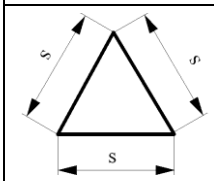	$Q = \frac{s^4}{185\mu L}(P_1 - P_2)$ (Merritt 1967) Triangular passage, equilateral triangle cross section.

Table 3.15 More restrictions with laminar flow

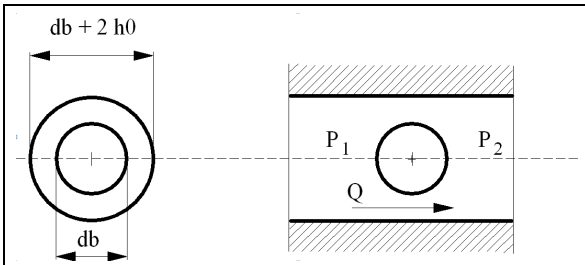	$Q = \frac{2d_b h_0^3}{9\mu\sqrt{h_0 d_b}}(P_1 - P_2)$ $\mathrm{Re} = \frac{2Q}{\pi d_b \nu}$ (Müller 1978) Ball in perfect cylindrical bore, centric.
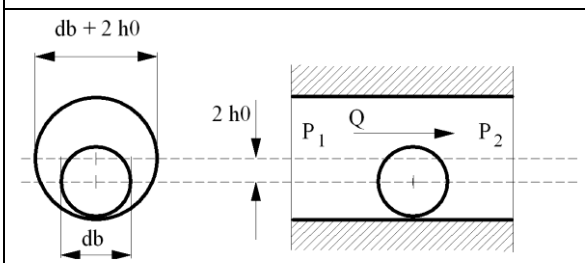	$Q = \frac{36(2h_0)^2\sqrt{2h_0 d_b}}{135\mu\pi}(P_1 - P_2)$ $\mathrm{Re} = \frac{2Q}{\pi d_b \nu}$ (Müller 1978) Ball in perfect cylindrical bore, maximum eccentricity

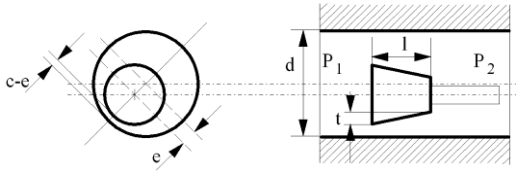

Tapered piston in perfect cylindrical bore

$$T = t/c, E = e/c, L = l/d$$

$$Q = \frac{\pi c^3}{12\mu L}(P_1 - P_2)\left[\frac{2(1+T)^2}{2+T} + \frac{3(2+T)^2}{4} + \frac{T^4}{8(2+T}\left\{\frac{2+T}{(2+T)^2 - 4E^2}\right\} - 1\right]$$

$$\approx \frac{\pi c^3}{12\mu L}(P_1 - P_2)\frac{1 + 1.75T + 1.5(1+0.5T)E^2}{L}$$

(Viersma1980)

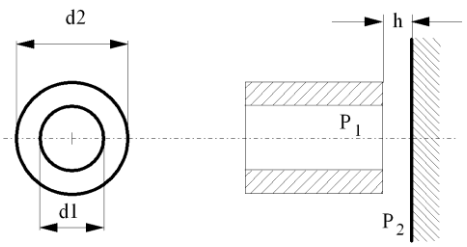

$$Q = \frac{\pi h^3}{6\mu}\frac{P_1 - P_2}{\ln\frac{d_2}{d_1}}$$ (Shute and Turnbull 1962)

3.5.2 Calculating Discharge Coefficient C_d For Turbulent Flow Through Orifices

When modeling turbulent flow through a thin sharp-edged orifice, equation 3.68 is usually written as:

$$Q = A \cdot C_d \sqrt{\frac{2}{\rho}}\sqrt{\Delta P} \tag{3.72}$$

with: Q flow rate through orifice,
$A = \pi D_0^2 / 4$ area,
C_d discharge coefficient,
ρ fluid density,
$\Delta P = P_1 - P_2$ pressure differential.

The value of C_d depends on many parameters, mostly geometry and the condition of the orifice inlet. Even minor deviations from a sharp-edged inlet, such as roughness or a slight local radius, can produce a significant increase in the discharge coefficient (Ohrn et al. 1991). Koivula et al. (1999) state that the oil type has approx. 5 % effect on the discharge coefficient in the range of oils used in their study. And while the equations and coefficients are defined for a constant or slow varying flow they are still valid for pulsating flow of up to 100 Hz (Lau et al. 1995, Schindler 1995, Ramdén 1999).

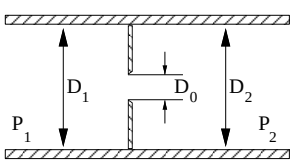

Figure 3.22 Sharp edged

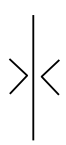

Figure 3.23 Orifice symbol

There are many references that give values of the discharge coefficient C_d in equation 3.71. The simplest model is

$$C_d = \text{const.} \tag{3.73}$$

Values for C_d vary between 0.6 and 1.0 depending on whether the orifice is sharp edged or rounded. Figure 3.24 shows the discharge coefficient as a function of Reynolds number (Merritt 1967, Weule 1974). Discharge characteristics for servo valve orifices are given by McCloy (1968).

All references agree that C_d goes towards zero as the pressure differential goes towards zero, some show an "overshoot" for low Reynolds numbers. Other models for C_d are given by Borutzky (2000) and Wu et al. (2003), who describe measured curves by an empirical formula.

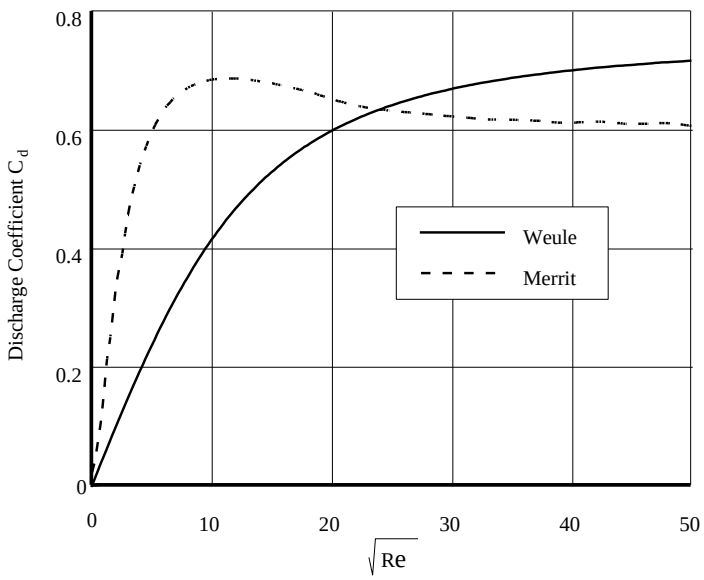

Figure 3.24 Discharge coefficient as a function of Reynolds number

Most orifices are not extremely thin but consist of a short tube, see Figure 3.25.

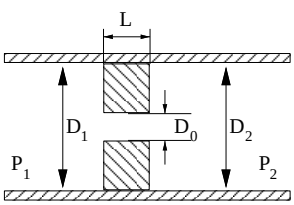

Figure 3.25 Short tube orifice

Merritt (1967) has the following model for this kind of orifice:

$$C_d = \begin{cases} \left[2.163 + 64\dfrac{L}{D_0\,Re}\right]^{-0,5} & \text{if} \quad \dfrac{D_0\,Re}{L} < 50 \\ \left[1.5 + 13.74\left(\dfrac{L}{D_0\,Re}\right)^{0.5}\right]^{-0,5} & \dfrac{D_0\,Re}{L} > 50 \end{cases} \tag{3.74}$$

with: $Re = \dfrac{4Q}{\nu\pi D_0}$.

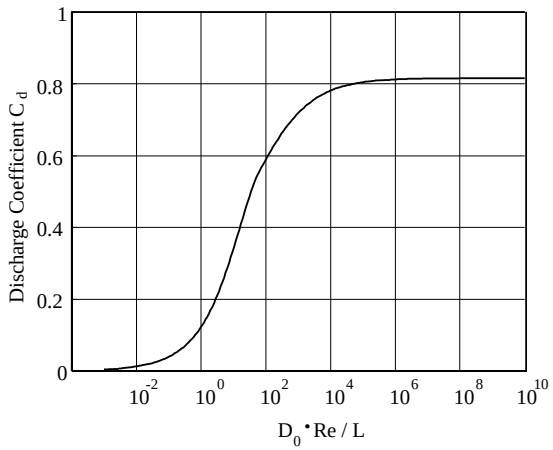

Figure 3.26 Discharge coefficient according to equation 3.74.

Lichtarowicz et al. (1965) give the following model, valid for $10 < Re_h < 20\,000$ and $2 < L/D < 10$, see Figure 3.27:

$$\frac{1}{C_d} = \sqrt{1-\beta^4}\left[\frac{1}{C_{D\max}} + \frac{20}{Re_h}\left(1 + 2.25\frac{L}{D_h}\right) - \frac{0.005\dfrac{L}{D_h}}{1 + 7.5(\log 0.00015\,Re_h)^2}\right] \tag{3.75}$$

with: $Re_h = \sqrt{\dfrac{2\Delta P}{\rho}}\dfrac{D_H}{\nu} = Re\dfrac{\sqrt{1-\beta^4}}{C_d}$

$$C_{d\max} = 0.827 - 0.0085\frac{L}{D_h},$$

D_h hydraulic diameter,
$\beta = D_0/D_1$ ratio of diameters.

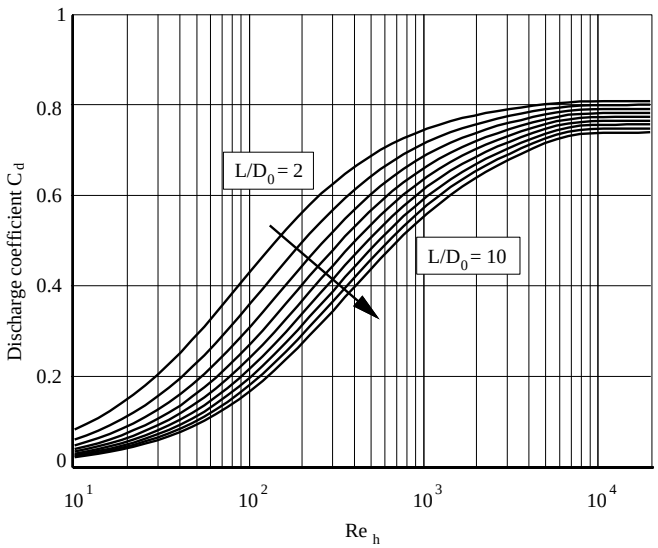

Figure 3.27 Discharge coefficient according to equation 3.75

3.5.3 Calculating Loss Coefficients or K-Factors

Another approach to calculate the resistance is the use of a *loss* or *resistance coefficient* or *K-factor*, K. It empirically describes the pressure drop by:

$$\Delta P = K \frac{\rho}{2} \frac{Q^2}{A^2} . \tag{3.76}$$

It is mostly used to calculate the pressure loss of complete hydraulic systems because the loss coefficients of several components can be added to give the total loss. This means for a tube type orifice that the entrance and exit losses and the laminar resistance of the tube can be modelled separately:

$$K = K_{entrance} + K_{tube} + K_{exit} \tag{3.77}$$

The loss coefficient of the entrance is given in Table 3.16.

Table 3.16 Loss coefficients of entrance

Geometry of entrance	$K_{entrance}$
very sharp edged	0.5
slightly rounded	0.25
smooth rounded	0.05

The loss coefficient of the exit is always 1.0, regardless whether it is sharp edged or rounded. Several references give values of the loss coefficient of orifices and experimental data. Winckler (1967) cites equations from Schaller (3.78) and Chaimowitch (3.79) to calculate K:

$$K = \frac{64}{Re} + \frac{64L}{ReD_0} + 1.4 \tag{3.78}$$

with: $Re = \frac{w_0 D_0}{\nu} < 2300$,

$L/D_0 > 1$,

$0.5 < D_0 < 4$ mm,

$D_0/D_2 \leq 0.5$.

This equation models the entrance resistance with 0.4 and the exit resistance with 1.0. Winckler mentions that other references state an entrance resistance of 0.5 if all edges are sharp. If the edges are slightly rounded this reduces to 0.25 and goes down to 0.06 if the edges are rounded with an radius R/D = 0.06:

$$K = \frac{64L}{D_1 Re} + 0.5\left(1 - \frac{D_0^2}{D_1^2}\right) + \left(1 - \frac{D_0^2}{D_2^2}\right)^2 \tag{3.79}$$

with: $Re = \frac{v_0 D_0}{\nu} < 2300$,

$L/D_0 > 2$.

For orifices as in Figure 2.1 Winckler (1967) gives experimental and calculated data for a model given by equation 3.91.

Table 3.17 Experimental and calculated data for orifices (Winckler 1967)

L	D_0	D_1	D_2	K_1 measured	K_2 measured	K_1 Eq. (3.78)	K_2 Eq. (3.78)	K_1 Eq. (3.79)	K_2 Eq. (3.79)
1	0.345	8	2.5	250	1.6	250	1.4	185	1.47
1	0.514	8	2.5	270	1.3	190	1.4	125	1.42

Will (1968) distinguishes between short restrictions with $L/D_0 \leq 1.2$, (3.80) and Figure 3.28, and long restrictions, (3.85) and Figure 3.30. The difference is that for a short restriction the narrowest area of the flow path, A*, lies behind the restriction, while it is within the restriction for a long restriction.

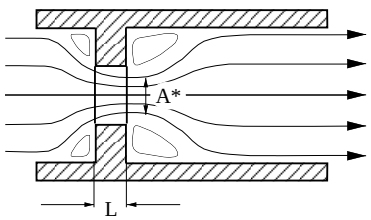

Figure 3.28 Flow through short restriction

$$K = \Phi_1 \Phi_2 \frac{64}{Re} \frac{L}{D_h} + \left(\frac{1 - m_2 \mu}{\mu} \right)^2 \Gamma \tag{3.80}$$

with: $m_2 = (D_0/D_2)^2$,
D_0, bore diameter,
D_1, diameter upstream,
D_2, diameter downstream,
Γ, models expansion losses,
Φ_1, models the geometric shape, see Table 3.18,
Φ_2, models the velocity profile, see Figure 3.29,
μ,contraction coefficient.

Table 3.18 Values for Φ_1 (Will 1968)

Geometric shape	Φ_1
circular cross section	1
annular gap	1 - 1.5
rectangular cross section (a » b)	1.5
quadratic cross section	0.89
rectangular cross section	0.89 - 1.5
equilateral triangle cross section	0.833

Φ_2 can be calculated by:

$$\Phi_2 = 1 + 0{,}5^{\frac{L}{D_h}} \tag{3.81}$$

or taken from Figure 3.29 as a function of the Reynolds number.

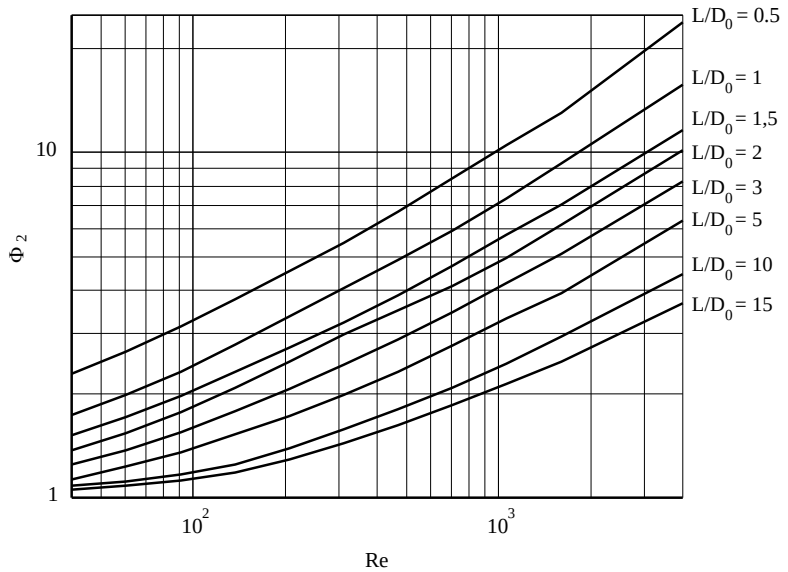

Figure 3.29 Parameter $\Phi_2$for annular restrictions as a function of Reynolds number (Will 1968)

For high Reynolds numbers and $m_1 = (D_0/D_1)^2 \approx 0$ the contraction coefficient μ is given in Table 3.19.

Table 3.19 Contraction coefficient μ (Will 1968)

Entrance	μ
very sharp edged	0.62 - 0.64
sharp edged	0.70 - 0.80
slightly rounded	0.90
smooth rounded	0.99

The contraction coefficient becomes higher if the Reynolds number is low and $m_1 > 0$. If the Reynolds number is high and the entrance edge sharp, μ can be calculated by:

$$\mu = 0.63 + 0.37 m_1^2 . \tag{3.82}$$

If the Reynolds number is high enough there are the following limits for Γ (sudden expansion of exit section)

$$L/D_0 < 0.5 \Rightarrow \Gamma = 1 , \tag{3.83}$$

$$L/D_0 > 1.2 \Rightarrow \Gamma = \left(\frac{\mu}{1 - m_2 \mu} \right)^2 \left[\left(\frac{1}{\mu} - 1 \right)^2 + (1 - m_2)^2 \right] . \tag{3.84}$$

If $0.5 < L/D_0 < 1.2$ Γ has to be determined by measurements. If the restriction is long, i. e. the area A* is within the restriction, the resistance is given by:

$$K = \Phi_1 \Phi_2 \frac{64}{\mathrm{Re}} \frac{L}{D_h} + \left(\frac{1}{\mu} - 1 \right)^2 + (1 - m_2)^2 . \tag{3.85}$$

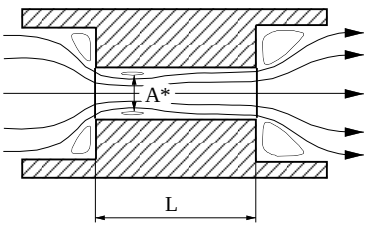

Figure 3.30 Flow through long restriction (Will 1968)

3.5.4 Cavitation

A short distance beyond the narrowest part of the flow path of a sharp edged orifice, the velocity of the liquid is at its greatest and the pressure least, see area A* in Figure 3.30. If this minimum pressure tends to decrease below the vapour pressure of the liquid, vapour bubbles appear in the liquid and pressure does not decrease below the vapour pressure. When the pressure increases downstream, vapour bubbles collapse, which can be heard as noise. This phenomenon, the emergence and collapse of vapour bubbles, is called *cavitation*.

If the ratio length to diameter of an orifice is higher than 0.5 there is a critical pressure differential ΔP_k, depending on the pressure upstream of the orifice, P_1. If the actual pressure differential becomes higher than the critical pressure differential ΔP_k, i. e. the pressure downstream, P_2, becomes very low, the flow doesn‘t increase significantly and equation 3.72 is no longer valid. This critical pressure differential ΔP_k is given by (Riedel 1973):

$$\Delta P_k = C_k^2 \left[\frac{\sqrt{P_1}}{C_{D\max}} + \frac{20\nu\left(1+2.25\frac{L}{D_H}\right)}{C_k D_H \sqrt{\frac{2}{\rho}}} \right]^2 \tag{3.86}$$

with: $C_k \approx 0.65$ and $C_{D\max} = 0.827 - 0.0085\frac{L}{D_H}$.

Will (1968) found that there is a loss coefficient K’ if cavitation occurs:

$$K' = \Phi_1 \Phi_2 \frac{64}{Re}\frac{L'}{D_h} + \frac{1-m_1^2\mu^2}{\mu^2} \tag{3.87}$$

with: L’ length from entrance to narrowest part of the flow path,
$L'/D_0 \approx 0.5$ for high Reynolds numbers and sharp edged entrance,
$L' = l$ for laminar throttling devices with $\mu \approx 1$.

If the upstream pressure is lower than the critical upstream pressure P_{2k} cavitation occurs:

$$\frac{P_{2k}}{P_1} = 1 - \frac{K}{K'}\left(1 - \frac{P_d}{P_1}\right) \tag{3.88}$$

with: P_d fluid vapour pressure.

If the quotient P_d / P_1 is neglected, equation 3.88 shows that cavitation can occur only if the loss coefficient K is smaller than K’.

Another model was given by Nurick (1976) and Schmidt and Corradini (1997) (see also Koivula 2000). They take equation 3.72 and use for C_d:

$$C_d = \min\left(0.84, 0.61\sqrt{\frac{P_1 - P_d}{P_1 - P_2}}\right). \tag{3.89}$$

3.5.5 Metering Edges of Valves

There are several models for the metering edges of valves. One uses the equation for a sharp edged circular orifice and varies the diameter of this orifice according to the position of the valve spool, i. e. the opened area of the valve and the orifice are the same. Another way is to measure the spool position, pressure drop and flow rate of the valve and use a look up table for the simulation. This method is the most accurate but requires an already existing valve and a lot of effort. The first method is usually good enough if the parameters of similar valves are known. Other models usually need a lot of parameters that are unknown when designing a system. A detailed study is presented by Borghi et al. (2005).

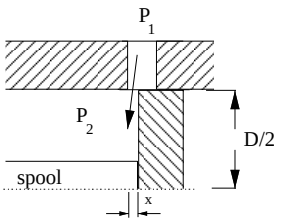

Figure 3.31 Spool valve

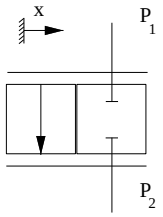

Figure 3.32 Symbol

3.5.6 Library Models for Orifices

When modeling turbulent flow through an orifice, equation 3.72 is usually used in the literature. If the pressure drop across the orifice becomes very low, however, and the Reynolds number is 200 or less even the flow through a sharp edged orifice becomes laminar. And equation 3.72 is not only a poor model for laminar flow but leads to severe numerical problems as the following example shows.

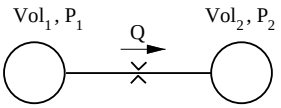

Figure 3.33 Example for orifice model

The flow rate Q in Figure 3.33 is modelled by:

$$Q = A \cdot C_d \sqrt{\frac{2}{\rho}} \sqrt{\Delta P} \tag{3.72}$$

with: $\Delta P = P_1 - P_2$.

The "gain" of the orifice, i. e. dQ / d(ΔP), is given by:

$$\frac{dQ}{d\,\Delta P} = \frac{d\left(A \cdot C_d \sqrt{\frac{2}{\rho}} \sqrt{\Delta P} \right)}{d\,\Delta P} = \frac{A \cdot C_d \sqrt{\frac{2}{\rho}}}{2\sqrt{\Delta P_{|op}}} \tag{3.90}$$

with: $\Delta P_{|op}$ pressure drop evaluated at the operating point.

Equation 3.90 shows that the gain goes to infinity as the pressure drop $\Delta P_{|op}$ goes towards zero. This may lead to severe numerical problems. Figure 3.34 shows the flow rate Q and the pressure drop for the initial conditions $P_1 = 10^4$ Pa and $P_2 = 0$ Pa. A second order Runge-Kutta-Fehlberg was used for this simulation (ACSL integration algorithm IALG = 8). Figure 3.35 gives the flow rate Q as a function of ΔP. The curve shows the familar "square root" shape.

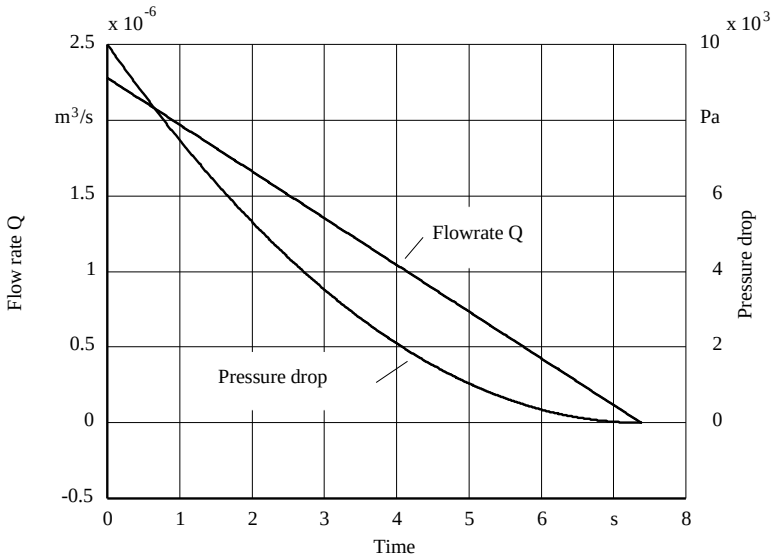

Figure 3.34 Simulation result for simple orifice model

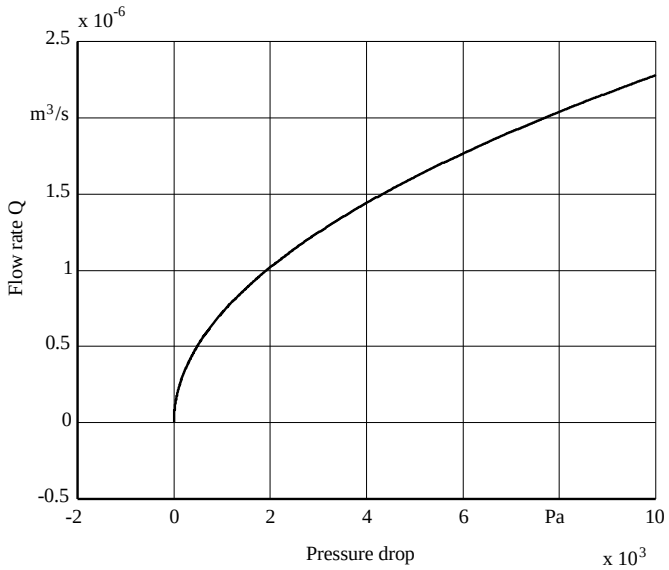

Figure 3.35 Flow rate as a function of pressure drop for simple model

The simulation result and the flow rate as a function of pressure drop show the expected results. Pressure differential and flow rate go to zero with increasing time. The problem with this simple model shows Figure 3.36. When the pressure differential approaches zero the step size of the variable step integration algorithm becomes very small and the number of integration steps per unit time increases dramatically. This means that it is not possible to use a stop time of the simulation that is much greater than the time at which the pressure drop approaches zero because the needed computing time is too long. Generally speaking this orifice model works only if the pressure drop is higher than zero or if an integration method with a fixed step size is used.

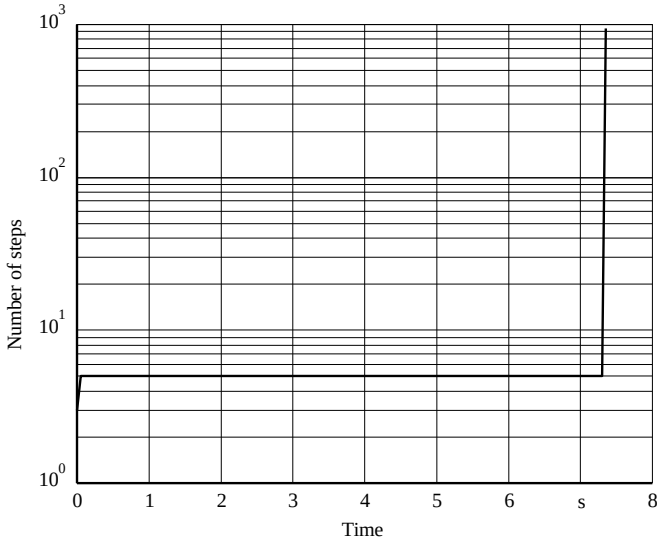

Figure 3.36 Number of integration steps per unit time. Huge increase at t = 7,39 s

Figure 3.37 show the time response after the pressure drop has become negative for the first time. It is a limit cycle around the origin caused by the infinite gain at $\Delta P = 0$.

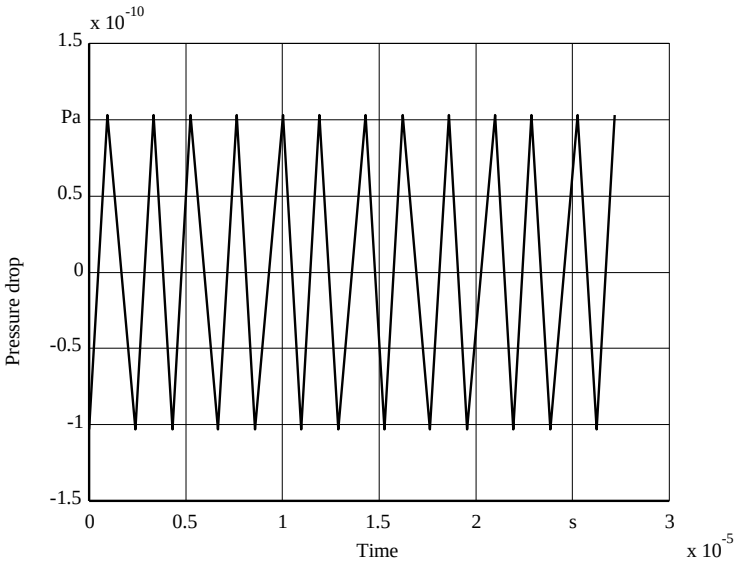

Figure 3.37 Time response shows a limit cycle after the pressure drop reaches zero for the first time

In the library the model *Orifice* uses the following equations to describe laminar/turbulent flow through fixed restrictions:

$$K = \frac{K_1}{Re} + K_2 \tag{3.91}$$

and

$$\Delta P = K \frac{\rho Q^2}{2A^2} \tag{3.92}$$

This equation was used in the German national standard TGL 38188 to describe the resistance characteristic of fixed hydraulic resistors. The coefficient K_1 determines the response at low Reynolds numbers when laminar flow exists:

$$\lim_{Re \to 0} K = \frac{K_1}{Re}, \tag{3.93}$$

which leads to:

$$\lim_{Re \to 0} Q = \frac{\pi D^3}{2K_1 \nu\rho} \Delta P \tag{3.94}$$

for an annular restriction. K_1 depends on the type of restriction. For tubes with a circular cross section K_1 is given by:

$$K_1 = \frac{64L}{D}. \tag{3.95}$$

For high Reynolds numbers, i. e. turbulent flow, K_1/Re goes toward zero and K_2 determines K:

$$\lim_{Re \to \infty} K = K_2. \tag{3.96}$$

The flow rate Q as a function of ΔP is given by:

$$\lim_{Re \to \infty} Q = \frac{\pi D^2}{4} \sqrt{\frac{2\Delta P}{\rho K_2}} \tag{3.97}$$

The relation between C_d, the discharge coefficient of equation 3.72 and K_2 is given by:

$$K_2 = \frac{1}{C_d^2}. \tag{3.98}$$

The gain dQ / d ΔP for (3.92) is given by:

$$\frac{dQ}{d\Delta P} = \frac{\pi D^3}{2\sqrt{K_1^2 \nu^2 \rho^2 + 8D^2 K_2 \rho \Delta P}} \tag{3.99}$$

and for the limit $\Delta P \to 0$ follows:

$$\lim_{\Delta P \to 0} \frac{dQ}{d\Delta P} = \frac{\pi D^3}{2K_1 \nu\rho}. \tag{3.100}$$

If $K_1 \neq 0$ the gain is not infinitely high. To understand this model better, a system as in Figure 3.33 was simulated, using the orifice model of the library, (3.92). From the computed flow and pressure drop values the C_d of a simple orifice model, (3.72), was calculated and plotted as a function of $Re^{0.5}$ in Figure 3.38. For high values of Re the computed C_d goes to $1/K_2^{0.5} = 0.6$, while for low values C_d goes towards zero. This agrees with measured data from the references (see also Figure 3.24).

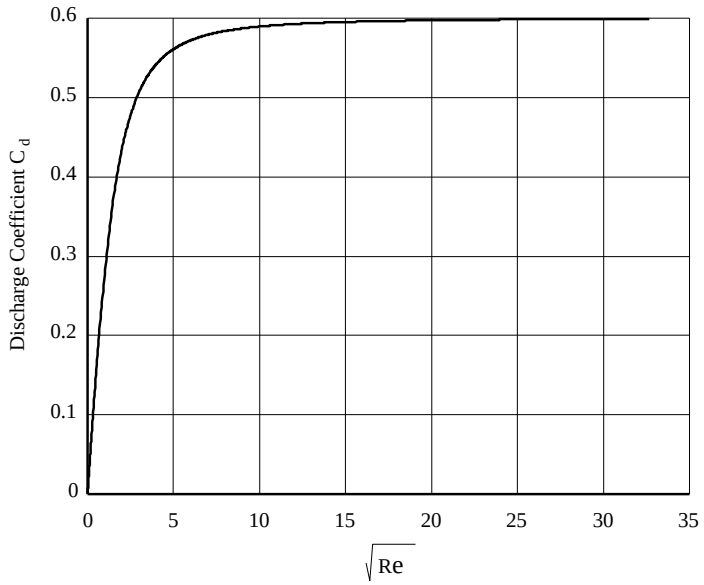

Figure 3.38 Calculated discharge coefficient as a function of Reynolds number

The library model also agrees with theoretical calculations. Wuest (1954) found that for laminar flow through an infinitely thin orifice the discharge coefficient is given by:

$$C_d = 0.2\sqrt{Re} \tag{3.101}$$

and van Mises (1917) determined C_d for turbulent flow through an infinitely thin orifice:

$$C_d = 0.611\,. \tag{3.102}$$

This means that theoretically the change from laminar to turbulent flow happens at about $Re \approx 9$. As real orifices are not infinitely thin the transition occurs at higher Reynolds numbers.

The model *OriPoly* is not based on physical reasons but tries to avoid the numerical problems of the simple model in (3.72) by an empirical polynomial approximation around $\Delta P \approx 0$ (Ellman and Piché 1996):

$$Q(\Delta P) = \begin{cases} C_{turb} A \sqrt{\frac{2|\Delta P|}{\rho}} \operatorname{sign}(\Delta P) & |\Delta P| > P_{tr} \\ \text{when} & \\ \frac{3A\nu \, Re_{tr}}{4D} \left(\frac{\Delta P}{P_{tr}} \right) \left(3 - \frac{|\Delta P|}{P_{tr}} \right) \operatorname{sign}(\Delta P) & 0 \le |\Delta P| \le P_{tr} \end{cases} \tag{3.103}$$

where the transition pressure difference P_{tr} occurs at:

$$P_{tr} = \frac{9 Re_{tr}^2 \rho \nu^2}{8 C_{turb} D^2} \tag{3.104}$$

This corresponds to a Reynolds number of 3/2 Re_{tr}. The Reynolds number is defined proportional to the orifice diameter D:

$$Re = \frac{Q \, D}{A \, \nu} \tag{3.105}$$

with: Q flow rate,
A orifice cross section area,
Re_{tr} transition Reynolds number,
C_{turb} orifice coefficient,
D orifice diameter.

To use this model the transition Reynolds number Re_{tr} has to be chosen. From that the transition pressure P_{tr} can be calculated.

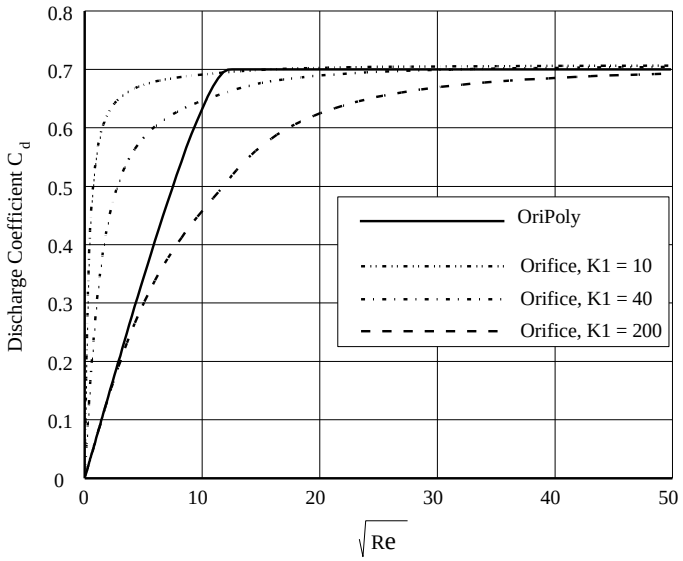

Figure 3.39 Comparison of the library models Orifice and OriPoly;
parameters are D_0 = 1.e-3 m, ν = 27e-6, c_{turb} = 0.7; ρ = 870; Re_{tr} = 100; k_2 = 2., k_1 varied

3.5.7 Library Models for Metering Orifices of Valves

There are two valve models in the library, both use (3.91):

$$K = \frac{K_1}{\mathrm{Re}} + K_2 \tag{3.91}$$

i. e. the model of a circular orifice. The orifice area is calculated according to the normalized position s of the spool. While for the *servo valve* model a linear relationship is used (zero lap)

$$\mathrm{A_{flow}} = \mathrm{A_{max}} \cdot \mathrm{s} \tag{3.106}$$

a quadratic relation is used for the *proportional valve*:

$$\mathrm{A_{flow}} = \mathrm{A_{max}} \cdot \mathrm{s}^2 \tag{3.107}$$

3.6 Spool Valves

Spool valves are used to direct the oil flow. Basic part of a spool valve are one or more metering orifices with variable area that is connected to the spool. Figure 3.40 show the diagram of a four port valve. There are six possible flow paths, from each port to the other three.

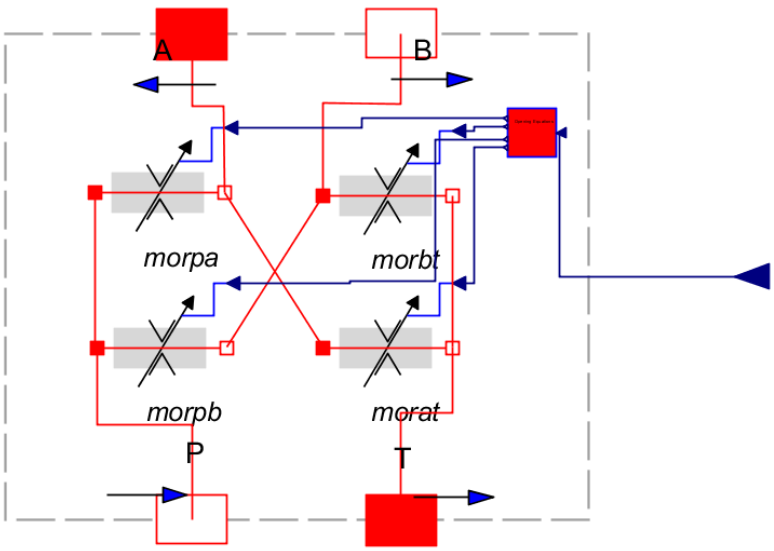

Figure 3.40 Connection of six metering orifices

The flow through a metering orifice can be modelled by equations 3.91 and 3.92. Needed is the flow area of each orifice as a function of the input signal. This functional relationship differs considerably between the different valve types.

3.6.1 Servo and Proportional Valves

Servo valves have a linear relationship between spool position s and flow area A:

$$A(s) \sim s\,. \tag{3.108}$$

Proportional valves usually have a considerable overlap and a nonlinear characteristic between position and flow area and a considerable overlap s_0 (Lausch 1990):

$$A(s) \sim \begin{cases} (s - s_0)^2 & s \geq s_0 \\ & if \\ 0 & s < s_0 \end{cases}. \tag{3.109}$$

Figure 3.41 and 3.42 gives the characteristics of servo and proportional valves. The figure for the servovalve shows that there is a linear relation between flow rate and position if the pressure drop is constant. The relation between pressure drop and flow rate is not linear, but described by the square root dependency for both types of valves. The relation between flow rate and position is quadratic for the proportional valve.

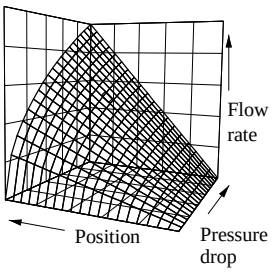

Figure 3.41 Characteristic of servovalve

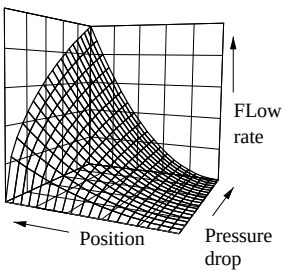

Figure 3.42 Characteristic of proportional valve

Important are also the nonlinearities of the mechanical part of the valve, the torque motor or the solenoid. (Vaughan and Gamble 1996). Ideally the position would linearly depend on the command input. But there are some nonlinearities, e. g. a limit of the spool velocity, hysteresis and friction. Figure 3.43 gives a signal flow diagram (Feuser 1983, see also Ferreira et al. 2002).

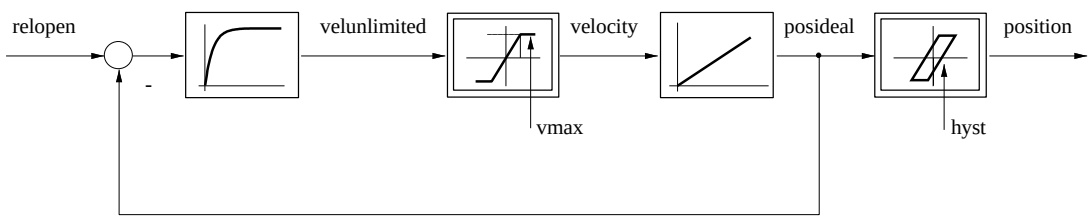

Figure 3.43 Signal flow diagram of mechanical part of valve

The values for the maximum velocity, hysteresis and friction depend on the type of valve. Usually servo valves are closed loop systems that have a mechanical or electronic feed back of the spool position and very small hysteresis. Simple proportional valves can have considerable nonlinearities.

The servo and proportional valves are modelled such that the input signal drives the mechanical part, i. e. spool position, and this determines the hydraulic part, flow through an orifice with variable flow area. But there is also a feedback of the hydraulic part to the mechanical part through the flow forces. This can limit the performance of a valve if the flow rate is high. This effect is not modelled in the library valves models because it depends very much on the actual valve design.

3.6.1.1 Steady state flow forces

A detailed model of a spool valve must include the steady state flow forces especially if there is no feedback of the spool position. The early work on flow forces was done by Lee and Blackburn (1952)

who also give a plot of the jet angle as a function of spool position. Nikolaus (1971) gives a formula for that plot. A survey on flow through spool valves is given by Chapple et al. (1999).

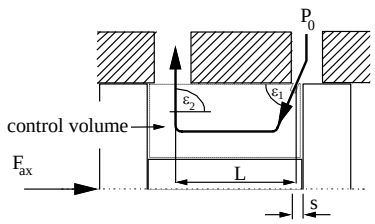

Figure 3.44 Flow through a spool valve

$$F_{ax} = -\rho \frac{Q^2}{A} \cos \varepsilon_1 \tag{3.110}$$

with: F_{ax} flow force,
ρ mass density,
A flow area,
s position of spool, $s = 0^+$ => valve opens,
Δr radial clearance.
ε_1 jet angle.

$$\cos \varepsilon_1 = \begin{cases} \dfrac{1.59}{2.69 + \dfrac{s}{\Delta r}} + 0.34 & s > 0 \\ \text{if} & \\ 0.934 & s \le 0 \end{cases} \tag{3.111}$$

Another formula for the jet angle ε_1 is given by Merritt (1967):

$$\frac{x_v}{C_r} = \frac{1 + (\pi/2)\sin\varepsilon_1 - \log_e \left|\tan(\pi - \varepsilon_1)/2\right| \cos\varepsilon_1}{1 + (\pi/2)\cos\varepsilon_1 + \log_e \left|\tan(\pi/2 - \varepsilon_1)/2\right| \sin\varepsilon_1} \tag{3.112}$$

with: x_V spool position,
C_r radial clearance.

Feigel (1992) gives approximations for different valve types.

One metering orifice: $F_{ax} = 0{,}077\ Q \sqrt{P}$. (3.113)

Two metering orifices: $F_{ax} = 0{,}077\ Q \sqrt{P}$. (3.114)

Four metering orifices: $F_{ax} = 0{,}109\ Q \sqrt{P}$ (3.115)

with: F_{ax} axial force on the spool in N,
Q flow rate in *l*/min,
P pressure differential in bar.

3.6.1.2 *Dynamic Flow Forces*

In addition to the steady state flow forces there are dynamic flow forces if the flow rate changes. They are caused by the inertia of the moving oil column.

$$F_{ax,dyn} = \rho L \frac{dQ(t)}{dt} \tag{3.116}$$

The effect of the dynamic flow forces is small, the magnitude is about the same as the viscous friction forces (Backé 1962). This force is therefore usually not included in a spool valve model.

3.6.2 Directional Control Valves

While servo and proportional valves have an analog input and metering orifices that can be opened gradually, directional control valves are switching valves that in steady state are either completely open or completely closed. Their command signals are therfore binary signals, “on” or “off”. Depending on the construction there may be one or two command signals: one if the valve has two stable states and two if the valve has three stable states.

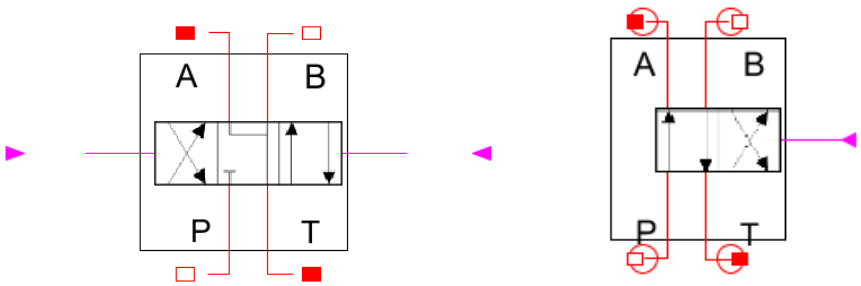

Figure 3.45 Icon of 4 port - 3 way and 4 port - 2 way directional control valves

The flow through one metering orifice can be modelled by (3.91) and (3.92). The diameter of each orifice as a function of the spool position is given by a piece wise defined linear function. This consists of segments where the flow is blocked, i.e. the diameter of the metering orifice set to a small value describing leakage. There are segments where the valve is completely opened, i.e. the diameter is set to a (maximum) value that is computed from the nominal pressure drop across one metering orifice and the flow rate. For example, the maximum diameter for the flow path from P to B is given by $dmax_{PB}$:

$$areamax_{PB} = qnom_{PB}\sqrt{\frac{\rho \cdot k_2}{2 \cdot dpnom}}$$

$$d_{max\ PB} = 2\sqrt{\frac{areamax_{PB}}{\pi}}$$

These segments are connected by straight lines to have a smooth transition when the spool moves from one position to another. In contrast to servo valves this “dynamic phase” is often not relevant for the analysis and the operation of the circuit. Typically, there is also no information from the valve manufacturer. In the library the spool dynamics is described by a first order system whose time constant can be set for the opening and closing operation separately.

More important than the spool dynamics are the flow paths that are opened or closed during the transition between the stable positions. Even if the stable positions are identical (identical valve symbol) the connections during the shifting of the spool may differ.

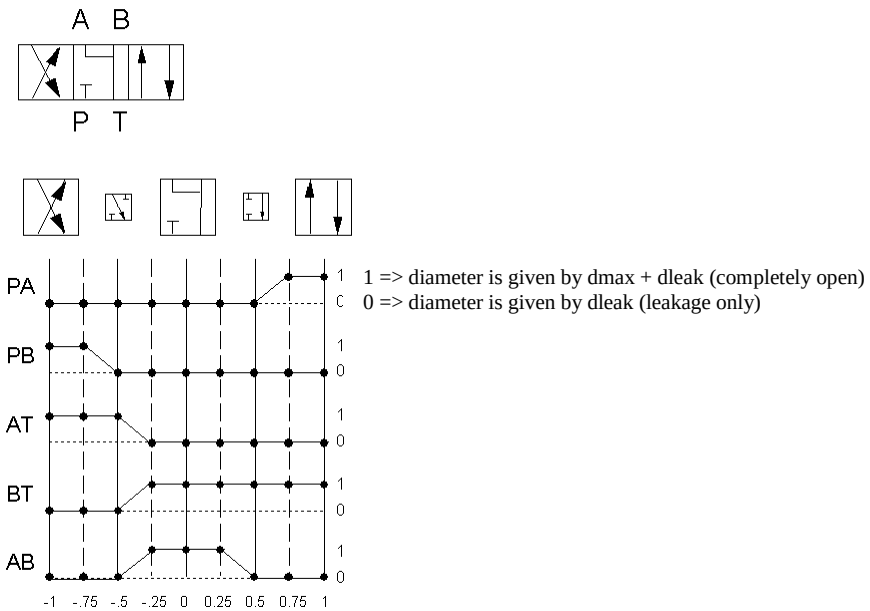

Figure 3.46 Icon and internal connections of a 4 port 3 way directional control valve (DCV_4_3_B)

When the pump pressure and the flow rate is high, the unbalanced forces and flow forces acting on the spool are higher than the force generated by the solenoid and the valve is partially closed. The effect can be modelled by the equations given above. However, the required detailed information is often not available and therefore the two parameters P_max and coeff_P are used to describe the valve behaviour. P_max specifies the maximum hydraulic power in W where the valve is still completely open and coeff_P is a reduction coefficient to adjust the model to the manufacturer's data. When the specified hydraulic power is exceeded, a warning is printed in the log window (Mode Simulation / Simulation / Show Log).

3.7 Flow and Pressure Control Valves

There are two types of control valves. One can be described as *shutoff valves*, e. g. check valves. They are either wide open or completely shut, having a minimum or maximum resistance. The transition from one state to the other is fast. Usually it suffices to describe only the static input-output relationship based on the pressure at the input and output port, because the speed of response of the valves is many times faster than the response of the overall system. A check valve is a typical example of this kind of shutoff valve.

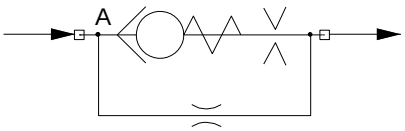

Figure 3.47 Check valve

The valve is considered open if the pressure at A, P_A, is higher than the pressure at B, P_B, plus a preload pressure given by the spring force, called popen. If the valve is open oil flows from port A through the orifice and the laminar resistance. If the valve is closed there is only the leakage through the laminar resistance. Figure 3.48 show the flow rate as a function of pressure drop for the library model *CheckValveTwo*.

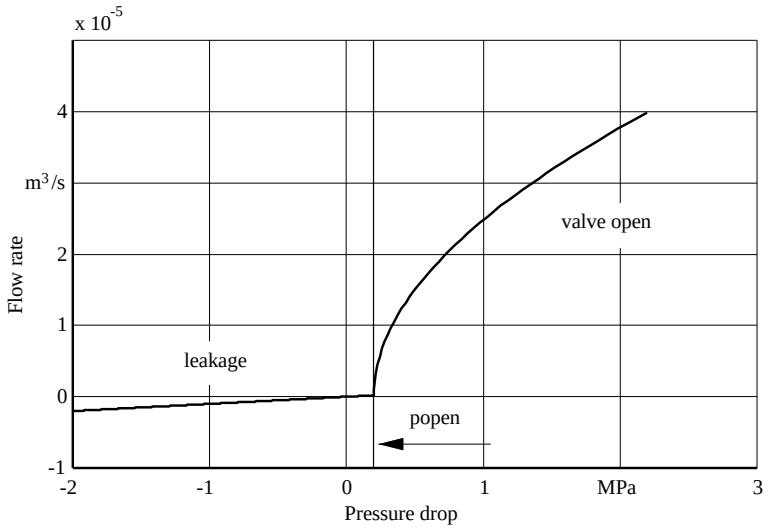

Figure 3.48 Flow as a function of pressure drop
model CheckValveTwo, popen = 0.2 Mpa, diameter = 0.001 m, $k_1 = 10$, $k_2 = 2$

There is a number of check valves who‘s response can be characterized by this model. But there are also valves that have a definite transition state between completely closed and wide open. They can be modelled by the library model *CheckValve*.

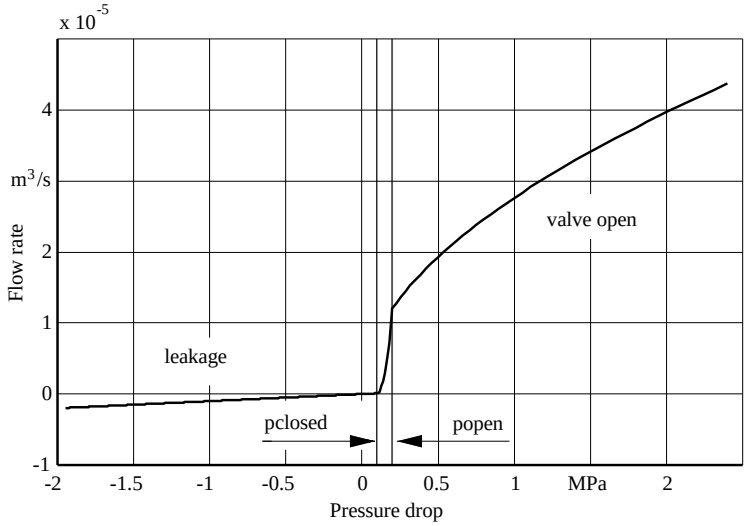

Figure 3.49 Flow as a function of pressure drop, model Checkvalve, pclosed = 0.1 Mpa, popen = 0.2 Mpa, diameter = 0.001 m, $K_1 = 10$, $K_2 = 2$

The other type of control valve can be described as *modulating valve*. These valves usually consist of a closed loop control system to control flow or pressure and vary their resistance according to the flow rate or pressure differential. A typical flow control valves consists of a closed loop control system that uses an orifice to measure flow rate and a variable restriction to reduce flow. When modeling a hydraulic system a first approach might be to use a detailed model of the flow control valve consisting of submodels for the orifice, the spool or poppet, the spring etc. The detailed model requires a number of parameters that are usually not readily available and it might use an enormous percentage of the simulation time because the masses and volumes in these valves tend to be very small leading to very small time constants. If the valve has a significant influence on the dynamics of the whole system a detailed model is necessary and can be build using the library models.

Usually it suffices to describe only the static input-output relationship. Because there is a control loop in the valve this input-output behaviour is very often (almost) linear. The necessary curves and parameters can be found in the manufacturers catalogues. Chong and Dransfield (1979) study the effects of choice of relief valve on the dynamic response of a hydraulic system. They state that for the system tested, the effect on response was noticeable and measurable rather than dramatic. They also show that for the system under test the relief valves could be represented by their steady-state discharge flow rate - pressure characteristics. Figure 3.50 gives as an example the model of a relief valve.

As pointed out in Sect. 2.6 there is also a third way, called *semi-empirical modeling*. Handroos gives models for pressure control valves (1990), counter balance valves (1993) and flow control valves (1991).

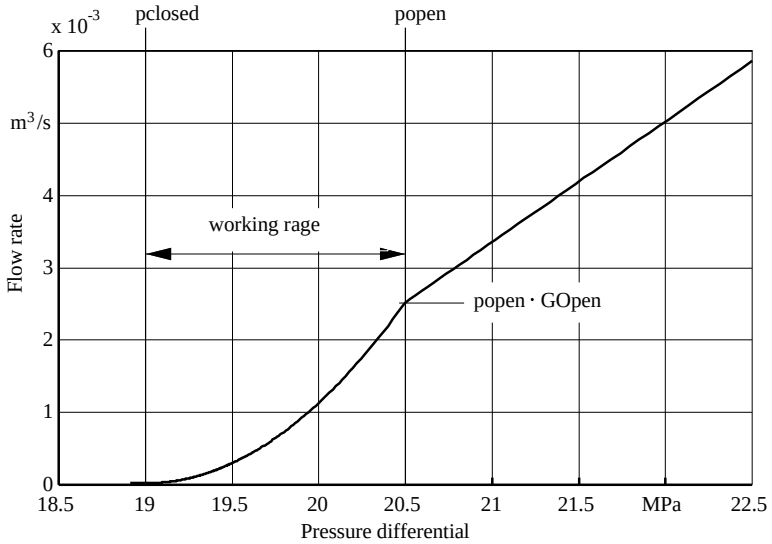

Figure 3.50 Flow rate as a function of pressure for a relief valve, ReliefValve, pclosed = 19 MPa, popen = 20.5 MPa, Gleak = 1.111e-12, Gopen = 1.666e-9

If the pressure differential is below a certain value, pclosed, there is only leakage. This leakage can be small but can also be considerably for bigger valves. The manufacturers' data sheets usually give some numbers. If the valve is working the resistance of the valve depends on the pressure differential. The resistance is decreasing with increasing pressure differential. If the pressure differential is too high the valve is wide open and its resistance is constant.

Sometimes it is necessary to make a detailed model of a valve. This has to include the inertia of the moving parts, the oil volumes under pressure and the restrictions. Table 3.20 gives some models for restrictions that are neither spools nor orifices.

Table 3.20 Models of different valve types

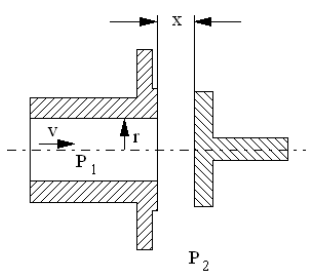 Disk Valve	$A_x = 2r\pi x$ $A_x = A_p \text{ when } x = r/2$ $A_p = \pi r^2 \quad L_w = 4\pi r$ $K = 1.3 + 0.2\left(\frac{A_p}{A_x}\right)^2$ (Lyon 1982)

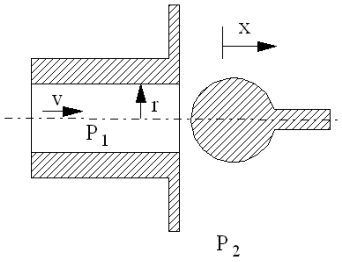 x = 0 => valve closed Simple Ball Valve	$A_x \approx 1.5\pi r x$ A_x is valid when $r \approx 1.3r$ $A_p = \pi r^2$ $L_w \approx 4\pi r$ $K = 0.5 + 0.15\left(\frac{A_p}{A_x}\right)^2$ (Lyon 1982)
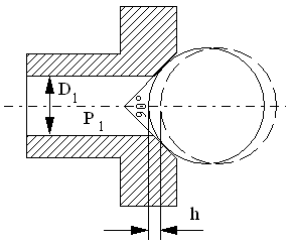	$K = 2.65 - 0.8\left(\frac{h}{D_1}\right) + 0.14\left(\frac{h}{D_1}\right)^2$ $0.1 < h/D_1 < 0.25$ (Chaimowitsch 1961)
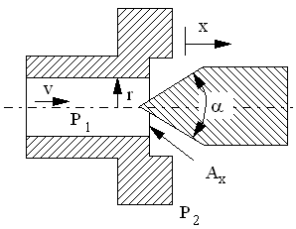 x = 0 => valve closed Needle Valve	$A_x = \pi\left(2rx\tan\frac{\alpha}{2} - x^2\tan^2\frac{\alpha}{2}\right)$, $A_x = 0$ when $x = 0$ $L_w = 2\pi\left(2r - x\tan\frac{\alpha}{2}\right)$, $K = 0.5 + 0.15\left(\frac{A_p}{A_x}\right)^2$ K is valid from A_x = 10 to A_x = 100 % of entry area, Ap. (Lyon 1982)
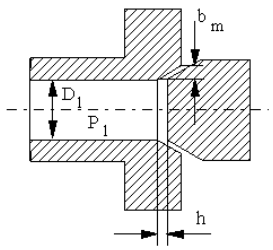 Poppet valve	$K = 2.65 - 0.8\left(\frac{h}{D_1}\right) + 0.14\left(\frac{h}{D_1}\right)^2$ $0.1 < h/D_1 < 0.25$ $b_m/D_1 = 0.1$ (Chaimowitsch 1961) see also (Bergada and Watton 2004)

3.8 Long Lines

In most hydraulic control systems the lines are short and are of reasonably large diameter to keep fluid flow velocities to a low value. In these situations it is usually reasonable to ignore line resistance as negligible relative to, for example, control valve resistance, line capacitance as negligible relative to, for example, actuator capacitance, and fluid inertia as a very minor dynamic effect relative to the inertia of the actuator and load. Alternatively, line resistance can be lumped with valve resistance and possibly with actuator inlet resistance, and line capacitance with actuator or other adjacent components' capacitance(s). There may be cases however where it is desirable to include some or all of a line's R, C and L effects in a dynamic model. The situation could arise:

- if the lines are long,
- if the lines are of small bore,
- if the system is being driven in a highly dynamic mode." (Dransfield 1981).

As Dransfield states the simplest line model is not to model it explicitly but adding only the line volume to the volume of the components connected by that line. The next step can be to model the oil compressibility by a lumped volume. This is acceptable if the length *l* of the line is shorter than

$$l < \frac{a}{10 f_{max}} \tag{3.117}$$

with: a speed of sound,
f_{max} highest frequency of interest.

If the highest frequency of interest leads to a length that is shorter than given by equation 3.117 or if the pressure drop across the line is important a detailed line model has to be used.

3.8.1 Steady State Pressure Loss in Lines

To model the pressure drop the *friction factor* f (3.118) is used. This number depends on the Reynolds number and, if the flow is turbulent, on the internal smoothness of the pipe.

$$f = \frac{2 \Delta P D}{\bar{u}^2 \rho L} \tag{3.118}$$

with: f friction factor,
ΔP pressure differential,
D inside diameter,
$\bar{u}$ (mean) velocity,
ρ mass density of fluid,
L pipe length.

The library model *RigidLine* models the losses for Reynolds numbers from 0 to 10^5 and uses the laws of Hagen-Poiseuille and Blasius from Table 3.21. The transition from laminar to turbulent flow is modelled as instantaneous; a dynamic model is given by Schindler (1995). In the library models there is no check whether the condition for smooth pipes is fulfilled.

Table 3.21 Friction factor f as a function of Reynolds number Re (Beitz and Küttner 1990)

Re	Law of	f
< 2320	Hagen-Poiseuille (laminar)	$\frac{64}{Re}$
2320 - 10^5	Blasius	$\frac{0{,}3164}{Re^{0.25}}$
10^5 - 10^8	Nikuradse	$(1.8\log(Re) - 1.64)^{-2}$
with: $Re = \frac{wD}{\nu} < \frac{65D}{k}$	as condition for hydraulic smooth pipes.	

Table 3.22 Guidelines for the wall roughness k (Findeisen and Findeisen 1984, Beitz and Küttner 1990).

Type of pipe	Wall roughness k
new seamless steel tubing	0.02 - 0.06 mm
narrow tube	up to 0.1 mm
rubber hose	0.02 - 0.05 mm
barrel slot	0.01 - 0.03 mm
valve housing	0.005 – 0.02 mm

The assumption of smooth pipes is usually valid for technical systems. Melchinger (1992) gives as an example data of an excavator where the actual Reynolds numbers are less than the limit given in Table 3.21. For an inner diameter of ID = 12 mm the admissible Reynolds number are between Re = 7800 up to Re = 39000 and for ID = 32 mm between Re = 20800 up to Re = 104000; the actual Reynolds numbers are much smaller. A second model is given by Will et al. (1990). It doesn‘t model the change from laminar to turbulent flow but uses an average friction factor.

Table 3.23 Friction factor f as a function of Reynolds number (Will et al. 1990)

Re	Law of	f
0 - 1404	Hagen-Poiseuille (laminar)	$\frac{64}{Re}$
1404 - 2320	(Transition)	$\lambda = 0.0456$
above 2320	Blasius	$\frac{0.3164}{Re^{0.25}}$

3.8.2 Modeling the Dynamics of Long Lines

In the past many methods were developed to describe and calculate the dynamic behaviour of long lines. The beginning was the need to understand the "water hammer effect" which occurred in long water hydraulic lines if valves were closed very fast. This lead to the *method of characteristics* which was a graphical method (Wylie and Streeter 1978). Later many more refined models were used. They all discretize the partial differential equations that describe the dynamics of long lines.

In the library a model given by Ham (1982) is used. Using a *frequency dependent viscosity function* $N(j\omega)$, it models laminar flow, including the dependency of the velocity profile on the driving frequency, see Figure 3.6. For the simulation $N(j\omega)$ is approximated by:

$$N(j\omega) \approx 1 + \frac{\alpha}{j\omega} + \sum_{i=1}^{3} \frac{k_i}{1 + \tau_i \frac{j\omega}{\alpha}} \tag{3.119}$$

with: $\alpha = \frac{32\nu}{D^2}$

and the following parameters k_i for $\omega / \alpha \leq 1000$:

$k_1 = 0.1918 \quad \tau_1 = 0.2496$

$k_2 = 0.0948 \quad \tau_2 = 0.0352$

$k_3 = 0.0407 \quad \tau_3 = 0.0024$

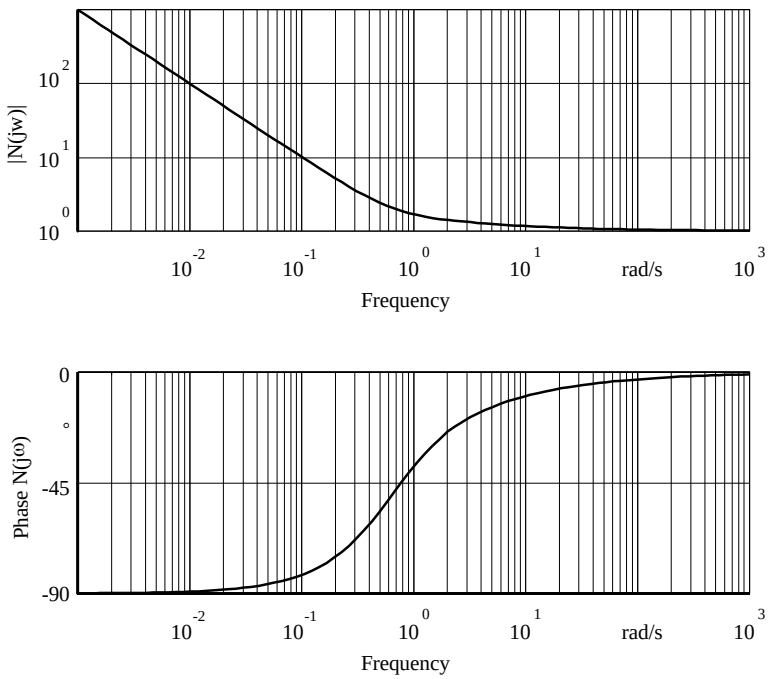

Figure 3.51 Bode plot of $N(j\omega)$ with $\alpha = 1$

Figure 3.52 shows the discretization of the line. There is one entrance segment, one exit segment and n-1 middle segments. For each the flow rate in the middle of the segment, $Q_{k+1/2}(t)$, is calculated, symbolised by the index k + ½. At the ends of each segment the pressure $P_k(t)$ is calculated.

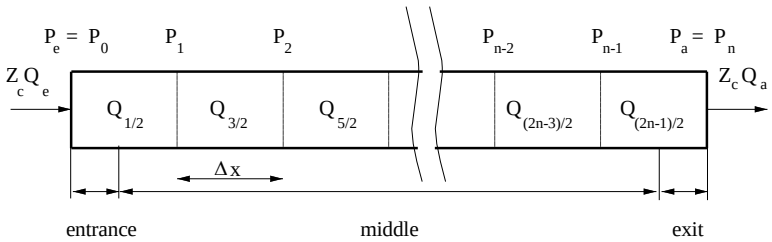

Figure 3.52 Segments of the long line

Using equation 3.119 the pressure and flow dynamics is given by:

$$\dot{P_k} = \frac{a}{\Delta x}\left[Z_c Q_{k-\frac{1}{2}}(t) - Z_c Q_{k+\frac{1}{2}}(t)\right], k = 1,2,3, \ldots n-1 \tag{3.120}$$

$$\dot{Q}_{k+1/2} = \frac{1}{Z_c}\left[\frac{a}{\Delta x}(P_k(t) - P_{k+1}(t)) - \alpha\left(1 + \sum_{i=1}^{3}\frac{k_i}{\tau_i}\right)Z_c Q_{k+1/2} + \alpha\sum_{i=1}^{3} w_{ki}(t)\right], \text{ k = 0, 1, ..., n-1} \tag{3.121}$$

$$\dot{w}_{ki}(t) = \frac{\alpha k_i}{\tau_i^2} Z_c Q_{k+1/2}(t) - \frac{\alpha}{\tau_i} w_{ki}(t), \text{ k = 0, 1, 2, ... , n-1} \tag{3.122}$$

For the first and the last segment of the line (3.120) cannot be used. Instead the pressure dynamic is described by:

$$\dot{P_e}(t) = \dot{P_0}(t) = \frac{2a}{\Delta x}\left[Z_c Q_e(t) - Z_c Q_{\frac{1}{2}}(t)\right], k = 0 \tag{3.123}$$

Pressure dynamics of the entrance segment

$$\dot{P_n}(t) = \dot{P_n}(t) = \frac{2a}{\Delta x}\left[Z_c Q_{k-\frac{1}{2}}(t) - Z_c Q_a(t)\right], k = n \tag{3.124}$$

Pressure dynamics of the exit segment

Using n segments there will be 5n+1 differential equations. To determine the necessary number of segments (3.125) is used. This gives the maximum frequency f_{max} that will be described by the model with an relative phase shift error of less than 2 %.

$$\Delta x = \frac{a}{10 f_{max}} \tag{3.125}$$

Another model of a long line was given by Gibson and Levitt (1991). They start with the general Navier-Stokes equations, make a number of assumptions and arise at the following set of ordinary differential equations:

$$\dot{P}_i(t) = -\frac{\beta_k}{2a\Delta x}(Q_{i+1} - Q_{i-1}) - \frac{Q_i}{2a\Delta x}(P_{i+1} - P_{i-1}), \text{ k = 2, 3, ... n-1} \tag{3.126}$$

$$\dot{Q}_k(t) = -\frac{a}{2a\rho_k}(P_{k+1} - P_{k-1}) - \frac{Q_k}{2a\Delta x}(Q_{k+1} - Q_{k-1}) - \frac{a}{\rho_k}F_f(k), \text{ k = 2, ..., n-1} \quad (3.127)$$

with: F_f friction terms according to Table 3.23

They describe the bulk modulus β as a function of pressure:

$$\beta = \frac{\gamma\,\beta_l\,P^2}{\gamma\,P^2 - R\,P_0^{1/\lambda}\,P^{2-1/\lambda} + \beta_l\,R\,P_0^{1/\lambda}\,P^{(\gamma-1)/\lambda}} \quad (3.128)$$

with: β_l bulk modulus of oil
γ a constant that depends on the thermodynamics of bubble formation, e. g., γ = 1, if bubble formation is isothermal, γ = 1.4 if it is adiabatic
P oil pressure
R the gas volume fraction at atmospheric pressure P_0

This model is available as function Interfaces.betaGibson.

Gibson and Levitt describe the mass density ρ as a function of pressure:

$$\rho = \begin{cases} \rho_0 (P/P_0)^{\alpha} \\ \cdot \exp((P - P_0)((1/\beta_l) + R/P)), & if\ \gamma = 1 \\ \alpha = R\,P_0 / \beta_l \\ \\ \rho_0 \cdot \exp((P - P_0)/\beta_l) \cdot \exp\left(\frac{R}{P^{1/\gamma}}(P - P)\right) & \\ \cdot \exp\left[\frac{\gamma}{\gamma - 1}\frac{R\,P_0^{1/\gamma}}{\beta}(P^{(\gamma-1)/\gamma} - P_0^{(\gamma-1)/\gamma})\right] & if\ \gamma > 1 \end{cases} \quad (3.129)$$

This model is available as function Interfaces.rhoGibson.

The dynamics of long lines depends on the effective bulk modulus. Gibson and Levitt use a function of pressure, in Ham‘s model a constant bulk modulus is assumed. This model assumes rigid lines, e. g. steel or copper. If rubber hoses are used the viscoelastic behaviour of these hoses might need modeling. For a description of the effect of viscoelasticity see e. g. McAdams et al. (1989). Muto et al. (1996) give a model for long lines with viscoelastic pipe walls. The expansion of these hoses is a function of the line pressure and time. Using a numerical analysis program like Maple, Muto‘s equation can easily be evaluated to give the frequency response, e. g. a Bode plot. However the model is not well suited for time domain simulations because the given approximations of the Bessel- and exponential functions lead to a parallel structure of the model instead of a series structure as with Ham‘s model, requiring a large number of difficult to determine coefficients.

Table 3.24 Effective bulk modulus and speed of sound (Viersma 1980)

	Steel tube D_i = 12.5 mm; D_o = 16 mm		High pressure hose D_i = 12.5 mm	
nominal pressure	$\beta_{effective}$	a	$\beta_{effective}$	a
50 bar	14600 bar	1270 m/s	5000 bar	746 m/s
90 bar	15100 bar	1296 m/s	5370 bar	772 m/s
130 bar	15700 bar	1320 m/s	5680 bar	795 m/s
225 bar	18900 bar	1450 m/s		

Table 3.25 Speed of sound of different hoses(Wacker 1985)

Hose type	pressure range	Speed of sound
3 TE (textile braid)	20 - 100 bar	≈ 700 m/s
2 STT (two-wire braid)	10 - 170 bar	≈ 975 m/s
4 SP (four light spiral wire)	20 - 170 bar	≈ 1025 m/s
ν = 34 mm^2/s; oil temperature 50 °C		

3.8.3 Examples using Model LongLine and LongLine_u_air

The model *LongLine* assumes laminar flow, i. e. Reynolds numbers below 2320. Figure 3.53 shows the pressure drop as a function of flow rate for the steady state. The pressure started at zero, was increased up to $6 \cdot 10^4$ Pa by opening a valve and then reduced to zero again. The hysteresis results from the necessary force, i. e. pressure drop, to accelerate the oil. The model *RigidLine* that computes only the resistance of the line shows no hysteresis but a jump when the critical Reynolds number is exceeded.

Table 3.26 Frequencies for example in Figure 3.54.

Number of segments n	Frequency f_{max}
4	17 Hz
9	38 Hz
39	163 Hz

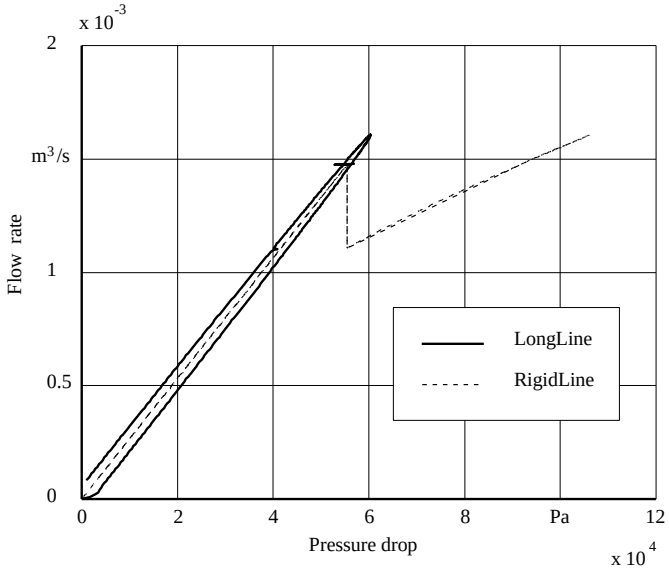

Figure 3.53 Pressure drop as a function of flow rate for models LongLine and RigidLine

The model LongLine or LongLine_u_air is used when the dynamic response of hydraulic lines has to be included in the model. To validate the models data from the literature was used. The first test is an example from Ham (1982) that consists of a pipe with diameter of 13 mm and a length of 31.98 m terminated by a laminar resistance. For three different numbers of segments, 4, 9 and 39, the frequency response was computed and is shown in Figure 3.52 to Figure 3.54. The top figures show the response of the model LongLine and the analytical solution, the bottom figures the response of the model LongLine_u_air for different values of the parameters R and γ.

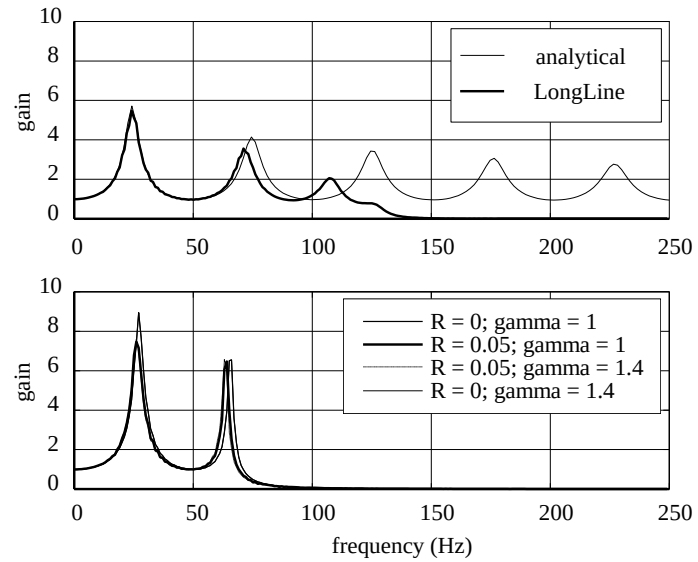

Figure 3.54 Magnitude plots of $|p_1 / p_0|$ for the analytical solution and model LongLine with 4 segments (top) and model LongLine_u_air with 4 segments for different values of R and γ

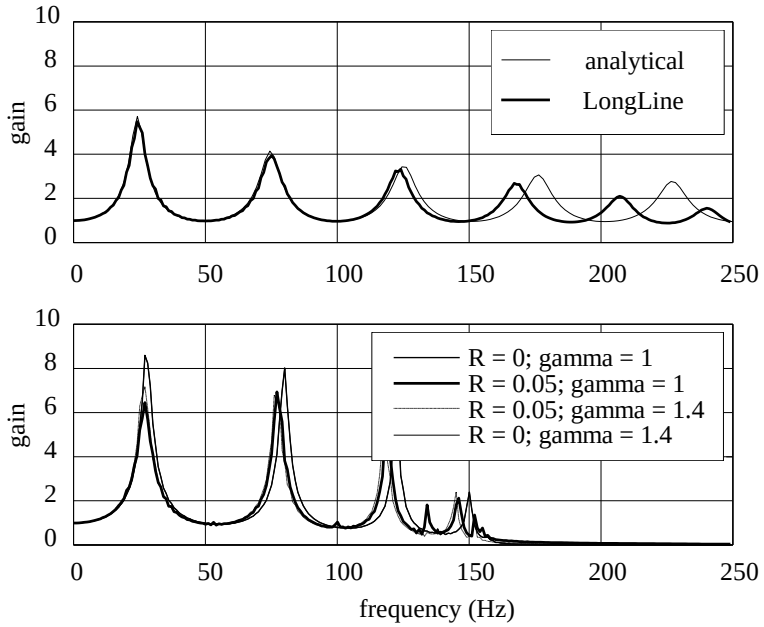

Figure 3.55 Magnitude plots of $|p_1 / p_0|$ for the analytical solution and model LongLine with 9 segments (top) and model LongLine_u_air with 9 segments for different values of R and γ

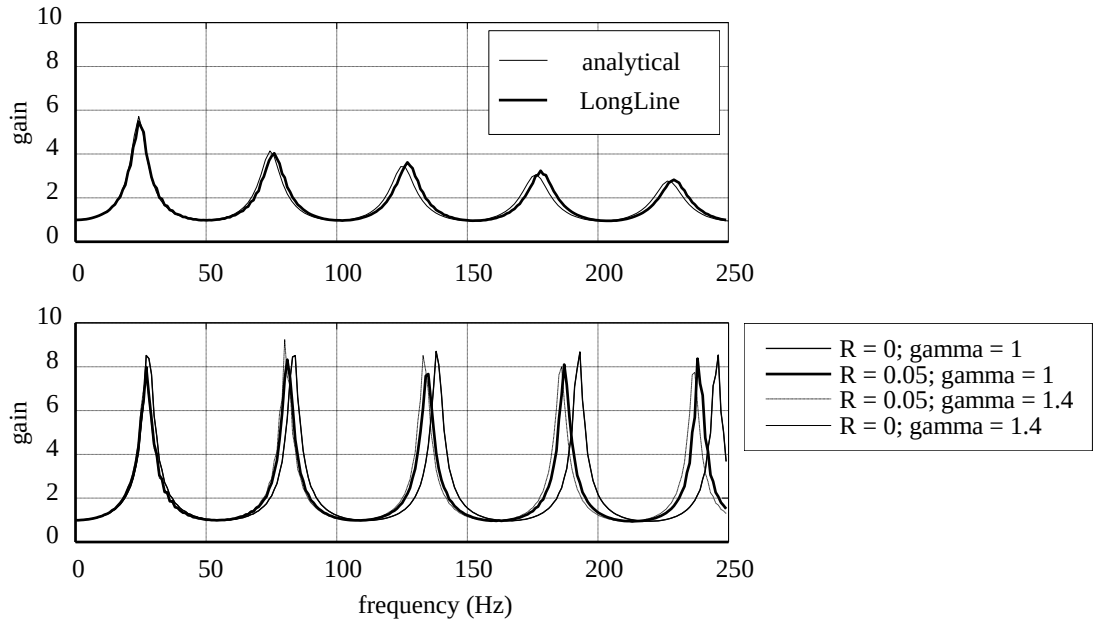

Figure 3.56 Magnitude plots of $|p_1 / p_0|$ for the analytical solution and model LongLine with 39 segments (top) and model LongLine_u_air with 39 segments for different values of R and γ

The results for R = 0, γ = 1.0 and R = 0, γ = 1.4 are almost identical for this set-up. In general the simpler model LongLine_u_air needs less computing time than the model LongLine. It doesn't describe the frequency dependent friction but can account for unsolved air. The greatest differences occur therefore for

step responses at low pressure (less than 10 MPa) where LongLine uses a constant bulk modulus - i. e. also a constant speed of sound - while the property is a function of pressure in LongLine_u_air.

A second test example is from Manhartsgruber (2000) who used a 5.6 m long blocked pipe with an entrance section and an exit section and measured the response up to 1000 Hz. The speed of sound is given in his paper to vary between 1375 m/s at a mean pressure of 50 bar and 1403 m/s at 125 bar. The viscosity has to be estimated from his figures.

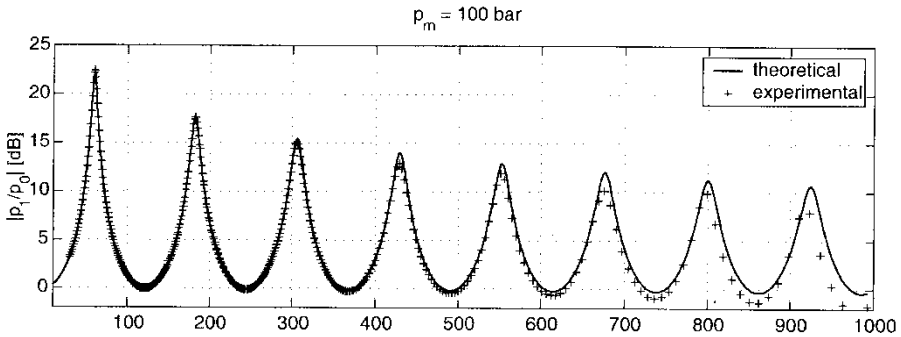

Figure 3.57 Magnitude plots for the analytical solution and measured response (Manhartsgruber 2000)

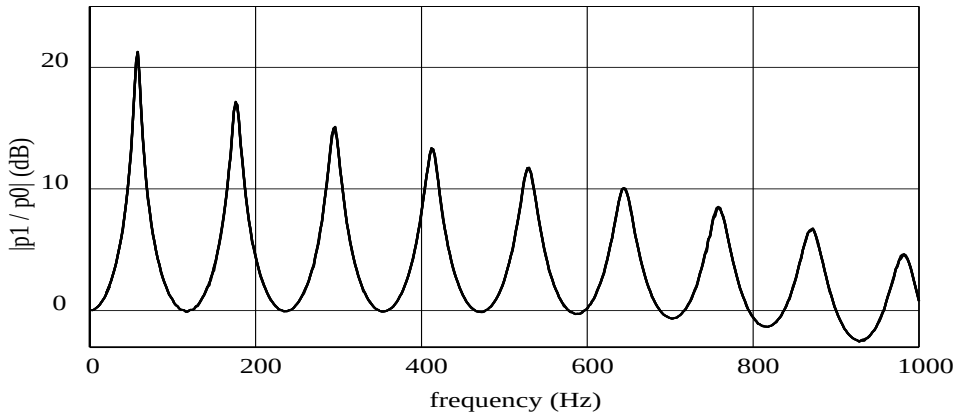

Figure 3.58 Magnitude plots of $|p_1 / p_0|$ for the model LongLine with 40 segments

Another reference model was given by Kajaste (1999). He studied the time response of hydraulic lines and used a test rig with a line length of 20.23 m and an inner diameter of 12 mm where he closed a directional control valve to produce the waterhammer effect. The following figures show a good agreement between his results and a simulation with the model LongLine.

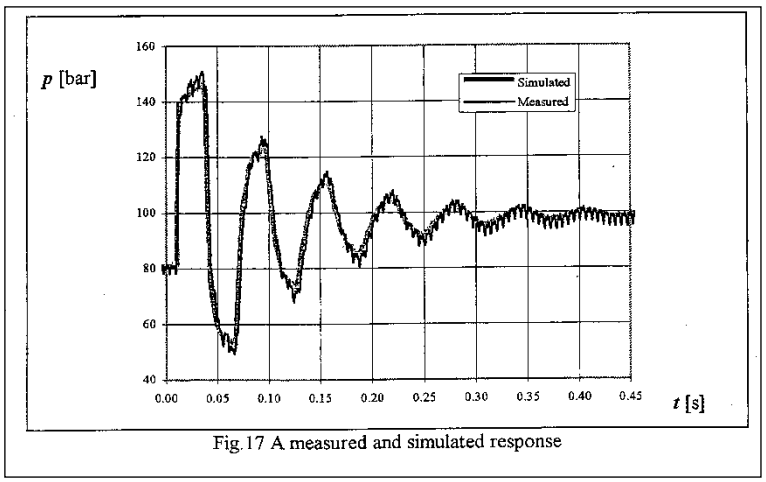

Figure 3.59 Result from Kajaste. Measured data and his simulation result

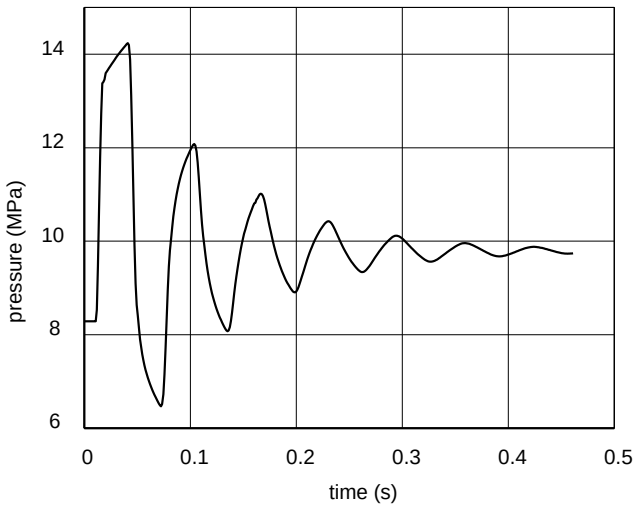

Figure 3.60 Simulation result with HyLib and model LongLine

3.9 Accumulators

There are different types of accumulators. The so called *spring accumulators* store energy by compressing a metal spring. More often a volume of gas, mostly nitrogen, is used to store the energy. These *hydro-pneumatic* accumulators are used to either reduce the pressure and flow fluctuations or to supplement a pump in a circuit, where the load cycle requires maximum power over a short period of time only, e. g. a system with secondary control, see Sect. 2.4. The design of accumulators differs depending on the task.

If an accumulator is used in a hydraulic circuit, it is usually necessary to model it because the compliance of the accumulator spring, i. e. the gas volume, is much smaller than the compliance of the oil spring. The accumulator reduces the effective bulk modulus of the system.

3.10 Filters and Coolers

Filters are used to keep the fluid clean. When modeling the system dynamics there are two points that may need consideration. There is always a certain amount of fluid in the filter and a filter has a resistance. The oil in the filter can be modelled by a lumped volume or added to a lumped volume that describes the lines connected to the filter. The resistance of a filter is usually small and doesn‘t influence the dynamics of the complete system.

If it is necessary to model the losses data from the manufacturer or measurements are needed because there are only few theoretical models mentioned in the literature. There are references to losses in flow normal to plane screens (Cornell 1958, Chaimowitch 1961) but they can‘t be used to model the losses of a filter. Fritsche (1984) made measurements with one particular type of filter and used the following polynomial:

$$K = a_0 + a_1 \frac{1}{\sqrt{Re}} + a_2 \left(\frac{1}{\sqrt{Re}} \right)^2 + a_3 \left(\frac{1}{\sqrt{Re}} \right)^3 \tag{3.130}$$

with $a_0 = 0.591 \cdot 10^1$

$a_1 = -0.305 \cdot 10^2$

$a_2 = 0.255 \cdot 10^4$

$a_3 = 0.997 \cdot 10^4$

To calculate the Reynolds number Re the diameter of the fitting, 16 mm, was used.

Coolers are needed to control the temperature of the fluid and there are the same problems as with filters when modeling them. There are some theoretical models (Anon. 1974) but when modeling a particular component measurements are needed. Fritsche (1984) used the same model as for filters and found the following coefficients:

$a_0 = 0.681 \cdot 10^1$

$a_1 = -0.274 \cdot 10^3$

$a_2 = 0.930 \cdot 10^4$

$a_3 = 0.543 \cdot 10^3$

References

Anon. (1974) VDI-Wärmeatlas. VDI-Verlag: Düsseldorf

Armstrong-Hélouvry, B. (1991) Control of Machines with Friction. Kluwer Academic Publishers, Boston

Armstrong B., Canudas de Wit C. (1996): Friction Modeling and Compensation. The Control Handbook, edited by W.S.Levine, CRC Press, pp. 1369-1382.

Backé, W. (1962) Über die dynamische Stabilität hydraulischer Steuerungen unter Berücksichtigung der Strömungskräfte. Thesis RWTH Aachen

Backé, W., Murrenhoff, H. (1994) Grundlagen der Ölhydraulik. RWTH Aachen

Beater, P. (1999) Entwurf hydraulischer Maschinen – Modellbildung, Stabilitätsanalyse und Simulation hydrostatischer Antriebe und Steuerungen. Springer Berlin Heidelberg New York.

Beater, P. Object-oriented Modeling and Simulation of Hydraulic Drives. Simulation News Europe. SNE 22, 1998. S.11 - 13.

Beitz W. , Küttner K.-H. Herausgeber (1990) Dubbel - Taschenbuch für den Maschinenbau. Springer, Berlin Heidelberg New York.

Bell, J., Bergelin, O., P., (1957) Flow Through Annular Orifices. Transactions of the ASME. 79:593 - 601

Bergada, J. M., Watton, J. (2004) A direct solution for flowrate and force along a cone-seated poppet valve for laminar flow conditions. Proceedings of the Institution of Mechanical Engineers / Journal of systems and control engineering. 218:197-210

Boes, C. (1995) Hydraulische Achsantriebe im digitalen Regelkreis. Ph.D. Thesis, RWTH Aachen

Borghi, M., Milani, M., Paoluzzi, R. (2005) Influence of the notch shape and number of notches on the metering characteristics of hydraulic spool valves. International Journal of Fluid Power 6(2):5-18

Borutzky, W., Barnard, B.,Thoma, J. U. (2000) Describing bond graph models of hydraulic components in Modelica. Mathematics and Computers in Simulation. 53:381-387

Bowns, D., E., Edge, K., Worton-Griffiths, J. (1993) The Effect of Air in the Fluid on the Operating Characteristics of a Hydrostatic Transmission. 3rd International Fluid Power Symposium, Turin, May 1973. pp A1 - 1:15

Briggs, L. J. (1950) Limiting Negative Pressure of Water. Journal of Applied Physics 21:721- 722

Chaimowitsch, E. M. (1961) Ölhydraulik. Grundlagen und Anwendung. VEB Verlag Technik Berlin.

Chapple, P., Grahl-Madsen, M., Lie, T. (1999) Flow Through Spool Valves - CFD and a Link to the Past. Int Workshop on Computer Software for Design of Fluid Power Systems. Trondheim 99

Chong, F. K. and Dransfield, P. (1979) The Effect of Choice on Relief Valve on the Response of a Hydraulic Control System. Proc. Conference on Control Engineering, Melbourne, pp 65 - 69

Conrad, F., Sorensen, P., M., Trostmann, E. (1990) On the Modelling of Flow- and Torque-loss in Hydrostatic Machines. 9th int Symp Fluid Power, Cambridge, 1990. pp. 3 - 17

Conrad F., Trostmann E., Zhang M (1993) Experimental identification and modelling of flow and torque losses in gerotor hydraulic motors. Proceedings of the 2nd JHPS International Symposium on Fluid Power Tokyo, 677 - 682

Cornell, W. (1958) Losses in flow normal to plane screens. Transaction ASME 80, 1958, Nr. 4

Doebelin E. O. (1972) System Dynamics: Modeling and Response. Charles E. Merrill Publishing Company. Columbus/Ohio

Dransfield, P. (1981) Hydraulic Control Systems - Design and Analysis of Their Dynamics. Springer, Berlin Heidelberg New York.

Ebertshäuser, H. (1993)Formelsammlung. o+p Konstruktionsjahrbuch 1993/94. Mainz: Vereinigte Fachverlage GmbH.

Eggerth, S. (1980) Beitrag zur Messung von Volumenströmen viskoser Flüssigkeiten in Druckleitungen. Ph.D. thesis Technische Universität Dresden.

Ellman, A., Koskinen, Vilenius (1995) Through Flow in Short Annulus of Fine Clearance. ASME International Mechnical Engineering Congress and Exposition, San Francisco, p 813 - 821

Ellman, A., Piché, P. A. (1996) A Modified Orifice Flow Formula for Numerical Simulation. ASME International Mechanical Engineering Congress and Exposition. Atlanta, USA

Elmqvist, H., Cellier, F. E., Otter, M. (1993) Object-oriented Modeling of Hybrid Systems. ESS'93, European Simulation Symposium, Delft, The Netherlands

Fassbender, A. (1993) Saugdrosselung - der Einfluß von Druckmedium und Temperatur. Ölhydraulik und Pneumatik 37:702 - 707

Feigel, H.-J. (1992) Strömungskraftkompensation in direktgesteuerten elektrohydraulischen Stetigventilen. Ph.D. Thesis RWTH Aachen.

Fensvig, A. T; Nielsen, T. H., Ovesen, T. B. (1975) On the Dynamics of Rubber Bag Accumulators - Analytical and Experimental Modeling. 4th International BHRA Fluid Power Symposium. Sheffield.

Ferreira, J. A.., Gomes de Almeida, F., Quintas, M. R. (2002) Semi-empirical model for a hydraulic servo-solenoid valve. Institution of Mechanical Engineers. Journal of systems and control engineering. 216 (3): 237-248

Feuser, A. (1983) Ein Beitrag zur Auslegung ventilgesteuerter Vorschubantriebe im Lageregelkreis. Ph.D. Thesis, Universität Erlangen-Nürnberg.

Findeisen, D., Findeisen, F. (1994) Ölhydraulik. Springer, Berlin Heidelberg New York

Fritzsche, M. (1984) Ölleitungsdimensionierung. FVA Frankfurt

Gibson, A., O., Levitt, J., A., (1991) Modeling and simulation of fluid flow in pipes and hoses. The 3rd triennial international symposium on fluid control, measurement, and visualization. FLUCOME'91. August 28-31, 1991, San Francisco, California. 67-75

Götz, W. (1983) Hydraulik in Theorie und Praxis. Robert Bosch GmbH. Stuttgart

Hahmann, W. (1973) Das dynamische Verhalten hydrostatischer Antriebe mit Servopumpe und ihr Einsatz in Regelkreisen. Ph.D. thesis TH Aachen

Ham, A. A. (1982) On the Dynamics of Hydraulic Lines supplying Servosystems. Ph.D. Thesis Technische Hogeschool Delft

Handroos, H. M., Vilenius, M. J. The Utilization of Experimental Data in Modelling Hydraulic Single Stage Pressure Control Valves. ASME Journal of Dynamic Systems, Measurement and Control, Vol 112, Number 3, Setember 1990, pp. 482 – 488

Handroos H; Halme J; Vilenius. Steady-state and Dynamic Properties of Counter Balance Valves. 3. Scandinavian International Conference on Fluid Power Linköping. 1993

Handroos H; Vilenius M. The influence of Semi-Empirical Control Valve Model Parameter Accuracy on Simulated Hydraulic System Responses. Transactions ASME Journal of Dynamic Systems, Measurement Control 1992

Handroos H; Vilenius M J. Flexible Semi-Empirical Models for Hydraulic Flow Control Valves Transactions of the ASME Journal of Mechanical Design 1991

Handroos M; Keskinen E K; Vilenius M.Effect of design parameters on vibrational behaviour of a counter balance valve equipped hydraulic crane. Proc of the 2nd JHPS Int Symposium on Fluid Power Toky 1993

Handroos, H., Halme, H. (1996) Semi-empirical model for a counter balance valve. The Third JHPS International Conference on Fluid Power, Yokohama, Japan, 4-6 Nov, 1996

Hayward, A., T., J. (1962) How Air Bubbles Affect the Compressibility of Hydraulic Oil. Hydraulic Power Transmission, No. 90, 384-388

Hayward, A. T. J. (1970) How to Estimate the Bulk Modulus of Hydraulic Fluids. Hydraulic Pneumatic Power (1)

Heumann, H. (1987) Ermittlung von Kennwerten hydrostatischer Geräte unter Berücksichtigung ihrer Verwendbarkeit bei der rechnergestützten Projektierung und Konstruktion hydraulischer Systeme. 7. Fachtagung Hydraulik und Pneumatik. Dresden.

Hibi, A., Ibuki,T., Ichikawa, T., Yokote, H. (1977) Suction Performance of Axial Piston Pumps. Bulletin of the JSME 20(139):79-84, 827:833

Hoffmann, W. (1981) Dynamisches Verhalten hydraulischer Systeme, automatischer Modellaufbau und digitale Simulation. Ph.D. thesis RWTH Aachen

Huhtala K., Karen J. K., Vilenius M. J. (1995) Semi-emperical modelling of losses in components of hydrostatic transmission systems. Proceedings of the 8th Bath International Fluid Power Workshop 237-253

Huhtala, K., Vilenius, M. (1997) Comparison of Steady-State Models of Hydraulic pumps. 5th Scandinavian Int Conf on Fluid Power, Linköping, 1997. pp. 139 - 156

Ivantysyn, J. , Ivantysynova M. (1993) Hydrostatische Pumpen und Motoren. Vogel, Würzburg.

Ivantysyn, J., Ivantysynova, M. (2001) Hydrostatic pumps and motors : principles, design, performance, modelling, analysis, control and testing. 1. Engl. ed. Akademia Books International. New Delhi.

Jinghong, Y., Zhaoneng, C., Yuanzhang, L. (1994) The Variation of Oil Effective Bulk Modulus With Pressure in Hydraulic Systems. Transaction of the ASME. Journal of Dynamic Systems, Measurement, and Control, 116:144 -150

Johnson, J. J. (2000) Designer's Handbook for Electrohydraulics, IDAS Engineering, East Troy, WI, USA

Johnston, D., N. (2002) Prediction of hydraulic inductance. Proceeding of the IMECE 2002, ASME International Mechanical Engineering Congress & Exposition, Nov. 17-22, 2002, New Orleans, Louisiana, pp 85-92

Kajaste, J. (1999) Pipeline models for large-scale fluid power systems, analysis and validation.The Sixth Scandinavian International Conference on Fluid Power, SICFP'99, May 1999, Tampere, Finland. pp 529 - 543

Kallies, H.-E. (1968) Über das Leistungsverhalten von Prallplattenventilen. Ph.D. Thesis. TU Berlin

Knight, G. C.; McCallion, H.; Dudley, B. R. (1972) Connection capacitance effects in hydrostatic transmission systems and their prediction by mathematical model. Proc Instn Mech Engrs 186:661

Koivula, T., Ellman, A., Vilenius, M. (1999) The Effect of Oil Type on Flow and Cavitation Properties in orifices and annular clearances. Workshop on Power Transmission & Motion Control 1999. Bath. p. 151 - 165

Koivula, T. (2000) On Cavitation in Fluid Power.1st FPNI-PhD Symposium, Hamburg 2000, pp. 371 - 382

Korkmaz, F. (1982) Hydrospeicher als Energiespeicher. Springer, Berlin Heidelberg New York

Kraft, W. (1996) Experimentelle und analytische Untersuchungen hydrostatischer Fahrantriebe am Beispiel eines Radbaggers. Ph. D. Thesis. RWTH Aachen.

Kürten, T. (1993) Modellbildung, Simulation und digitale Regelung hydraulischer Antriebe mit elektrohydraulischen Schaltventilen. Ph.D. Thesis Universität -GH- Duisburg. Duisburg: F. Seidelt.

Lallement J. (1989) Hydropneumatic Accumulators. Second Bath International Fluid Power Workshop 43-57

Lausch, H. (1990) Digitale Regelung hydraulischer Antriebe mittels pulsbreitenmoduliert angesteuerter Proportionalventile. Ph.D. Thesis. Universität -GH- Duisburg.VDI-Fortschrittsbericht 213, Reihe 8. Düsseldorf. VDI-Verlag.

Lau, K. K., Edge, K. A., Johnston, D. N. (1995) Impedance characteristics of hydraulic orifices. ImechE Vol 209, p 241 – 253

Lee, S., Y., Blackburn, J., F., (1952) Contributions to Hydraulic Control 1 Steady-State Axial Forces on Control-Valve Pistons. Transactions of the ASME. 74:1005 - 1111

Lee, K. I. (1977) Dynamisches Verhalten der Steuerkette Servoventil - Motor- Last. Ph.D. thesis RWTH Aachen.

Lennevi, J. (1995) Hydrostatic Transmission Control. Desing Methodology for Vehicular Drivetrain Applications. Ph. D. Thesis Linköping University, Sweden

Leonhard, W. (1985) Control of Electrical Drives. Springer, Berlin Heidelberg New York

Lichtarowicz A., Duggins, R. K., Markland, E. (1965) Discharge Coefficients for Incompressible Non-Cavitating Flow Through Long Orifices. J. Mech. Eng. Sc. Nr. 2:210 - 219

Lyon, J. L. (1982) Lyon‘s Valve Designer‘s Handbook. Van Nostrand Reinhold Company, New York

Mäkinen, J., Ellman, A., Piché, R (1997) Dynamic Simulations of Flexible Hydraulic-Driven Multibody Systems using Finite Strain Beam Theory. Proc. 5th International Conference on Fluid Power, Linköping 2:119-134

Manhartsgruber, B. (2000) Experimental validation of mathematical models of hydraulic pipelines with high-frequency excitation. Bath Workshop on Power Transmission and Motion Control (PTMC 2000), Bath, 2000. 29-41

Manring, N. D. (1997) The Effective Fluid Bulk-Modulus Within a Hydrostatic Transmission. Transactions of the ASME Journal of Dynamic Systems, Measurement, and Control. 119:462-466

Martin, H. R. (1981) Effects of Pipes and Hoses on Hydraulic Circuit Noise and Performance. 37th Nat. Fluid Power Conference, Chicago, 35:71 - 76

Martin, H. (1995) The Design of Hydraulic Components and Systems. Ellis Horwood, London

McAdams, J. P., Manuel, W. S., Hall, H. E. (1989) Comparison of Response-Time Tests with Computer Simulations for Control Hoses in Subsea Production Service. Proc. 21st Annual Offshore Technology Conf., Houston. Texas. Paper OTC 5917:367-376

McCloy, D. (1968) Discharge Characteristics of Servo Valve Orifices. Fluid Power International Conference, Olympia, 43-50

Melchinger, U. (1992) Simulation der Arbeitsbewegungen und Antriebssysteme von Hydraulikbaggern. VDI-Fortschrittsbericht 212. Reihe 1. Düsseldorf: VDI-Verlag.

Merritt, H. E. (1967) Hydraulic Control Systems. New York: John Wiley & Sons

van Mises, R. (1917) Berechnung von Ausfluß- und Überfallzahlen.Z. Ver. Deutsch. Ing, 61:447-452, 465-474, 493-498

Müller, H. (1978) Die Kugel als Kolben hydrostatischer Maschinen. Ph.D. Thesis Technische Universität Braunschweig

Muto, T., Yamada, H., Kato, H. (1996) A Fast and Convenient Method for Simulating Transient Response of Fluid Lines with Viscoelastic Pipe Walls. 12. Aaechener Fluidtechnisches Kolloquium. RWTH Aachen

Nikolaus, H. (1971) Stationäres und dynamisches Verhalten von hydraulischen Zeiwegestromregelventilen. Habilitationsschrift Universität Karlsruhe.

Nikolaus, H. (1981) Hydrospeicher als hydraulische Batterie für hydrostatische Getriebe. Ölhydraulik und Pneumatik. 25:p 563 - 566.

Nurick, W., H. (1976) Orifice Cavitation and Its Effect on Spray Mixing. Transactions of the ASME Journal of Fluids Engineering. 98:681 - 687

Nykänen, T., H., A., Esqué, S., Ellman, A., U. (2000) Comparison of different fluid models. Bath Workshop on Power Transmission and Motion Control (PTMC 2000), Bath, 2000, 101-110

Ohrn, T., R., Senser,D., W., Lefebvre, A., H. (1991) Geometrical Effects on Discharge Coefficients for Plain-orifice Atomizers. Atomization and Sprays. 1:137 - 153

Otis, D. R., (1974) New Developments in Predicting and Modifying Performance of Hydraulic Accumulators National Conference on Fluid Power, Chicago, Vol. 28, 30th ann mtg. 473 - 489

Pettersson M, Weddfelt K; Palmber J-O (1993) Modelling and Measurement of Cavitation and Air Release in a Fluid Power Piston Pump. Proc. 3rd Scandinavian International Conference on Fluid Power. Linköping, Sweden

Ramdén C, (1999) Experimental Methods in Valve Characterisitic Assesment. Ph. D. thesis Linköping University, Sweden.

Riedel, H.-P. (1973) Untersuchung von Kavitationserscheinungen an hydraulischen Widerständen. Ph.D. thesis RWTH Aachen.

Rotthäuser, S.; Finke, T. (1990) Hydrospeicher als lineares Übertragungselement ölhydraulik und pneumatik 34:348

Rotthäuser, S. (1993) Verfahren zur Untersuchung hydro-pneumatischer Speicher.Ph.D. thesis RWTH Aachen

Rupprecht, K.-R. (1988) Hydrospeicher - Experimentelle und analytische Untersuchungen zur Energiespeicherung. Ph.D. Thesis RWTH Aachen.

Schindler, D. (1995) Numerische und experimentelle Untersuchungen über pulsierende Strömungen in Rohren und Ventilen als Grundlage für die Entwicklung energieeffizienter Schalttechniken in der Ölhydraulik. Ph.D. thesis Johannes Kepler Universität Linz.

Schlösser, W. M. (1968) Über den Gesamtwirkungsgrad von Verdrängerpumpen. Ölhydraulik und Pneumatik 12:415 - 420.

Schlösser W. (1961) Mathematical model for displacement pumps and motors.Hydraulic power transmission 252 - 257, 269-328

Schmidt, D., P., Corradini, M., L. (1997) Analytical Prediction of the Exit Flow of Cavitating Orifices. Atomization and Sprays. 7:603 - 616

Schulz, R. (1979) Berechnung des dynamischen Verhaltens hydraulischer Antriebe großer Leistung für Umformmaschinen. Ph.D. Thesis. RWTH Aachen

Shute, N. A., Turnbull D. E. (1962) The minimum power loss of hydrostatic slipper bearings.Brit. Hydromech. Research. Ass. (B.H.R.A) Special Paper SP 721 (April (1962)

Stern, H. (1997) On the Bulk Modulus of Hydraulic Fluids in the Presence of Dissolved Gas. FPST-Vol.4/DSC-Vol 63. Fluid Power Systems and Technology, Collected Papers, ASME. pp. 113 - 123

Stern, H. (2000) The role of dissolved and nascent air in oil-hydraulic systems. Fluid Power Systems & Technology 2000, McLain Editor, pp. 91 - 98

Svoboda, J. (1979) Analogue and Digital Modelling in the Design of a hydraulic vehicular transmission. Proc Instn Mech Engrs 193:277

Tao J. (1991) Untersuchung der physikalischen Vorgänge im Dichtspalt und des Reibverhaltens von Hydraulik-Stangendichtungen. Ph.D. Thesis. RWTH Aachen.

Theißen, H. (1983) Die Berücksichtigung instationärer Rohrströmung bei der Simulation hydraulischer Anlagen. Ph.D. thesis RWTH Aachen.

Tsung T.-T. (1991) Analytische und experimentelle Untersuchungen zur Bestimmung der hydraulischen Induktivität von Schlitzen und Bohrungen. Ph.D, thesis RWTH Aachen.

Tustin, A. (1947) The effects of Backlash and of Speed-Dependent Friction on the Stability of Closed-Cylce Control Systems. IEE-Journal, vol 94, part 2A, p. 143 - 151

Vaughan, N., D., Gamble, J., B. (1996) The Modeling and Simulation of a Proportional Solenoid Valve. Transactions of the ASME. 118:120 - 125

Viersma, T. J. (1980) Analysis, Synthesis and Design of Hydraulic Servosystems and Pipelines. Amsterdam: Elsevier Scientific Publishing Company.

Wacker, K. (1985) Flüssigkeitsschall in Rohrleitungssystemen mit kleinem Durchmesser. Ölhydraulik und Pneumatik 29:818 - 825 and 908 - 915

Wacker, K. (1987) Bestimmung der akustischen Impedanz von Drosselventilen. Ölhydraulik und Pneumatik 31:227 - 233

Weule, H. (1974) Eine Durchflußgleichung für den laminar-turbulenten Strömungsbereich. Ölhydraulik und Pneumatik 18:57 - 67

Will, D. (1968) Der Einfluß der Öltemperatur auf das Durchflußverhalten von Drosselventilen unter besonderer Berücksichtigung der Kavitation. Ph.D. thesis. Technische Universität Dresden.

Will, D. et al. (1990) Modellierung und Berechnung hydraulischer Elemente und Anlagen. 9.Aachener Fluidtechnisches Kolloquium, RWTH Aachen

Will, D., Stöhl, H. (1985) Einführung in die Hydraulik und Pneumatik.VEB Verlag Technik, Berlin

Wilson, W. E. (1946) Rotary-Pump Theory. Trans of the ASME 68, pp 371

Winckler, R. (1967) Die Zylinderspaltdrossel als variabler Widerstand in elektrohydraulischen Regelgeräten. Ph.D. thesis, Technische Universität Berlin

Wochnik, J. and Frank, P. M. (1993) Dieselhydraulischer Antrieb. VDI Berichte 1026. pp 113 - 124. VDI Verlag, Düsseldorf

Wu, D., Burton, R., Schoenau, G. (2003) An empirical discharge coefficient model for orifice flow. International Journal of Fluid Power. 3(3)13-18

Wuest, W. (1954) Strömung durch Schlitz- und Lochblenden bei kleinen Reynolds-Zahlen. Ingenieur-Archiv 22:357 - 367

Wylie, E. B., Streeter, V. L. (1978) Fluid Transients. McGraw Hill, New York

Zimmermann, H. L. (1985) Untersuchung des statischen und dynamischen Verhaltens vorgesteuerter Druckminderventile. Ph.D. thesis RWTH Aachen.

Yeaple, F. (1990) Fluid Power Design Handbook. Marcel Dekker, Inc. New York and Basel

Zalka, A. Látrányi, J. (1971) Suction Capability and Cavitation of Gear Pumps. Second Fluid Power Symposium, Organised by the British Hydromechanics Research Association, BHRA. Guildford UK

Index

A

Abstract Mathematical Models, 29, 31
Accumulators, 85, 111, 113, 115
air
  disolved, 18
  entrained, 18
annulus, 48

B

ball in bore, 49
ball valve, 74
Base Classes, 93
basic component models, 5, 6
Beattie-Bridgeman equation, 87, 88
Break-Away, 41
bulk modulus, 3, 17, 18, 19, 20, 22, 44, 45, 79, 83, 85, 86, 102
  effect of entrained air, 17
  hoses, 80
  hoses, 79

C

Cavitation, 57, 113, 114, 115, 116
Cavitations, 35
CheckValve, 71
CheckValveTwo, 71, 97
circular tube, 48
closed circuit transmission, 10
compliance, 6, 17, 19, 40, 85, 101
compressibility, 21, 22, 40, 75, 85, 96
conductance, 3, 5, 15, 33, 34, 38, 39, 46, 94
connection of volumes, 4
coolers, 92
Coulomb friction, 41
cylinder, 40
  mechanical efficiency, 43
  seal friction, 40

D

direct connection of two lumped volumes, 4
Discharge Coefficient, 50
disk valve, 73
dissolved air, 18
Dynamic friction, 41
dynamic viscosity, 22, 23

E

bulk modulus, 17
effective bulk modulus, 18, 19
Efficiency, 27, 43
elliptical tube, 48
external leakage, 12, 27

F

filter, 92
fluid, 17
  Newtonian fluid, 22
frequency dependent viscosity function, 77
friction, 13, 24, 27, 29, 31, 34, 35, 38, 40, 41, 42, 43, 67, 69, 75, 76, 79, 82
Friction factor, 76

H

hydraulic diameter, 47, 52
hydraulic fluid, 18, 19
hydro-pneumatic, 85

I

ideal gas, 85, 86, 87, 102
ideal pump, 27, 38
Inductance, 25, 101
internal leakage, 13, 27, 94
internal or cross-port leakage, 1

K

K-Factors, 53
kinematic viscosity, 22, 23, 24, 26, 46
kinetic friction, 41

L

line resistance, 75
long line, 78, 101
loss coefficient, 53, 54, 57
lumped volumes, 4, 5, 6, 7, 9, 12, 15, 95, 98, 105, 106, 108

M

main models, 7
main windows, 7
mass density, 22, 68, 75, 79
mechanical efficiency, 35
Metering Edges, 58
method of characteristics, 77
modulating valve, 72
motor
  torque loss, 38
  volumetric loss, 38

N

negative pressure, 10, 17, 44
Negative Viscous Friction, 41

O

object diagram, 3
open circuit, 11
orifice, 2, 46, 47, 50, 51, 52, 53, 57, 58, 59, 60, 63, 64, 65, 66, 72, 99, 107, 108, 115, 116
over-all efficiency, 28

P

positive displacement pumps, 27
proportional valves, 67, 69
Pumps, 27

R

rectangular passage, 48
Rectangular passage, 48, 49
reduced inlet pressure, 36
resistance coefficient, 53
restrictions, 5, 46, 49, 54, 55, 62, 73
Reynolds numbers, 2, 51, 56, 57, 62, 63, 75, 76, 80, 99, 108
RigidLine, 75, 80, 81, 101

S

secondary control, 12, 85
semi-empirical modeling, 72
Servo valves, 66
shutoff valves, 71
speed of sound, 75, 80, 83
spring accumulators, 85
spring effect, 17
Static Friction, 41
Stiction, 41
stiffness
  fluid, 17
Stop, 41
Stribeck Effect, 41
Stribeck friction, 41

T

tapered piston in bore, 50
torque efficiency, 27
triangular passage, 49
tube
  circular, 48
  elliptical, 48
turbulent flow, 26, 46, 47, 48, 50, 58, 62, 63, 75, 76, 97, 99, 101, 106, 108

V

valve
  metering edge, 58
Valve, 65, 66, 67, 69, 71
viscosity, 22
  dynamic, 23
  function, 77
  kinematic, 22
  pressure dependency, 24
  temperature dependent, 24
viscous drag, 24
viscous friction, 29, 41
volume, 3, 4, 5, 6, 7, 22, 44, 45, 85, 87, 88, 89, 90, 92, 102, 108
volumetric efficiency, 27